AN ABSTRACT OF THE DISSERTATION OF

Tosapol Maluangnont for the degree of Doctor of Philosophy in Chemistry presented on October 10, 2011.

Title: Novel Ternary Graphite Intercalation Compounds of Alkali Metal Cations and Amines.

Abstract approved:

_____

Michael M. Lerner

Novel ternary graphite intercalation compounds (GICs) of alkali metal cations and a wide variety of amines have been synthesized by one-pot chemical syntheses. Alkali metals studied includes Li, Na and K. The families of amines employed are *n*-alkylamines, branched alkylamines, and different structural isomers of diamines and polyamines. Intragallery structures of the amine co-intercalates residing between the graphene sheets are proposed based on powder X-ray diffraction (PXRD), supplemented by compositional analyses, thermal analyses, and structure optimization when appropriate.

A homologous series of M-*n*-alkylamine-GICs (M = Na, Li) is reported for the first time, with the *n*-alkylamines of 3-14 carbon atoms (nC3-nC14). The following new GICs with indicated stages and intercalate arrangements are obtained: stage 1, d_i ~

0.70 nm, monolayer (nC3, nC4); stage 1, d_i ~ 1.10 nm, bilayer (nC6, nC8); and stage 2, d_i ~ 1.10 nm, bilayer (nC12, nC14). Here d_i is the gallery height. Two features new to donor-type GICs found are (i) an intercalate bilayer arrangement with guest alkyl chains parallel to encasing graphene layers, and (ii) the transition from an intercalate bilayer to monolayer arrangement upon evacuation for nC6.

GICs containing branched alkylamines co-intercalates are prepared and their intragallery structures compared to those of selected *n*-alkylamines. A notable difference is observed for amines with 4 carbon atoms. While the linear *n*-butylamine forms parallel monolayers (d_i ~ 0.70 nm), the branched analogs (*iso*-butylamine and *sec*-butylamine) instead form bilayers with d_i ~ 1.30 nm. This result contrasts with the general observation that more sterically-hindered intercalates tend to intercalate at lower concentrations. This structural difference is not observed, however, between *n*-propylamine and *iso*-propylamine (d_i ~ 0.70 and 0.76 nm respectively).

A rare example of a ternary GIC exhibiting cation-directed orientation of the diamine co-intercalate (1,2-diaminopropane, 12DAP) is reported. Depending on the cation M^+, this diamine can exhibit either perpendicular (M = Li, d_i ~ 0.81 nm), parallel (M = K, d_i ~ 0.70 nm) or a tilted orientation (M = Na, d_i ~ 0.75 nm). Interestingly, the gallery expansions increase as the cationic radii decrease.

The structural effect of the diamines is systematically investigated, employing diamines with different alkyl chain lengths, different positions of an $–NH_2$ group, and different $–CH_3$ substituent patterns. The first example of a monolayer perpendicular-

to-parallel transition in a GIC is reported for Li- ethylenediamine (EN)-GIC, with the respective change in d_i from 0.85 to 0.68 nm. The sodium analog, Na-EN-GIC, is also prepared and described. We also report quaternary compounds of mixed cations (Li,Na)-12DAP-GIC and mixed amines Na-(EN,12DAP)-GIC.

Ternary graphite intercalation compounds (GICs) of alkali metals and polyamines are prepared. Structural modifications similar to the diamines indicated above are also observed for polyamine intercalates. The polyamines studied include diethylenetriamine, triethylenetetramine, tetraethylenepentamine, *N*,*N*,*N'*,*N'*,*N'*-pentamethyldiethylenetriamine, and tris(2-aminoethyl)amine. Most of the new GICs have amine intercalates in parallel orientation (d_i ~ 0.76-0.86 nm for monolayers, and 1.13 nm for bilayers), though the GIC stage numbers depend on the size of the polyamine. In contrast, the star-shaped polyamine tris(2-aminoethyl)amine shows a perpendicular monolayer orientation with d_i ~ 1.06 nm.

Novel Ternary Graphite Intercalation Compounds of Alkali Metal Cations and Amines

by

Tosapol Maluangnont

A DISSERTATION

submitted to

Oregon State University

In partial fulfillment of

the requirements for the

degree of

Doctor of Philosophy

Presented October 10, 2011

Commencement June 2012

Doctor of Philosophy dissertation of Tosapol Maluangnont presented on October 10, 2011.

APPROVED:

Major Professor, representing Chemistry

Chair of the Department of Chemistry

Dean of the Graduate School

I understand that my dissertation will become part of the permanent collection of Oregon State University libraries. My signature below authorizes release of my dissertation to any reader upon request.

Tosapol Maluangnont, Author

ACKNOWLEDGEMENTS

I would like to dearly thank my advisor Prof. Michael Lerner for his guidance, patience, encouragement, and sympathy. He has given me a nice welcome, yet willing to let me go to Japan, where he helps securing me a post-doc position. I appreciate the time and interest of the thesis committee, including Prof. Ethan Minot, Prof. Mas Subramanian, Prof. William Warnes, and Prof. Phillip Watson.

The following persons have helped in different projects which are not included in this thesis: Dr. Victor Koch (Covalent Associates, Inc.) for suggestion and supplies of ionic liquids; Prof. Mingdi Yan and Dr. Li-Hong Liu (PSU Chemistry) for collaboration on graphene production from GICs; Prof. John Simonsen and Dr. Melissa Taylor (OSU Forestry) for dynamic light scattering measurements; Prof. Chin-hung (Alex) Chang and Wei Wang (OSU Chemical Engineering) for Raman measurements; Prof. Ethan Minot, Dr. Matthew Leyden, and Mr. Tristan Deborde (OSU Physics) for AFM and Raman measurements. Others who have contributed to the published works are co-authors in the manuscript or have been acknowledged in the Chapters to follow.

I would also like to acknowledge the company and discussion of the past and present members of Lerner group: Dr. Bahar Özmen-Monkul, Weekit Sirisaksoontorn, and Amila Liyanage. I would like to thanks friends for supports, especially during the critical period at the very last phase of my PhD. My best wishes to all of them. I thank

OSU Chemistry for financial supports throughout my time here in general. I appreciate the following awards given to me in particular: OSU Teaching Award (2009), and Whiteley Fellowship in Materials Sciences for Summer 2010.

I reserve the last place in Acknowledgement for my parents, with love.

CONTRIBUTION OF AUTHORS

Prof. Michael Lerner has contributed to the design and writing of each manuscript. Mr. Giao Bui and Mr. Benjamin Huntington assisted in sample preparation in Chapter 2. Mr. Weekit Sirisaksoontorn assisted in capillary zone electrophoresis experiments in Chapter 3. Prof. Kazuma Gotoh and Mr. Kazuya Fujiwara performed the measurements and interpreted the results on Li NMR in Chapter 4.

TABLE OF CONTENTS

TABLE OF CONTENTS (Continued)

TABLE OF CONTENTS (Continued)

Page

TABLE OF CONTENTS (Continued)

Page

TABLE OF CONTENTS (Continued)

Page

TABLE OF CONTENTS (Continued)

Page

LIST OF FIGURES

LIST OF FIGURES

LIST OF FIGURES (Continued)

LIST OF FIGURES (Continued)

LIST OF FIGURES (Continued)

LIST OF TABLES

LIST OF TABLES (Continued)

CHAPTER 1

INTRODUCTION

1.1 INTRODUCTION TO INTERCALATION CHEMISTRY

Intercalation is the insertion of guest species (atoms, ions, molecules) between the strongly bound layers of a two-dimensional host structure while retaining the host framework.[1, 2] In some cases, subtle changes are observed in the host, such as a new stacking order or changes in bond lengths. From one viewpoint, intercalation chemistry allows the study of molecular confinement in two dimensions, and thus complements related studies on one- and three-dimensional hosts. There are numerous important applications of intercalation compounds, including their use in energy storage, adsorption of toxins, as photo- and electro-functional materials, and as precursors for novel composites.[3] Intercalation reactions can also sometimes be used as a means to completely separate (delaminate) the host sheets, a process known as *exfoliation.* This route can even lead to single sheets that can exhibit properties different from the original bulk materials.[4]

One way of categorizing the large number of intercalation reactions and materials is using the reaction mechanism involved, as shown in Table 1.1.

Table 1.1 Classification through intercalation mechanism, with examples of hosts and guests

Mechanism	Host[a]	Examples of Guest[b]
Ion exchange	Clay, metal phosphate and metal phosphonate	M^{n+}; NR_4^+; protonated form of amine, alcohol, ether, ketone, *etc.*
	Layered metal hydroxide (LDH)	A^{n-}; X^-
Acid-base	MCh_2, MPS_3, MX, MOX, Clay, metal phosphate and metal phosphonate,	amines, alcohol, ether, ketone, *etc.*
Reduction	Graphite, MCh_2, MPS_3, MO_y, BN	M^{n+}, NR_4^+
Oxidation	Graphite, BN	$R_FSO_3^-$, $N(SO_2R_F)_2^-$, $C(SO_2R_F)_3^-$, $P(R_F)_6^-$, $B(R_F)_4^-$, MX_n^-, X^-

[a]MCh_2 = metal dichalcogenide, MPS_3 = metal phosphorus trichalcogenide, MX = metal halide, MOX = metal oxyhalide, MO_y = metal oxide, BN = boron nitride

[b]M^{n+} = alkali, alkaline earth, transition metal cations *etc.*; NR_4^+ = tetraalkylammonium (or simply any ammonium), imidazolium cations, *etc.*; A^{n-} = NO_3^-, SO_4^{2-}, ClO_4^- *etc.*; R_F = (per)fluoroalkyl group; MX_n^- = metal halide anions; X^- = halide anions

In ion exchange intercalation, the host layers are inherently charged, and this charge is compensated by intercalate ions of opposite charge located between the host layers. Some examples include alkali or alkaline earth cations M^{n+} in clays, H^+ in metal phosphate and metal phosphonate, and CO_3^{2-} in LDH. Ion exchange reactions can be performed with species whose charges are opposite to the framework, and numerous examples include inorganic, organic, or organometallic ions. Examples are the ion exchange of H^+ in α-$Zr(HPO_4)_2 \cdot H_2O$ by divalent cations,[5] of Na^+/EN complex (EN = ethylenediamine) in Na-EN-GIC by tetrabutylammonium[6] (GIC = graphite intercalation compound), and of chloride in $Zn_2Cr(OH)_6Cl \cdot 2H_2O$ by ferrocenesulfonate.[7] Note from the first example above that ions with different valencies can often be exchanged.

The formation of new intercalation compounds through acid-base interactions is well known. In Brönsted acid-base reactions, the interaction between H^+ from the host structure and guest molecule drives the intercalation reaction. The details of the proton transfer, however, depend on both the host and the guest. Examples below relate to the intercalation of aliphatic amines, RNH_2. Pan *et al.*[8] showed that in $H_2W_2O_7$ the amine intercalates exist as the protonated species, RNH_3^+. On the other hand, a combination of both RNH_3^+ and neutral RNH_2 intercalate are present in kaolinite, as reported by Kuroda *et al.*[9] Matsuo *et al.*[10] suggested the presence of hydrogen-bonding (both for neutral and protonated species) in amine-intercalated graphite oxide.

Additionally, the metal atoms at the framework of the host structure can act as Lewis acids, and interact with non-bonding electron pairs (Lewis base sites) present on the intercalates. Clearfield *et al.*[11] reported the intercalation of amines into $Cu(O_3PR)\cdot H_2O$ (R = CH_3, C_6H_5 and $CH_2C_6H_5$), in which the water coordinated to framework Cu ions is displaced by amines.

Lastly, there are many intercalation reactions that are tied to electrochemical reduction or oxidation reactions. The host will accept (donate) electrons concomitant with the intercalation of cationic (anionic) guests. In such reactions, additional considerations can become important, including the use of oxidants or reductants with appropriate redox activities to drive the redox reactions, and the selection of guests and solvents that are stable under the experimental conditions. Selected examples are shown in Fig. 1.1.[12] The figure indicates the electrochemical potentials required to intercalate Li^+ into different hosts (relative to the reference Li^+/Li potential). For example, Li^+ first starts to intercalate into graphite at a potential of ~+0.5 V, and will fully intercalate graphite, to form LiC_6 at ~+0.2 V. The amount of intercalated Li (indicated by x in Fig 1.1) increases as the potential is decreased. The vertical axis on this plot therefore relates to the driving force (electrochemical potential) required for intercalation.

As hosts, graphite and BN are unique in that they can undergo either oxidative or reductive intercalation chemistry. The intercalation chemistry of graphite will be the focus of the remainder of this thesis.

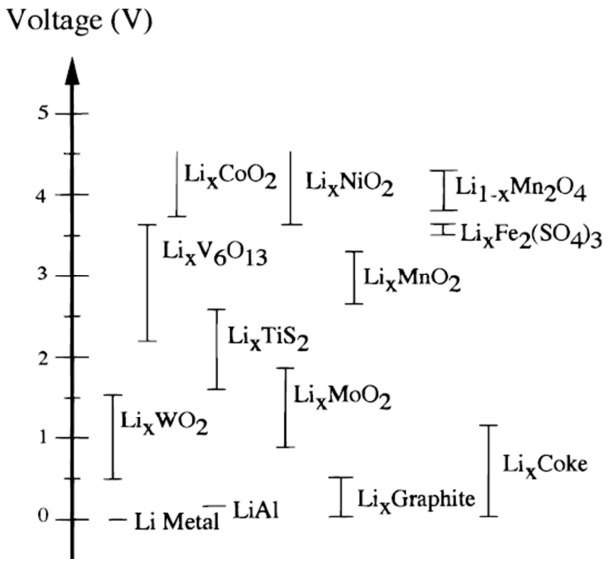

Figure 1.1 Reduction potentials of selected host structures. Reprinted with permission from ref.[12] Copyright 1998 American Chemical Society.

1.2 GRAPHITE INTERCALATION COMPOUNDS (GICs)

1.2.1 Crystal Structure of Graphite

Graphite is a planar layered material comprised of sp^2 carbon atoms bound in hexagonal sheets (called graphene sheets). Each sheet exhibits strong π-bonding that is delocalized through all C-C bonds. Graphite exists in two common forms: hexagonal and rhombohedral. The hexagonal structure (space group $P6_3/mmc$) is more common, and is shown in Fig. 1.2. Each unit cell contains four atoms (A, A', B, and B'); the sheet stacking sequence is $(AB)_n$. The A-A' distance of 0.335 nm defines the graphene sheet thickness and c = (2×0.335 nm) = 0.671 nm. Hexagonal graphite may be transformed into the rhombohedral structure by mild mechanical treatment.[13] The

latter has the stacking sequence $(ABC)_n$, and is far less common. According to Rüdorff,[13] the two forms do not show different reactivities when forming GICs.

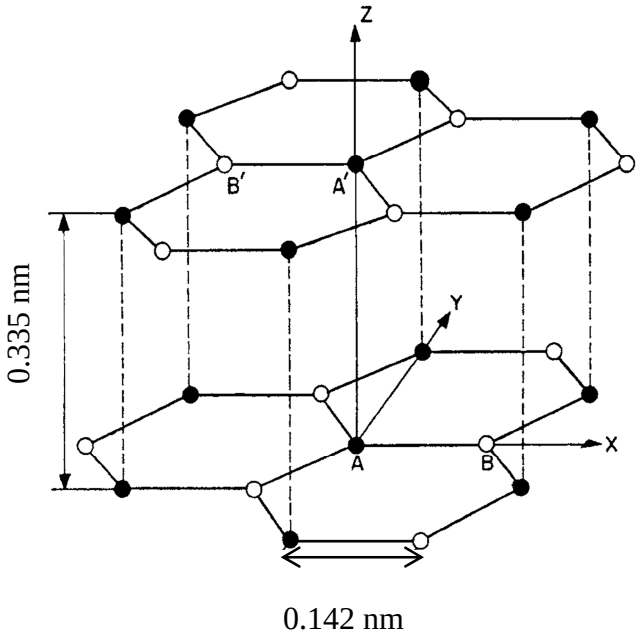

Figure 1.2 The crystal structure of hexagonal graphite along the *c*-direction. Adapted from ref.[14]

1.2.2 Intercalation Chemistry of Graphite: Donor *vs* Acceptor

As mentioned in Section 1.1, graphite is one of the few layered host materials that can intercalate either cations or anions, depending on experimental conditions. Representative reactions are indicated by eq (1.1) and (1.2) respectively.

$$M(s) + xC(s) \rightarrow M^{+}C_x^{-}(s) \quad (1.1)$$

$$MY_n(g) + xC(s) \rightarrow C_x^{+}MY_n^{-}(s) \quad (1.2)$$

In eq (1.1) the metal M reduces graphite, resulting in a *donor-type* GIC $M^{+}C_x^{-}$ where the graphene sheets accommodate the cation M^{+}. GICs of some alkaline earth[15]

and rare earth metals[16] are also known. The synthesis of donor-type GICs will be described later in Section 1.2.4, and more details on the GICs relevant to this thesis can be found in Section 1.3.

In eq (1.2), the metal halide MY_n oxidizes graphite to yield the *acceptor-type* GIC, $C_x^+MY_n^-$, containing anion intercalates between graphene sheets. In addition to a variety of metal halides, other guest species include anions (and organic derivatives) of boric, nitric, perchloric, phosphoric, sulfuric acids, and halogens. In cases where the guest species themselves cannot oxidize graphite, the addition of oxidizing agents such as F_2, or compounds containing high oxidation state metals, can be included as reagents in the GIC syntheses, or electrochemical oxidation may provide an alternate route. To date, acceptor-type GICs have shown a richer chemistry than the donor-type.

1.2.3 Staging

Staging is the periodic sequencing of the intercalates and the graphene sheets along the *c*-axis.[17] Stage one indicates the presence of intercalate between all graphene sheets, stage two indicates the presence of intercalate between every two graphene sheets, and so on. The observation that GICs can readily undergo a staging transition from *n*th to *(n-1)*th or *(n+1)*th, gave rise to what is now known as Daumas-Herold staging model, Fig. 1.3.[18] In this model there are no completely unfilled layers; instead, the graphene sheets bend, forming intercalate islands. Different structural regions in GICs are indicated in Fig. 1.3, including the boundaries of guest islands ("1"), an interlayer defect ("2"), and a terminating graphene layer ("3").[18] Thomas *et al.*[19]

published the high-resolution transmission electron microscopy (HRTEM) images of the acceptor-type $FeCl_3$-GIC, showing directly the formation of intercalate islands as suggested by this DH model. Staging is common in GICs[17] but is rare in other layered materials.[20] The flexibility of graphene sheets,[17, 21] has been identified as the principal reason for this novel phenomenon.

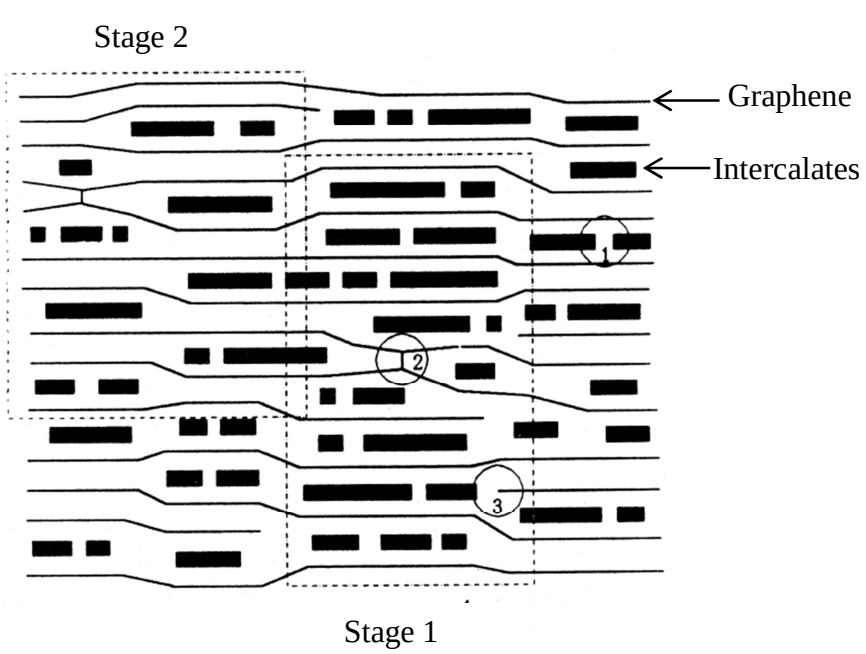

Figure 1.3 The Daumas-Herold model of staging, where the regions of stage 1 and stage 2 are highlighted. Other regions are also shown including the boundaries of guest islands ("1"), an interlayer defect ("2"), and a terminating graphene layer ("3"). Adapted from ref 18.

This thesis will use notation as indicated in Fig. 1.4 to describe GIC structures. The *(00l)* reflections from PXRD are first indexed according to the relation $I_c = d_i + (n\text{-}1)(0.335\text{ nm})$, where I_c is the identity period obtained directly from diffraction data,

d_i is the gallery height, n is the GIC stage number, and 0.335 nm is the distance between two adjacent graphene sheets. The gallery expansion, Δd, is defined as $\Delta d = d_i - 0.335$ nm. Also, a tilt angle θ, will be defined as the angle between the axis along the longest direction of a co-intercalate *vs* the adjacent graphene sheets. Fig. 1.4(a) shows the case where θ = 90º and the guest species are said to have a perpendicular orientation. The most common intercalate orientation is θ = 0º, where the intercalate species have a parallel orientation to the graphene sheets, Fig. 1.4(b). Also observed are tilted orientations with intermediate values of θ, Fig. 1.4(c).

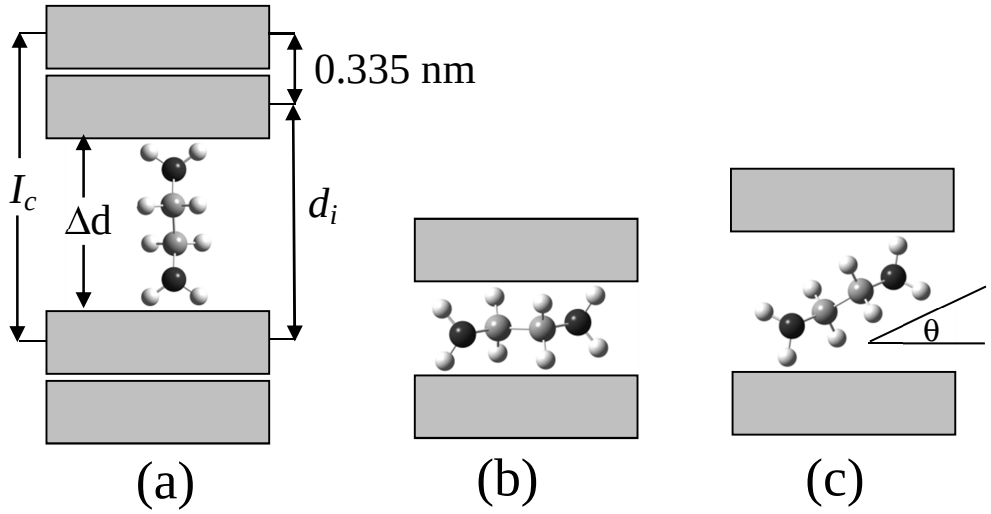

Figure 1.4 (a) Structural parameters of GIC, shown here as a stage 2 compound. The orientations of the intercalates are: (a) perpendicular [θ = 90°], (b) parallel orientation [θ = 0°], and (c) tilted, where the tilt angle θ is shown in (c).

1.2.4 Preparation of Donor-Type GICs

1.2.4.1 Thermodynamics Considerations

As a simple example, the formation of binary M-GICs from the elements can be separated into the following energetic contributions:

$M(s) \rightarrow M(g)$	ΔH_{atm}	(1.3a)
$M(g) \rightarrow M^{+}(g) + e^{-}$	I_1	(1.3b)
$C_x(s) + e^{-} \rightarrow C_x^{-}(g)$	$-E_1$	(1.3c)
$M^{+}(g) + xC^{-}(g) \rightarrow MC_x(s)$	$-\Delta H_L$	(1.3d)
$M(s) + xC(s) \rightarrow MC_x(s)$	ΔH_f	(1.3e)

Summation of steps (1.3a) to (1.3d) gives step (1.3e), which is the formation enthalpy ΔH_f of the GIC. The term E_1 combines the energy relating to sheet separation of graphite and addition of the electron, and x is the number of graphitic carbons bearing the negative charge. This simple energy scheme helps to identify some important issues in designing GIC syntheses. For example, consider the syntheses of the binary M-GICs (M = Na, K, Rb and Cs). For GICs with the same stoichiometry, MC_8, the terms in 1.3c are identical, and 1.3a and b are well known in the literature. Also, when the in-plane arrangements of the intercalate cations are similar, the differences in lattice enthalpies can be deduced from the differences in observed Δd. The differences in ΔH_f then relates to the terms in Table 1.2.

Table 1.2 Selected energetic contributions (kJ/mol) in the formation of GICs

Metal	ΔH_{atm} [22, 23]	I_1 [24]	ΔH_L [25]
Li	150	513	(440)[a]
Na	100	496	Not available
K	82	418	234
Rb	74	403	207
Cs	70	376	180

[a]For a LiC_6 stoichiometry. The calculated value for LiC_8 was not reported.[25]

It can be seen that the decreasing atomization and ionization enthalpies more than compensate for the decreasing lattice enthalpies for the GICs formed with larger alkali metals. Boersma[26] showed that stage 1 MC_8 and stage 2-5 MC_{12n} (Section 1.3.1) have negative free energies of formation for M = K, Rb and Cs, whereas those of M = Na and Li have positive values. Interestingly, while the binary compounds are unknown or little known, several *ternary* Na-solvent-GICs are readily prepared, as will be outlined in Section 1.5.

A somewhat more detailed description of the lattice enthalpy ΔH_L for reaction (1.3d) takes the form:

$$\Delta H_L = A(-\sum z_a z_c/r_{ac} + \sum z_a z_a/r_{aa} + \sum z_c z_c/r_{cc}) \qquad (1.4)$$

where A is the constant, z_a and z_c is the charge of the anion and cation respectively, r is the distance between anion-cation (r_{ac}), anion-anion (r_{aa}) and cation-cation (r_{cc}). For donor-type GICs, the anionic term refers to the negatively-charged graphene sheets.

Therefore ΔH_L is both composition- and structure-dependent. The term r_{ac} is most affected by the distance between graphene sheets and the cation M. On the other hand, r_{cc} is affected by the in-plane arrangement of the intercalate cations. Selected values of ΔH_L calculated by Setton[25] are shown in Table 1.2.

GIC lattices are more stabilized (*i.e.*, larger value of ΔH_L) for M-GICs with small gallery expansions and highly concentrated intercalates. For stage 1 binary GICs, LiC_6 has the highest value of ΔH_L and CsC_8 has the lowest. The stability of LiC_6 can then be explained due to the favorable ΔH_L compensating for the energy-intensive contributions from ΔH_{atm} and I_I.

The incorporation of metal cations solvated by organic molecules leads to ternary GICs, Section 1.3.3. These solvent molecules are termed co-intercalates. This thesis focuses on the synthesis and compositional and structural details of such compounds. The presence of organic co-intercalates qualitatively introduces the following modifications to the above simple energy model; (i) GICs are stabilized by the presence of additional ion-dipole interactions, (ii) intra-layer repulsions are reduced due to the screening by the co-intercalates, and (iii) GIC lattice enthalpies decrease due to the steric requirements of the co-intercalates. These effects are similar to those in forming three-dimensional hydrates or other solvates. Item (iii) above explains why there is often a preference for guest parallel orientation and therefore minimal gallery expansions, as this maximizes ΔH_L for the GICs produced. The interaction energies in K-THF-GIC (THF = tetrahydrofuran) have been calculated by Charlier *et al.*[27] and support the above description.

1.2.4.2 Chemical Reduction

The chemical reduction of graphite can be carried out with reagents either in the vapor, liquid, or solution phase. The synthesis of the binary GICs employing vapor phase reactions has been well established in the literature. In this method, graphite and alkali metal are placed at different temperature at the two ends in an evacuated Pyrex glass tube. The stage number can be precisely controlled through the temperature difference, *e.g.*, as shown for M-GICs of the composition MC_{12n} (M = K, Rb, Cs; $n \geq 2$).[28] The materials obtained can be of high quality suitable for physical properties measurement, but the quantity produced is usually limited.

Liquid-solid phase reactions can be performed by heating a mixture of alkali metal and graphite at elevated temperatures. This method was employed for the synthesis of K-GIC of different stages.[29] This method is attractive because it is simple and scalable, although the inhomogeneous nature of some products might be problematic. In a more recent study,[30] KC_8 can be made within 3 minutes employing high power (500 W) sonication. The formation of CaC_6, SrC_6, and BaC_6 through the high-energy ball milling has also been reported.[31] The extension of these methods to the syntheses of other synthetically-challenging GICs warrants further investigation.

Syntheses of GICs using reactants in solution involve the reaction of graphite, alkali metal, and a chosen solvent. These can be done either (i) without auxiliary agents, or (ii) with electron transfer agents such as anthracene, biphenyl, naphthalene, phenanthrene, or $Co(C_2H_4)(P(CH_3)_3)_3$. The solvents applicable for route (i) are highly polarizing and capable of directly solubilizing alkali metals, *e.g.*, liquid ammonia,

methylamine, ethylenediamine.[13] The products formed are typically ternary M-solvent-GICs. This method will be employed extensively in the following chapters. When additives are included, in route (ii), other less-polar solvents can be employed, such as ethers, or even non-polar solvent such as *n*-pentane or toluene in the case of the Co complex.[32] Since the GIC products usually contain the solvent as co-intercalates, the choice of solvent can play a critical role in the structure of the GICs obtained.

1.2.4.3 Electrochemical Reduction

With this method, a graphite electrode is reduced in an electrolyte that contains dissolved intercalate cations such as alkali metal cations, M^+, or tetraalkylammonium cations, R^+. The graphene sheets are reduced, and cations intercalate to form GICs. Until recently, the electrochemical synthesis was the *only* reported way to synthesize the binary R-GICs. As with the solution phase syntheses, this method usually gives the ternary M-solvent-GIC (M = Na to Cs, and tetramethylammonium; solvent = dimethylsulfoxide DMSO).[33] The electrochemical intercalation of K^+ from molten KF at 1163 K has also been reported.[34] However, due to the demanding reaction conditions, this method is unlikely to find a practical use. Electrochemical syntheses using liquid ammonia as electrolyte have been reported, yielding ternary M-NH_3-GICs (M = Be, Mg, Al, Sc, Y and La).[35] These ternary compounds cannot be made by chemical reduction.

1.2.4.4 Ternarization

Ternarization can be accomplished by reacting a binary GIC with the co-intercalate liquid or vapor. The following general rules can be deduced from the literature. Firstly, stage 2 GICs are more likely to yield ternary GICs than stage 1 precursors.[36,37] Similar reactions with higher stage compounds ($n \geq 3$) appear to be facile, although fewer examples have been reported.[38] The high ΔH_L values for stage 1 binary M-GICs help to explain their non-reactivity towards ternarization. Secondly, protic species (*e.g.*, alcohols[39] or water[40]) are unstable with respect to H_2 formation, and do not form ternary GICs. Finally, the ternary GICs often unstable in the mother liquor, as observed in the slow degradation of GICs prepared by ternarization of KC_8 or KC_{24} with liquid THF.[41]

1.2.4.5 Ion Exchange/ Guest Replacement

This method, although very well known for the intercalation chemistry of other layered hosts,[1] has so far been explored to only a limited extent in GICs. One challenge lies in the choice of solvents, which should dissolve the reactants to high concentrations, remain stable at very low chemical potential, and not themselves act as co-intercalates or otherwise complicate the reaction chemistry. One known example is the preparation of M-THF-GIC (M = Li, Na) by reaction of KC_8, LiC_6, or Na-NH_3-GIC, with a salt MX (X = Cl, I) in THF, as reported by Stumpp *et al.*[42] The synthesis of EuC_6 from the mixture of graphite, Li, and Eu was reported.[43] A product sequence of LiC_6, a mixture of LiC_6/EuC_6, and finally pure EuC_6 was observed as the reaction

time increased. Therefore, this is an example of the exchange of Li^+ for Eu^{n+}. A ternary Li-Eu-GIC was not detected in that study.

Recently, our group has utilized Na-EN-GIC as a precursor for the first chemical synthesis of GICs containing tetraalkylammonium[6] through an ion exchange route, which were previously only prepared by electrochemical methods. As will be described in Chapter 5, new compounds can also be obtained this way.

1.2.5 Applications of GICs

Many reviews describing the applications of GICs are available.[18,44,45] Two major existing applications of GICs are their use as anodes for Li-ion batteries,[18] and as precursors for the manufacture of thermally exfoliated graphite (TEG).[46,47] C_x/LiC_6 is a reversible anode with a theoretical capacity of 372 mAh/g.[18] Practical cells can now achieve reversible capacities exceeding 340 mAh/g. A typical voltage profile for lithium intercalation (charge) and de-intercalation (discharge) is shown in Fig. 1.5.[48]

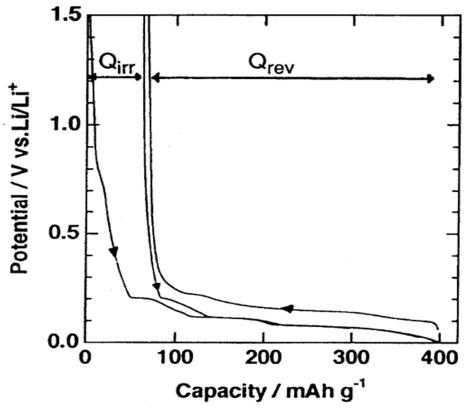

Figure 1.5 A typical voltage profile for lithium intercalation (charge) and de-intercalation (discharge) of a graphite electrode.[48] Reprinted with permission from ref. 48. Copyright 1998 Chemical Society of Japan.

The plateau observed at 0.8 V *vs* Li/Li^+ is due to the formation of the solid-electrolyte interface (SEI) during the first formation of the GIC. The majority of lithium ion intercalation into graphite occurs below 0.25 V. The charge consumed by the first charging (~400 mAh/g) is not fully recovered by the following discharge (~320 mAh/g). The capacity that can or cannot be recovered is called, respectively, the reversible Q_{rev} and irreversible capacity Q_{irr}, shown in Fig. 1.5. The efficiency (Q_{rev}/Q_{irr}) for the first charge is relatively low,[49] 0.7-0.9, but for subsequent cycles the charge discharge efficiencies usually exceed 99.8%. Several groups are exploring the use of new graphitic materials, *e.g.* carbon nanofiber[50] or graphene[51] to achieve superior electrode performance.

GICs are also currently used as precursors for materials called thermally exfoliated graphite, expanded graphite, or sometimes graphite nanoplatelets.[46,47] These are made through the rapid thermolysis of GICs, leading to the vaporization of the intercalates and the delamination of stacks of graphene sheets into thinner ones. Due to their remarkable properties (including extrudability, thermal stability, mechanical flexibility and high surface areas), TEGs find unique applications such as making high temperature seals,[52] and sorbents for oil spills.[53] Other proposed uses include *e.g.*, electrical conduction[45] and catalysis.[54]

In the above cases, binary GICs are utilized. Recently the application of ternary GICs has been proposed for hydrogen storage. Computational work on Li-benzene-GIC by Zhao *et al.*[55] and on Li-THF-GIC by Han and Jang[56] suggests that the presence of solvent co-intercalates enables the adsorption of multiple H_2 molecules per intercalate cation in Li-solvent-GICs. The ternary M-amine-GICs reported in this thesis may prove interesting as H_2 storage materials. An overview of different families of ternary M-amine-GICs is provided in Section 1.3.3.

1.3 STRUCTURAL FEATURES OF DONOR-TYPE GICs

1.3.1 Binary M-GICs and Ternary (M,M')-GICs

The general formula of a stage 1 binary M-GICs is MC_8 (M = K, d_i = 0.535 nm; M = Rb, d_i = 0.565 nm; and M = Cs, d_i = 0.594 nm) and MC_{12n} ($n \geq 2$) for higher-stage compounds.[14] The d_i values of the higher stage compounds are close to that of the stage 1 compounds. The in-plane structure, however, is different.[13] The in-

plane structure of MC_8 is shown in Fig. 1.6(a), that of MC_{12} (present in higher stage compounds) in Fig. 1.6(b), and that of LiC_6 in Fig. 1.6(c).

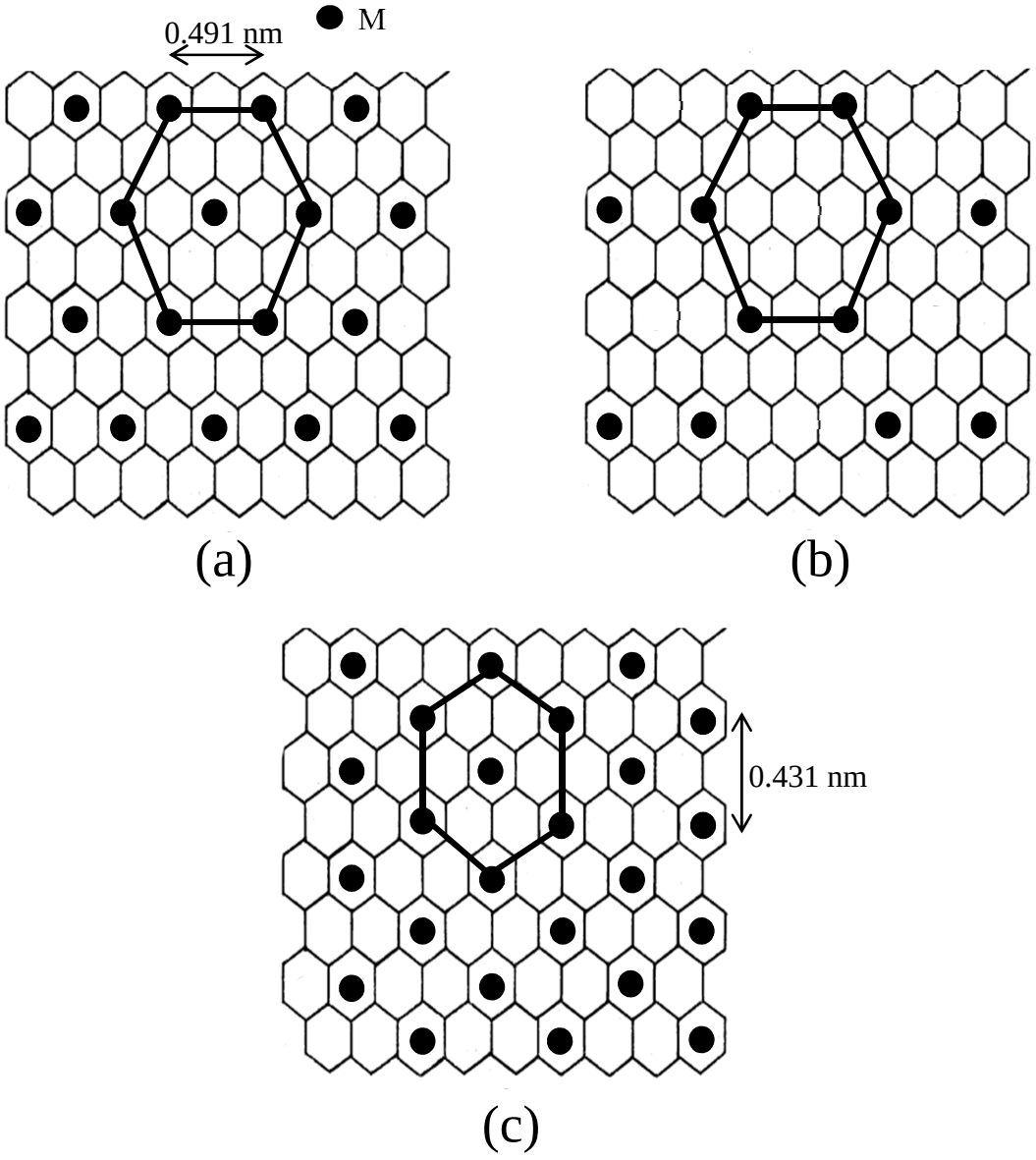

Figure 1.6 The in-plane structure of (a) MC_8, (b) MC_{12} (M = K, Rb and Cs)[13] and (c) LiC_6.[57]

The stage 1 to stage 5 Li-GICs (d_i = 0.371 nm) of the composition LiC_{6n} ($n \geq$ 1-5) have been reported,[58] though their syntheses require higher reaction temperatures than those with the larger alkali metals, and the products frequently contain impurities. The in-plane structure of Li-GICs has been studied extensively due to the importance of Li-batteries, and models for high stage compounds are available.[59,60] The dense packing of cations in LiC_6 results in a higher ΔH_L, and thus helps to stabilize the structure. For M = Na, K, Rb and Cs, cation-cation repulsions appear to be too great to adopt the MC_6 structure. Chung[14] applied a similar argument to rationalize the stability of LiC_6 *vs* MC_8.

Solid solutions of the M-GIC type can also be prepared, yielding ternary (M,M')-GICs where the two cations M and M' are statistically distributed within each layer. Examples include $Na_xM_{1-x}C_8$ (M = K, Rb, or Cs)[61] and $K_xRb_{1-x}C_8$.[62] Similarly, the formation of solid solutions with composition-dependent lattice dimensions, either linear or with an anomaly, are well known for 3-dimensional solid solutions.[63]

1.3.2 Ternary M-M'-GICs and M-Y-GICs

Some ternary M-M'-GICs show an ordered filling of galleries with different metals residing in separate layers; such gallery structures are known as *polylayers*. Several examples are known for the mixed-cation GICs prepared from Li alloys. These include the Li-M-GICs with the intercalate ordering comprising a 5-layer C-Li-M-Li-M-Li-C sequence (M = Ca, d_i = 0.776 nm;[64] M = Eu, d_i = 0.804 nm[65]) and 7-layer Li-M-Li-Li-Li-M-Li (M = Ca, d_i = 0.970 nm[64]).

A related example is the ternary M-Y-GIC, where M is the alkali metal and Y is an element less-electropositive than M, including H, Hg, Tl, Bi, O, P, S, Se, and Te.[66-68] The polylayer sequence C-M-Y-M-C is most often observed, although more complex cases are reported. Y is not limited to a single element, but can also indicate an ion pair such as NaX (X = OH, Cl, Br, I)[66] or even more complex combinations.[68] However, this family of GICs is difficult to prepare and the structures are not well characterized.

1.3.3 Ternary M-solvent-GICs

Reviews on ternary GICs containing metal cations and organic co-intercalates focusing on *e.g.*, their physics[69] or chemistry[70] are available. Sometimes these GICs are called ternary M-solvent-GICs, as they are usually prepared using a solution method with the organic solvent serving as the co-intercalate. The solvents include amines, ethers, alkane, alkene, aromatics, and others. For completion, quaternary compounds will be discussed as well in Section 1.3.3.7.

1.3.3.1 Amine Co-intercalates

Table 1.3 gives examples of ternary GICs containing amine co-intercalates. The M-NH_3-GIC (M = Li, Na, K, Rb, Cs) series investigated by Rüdorff *et al.*[71,72] appears to be the first report of ternary GICs containing a metal cation and solvent. An extension of the ammoniated GICs to M = Ca, Sr, Ba[73] and M = Be, Mg, Al, Sc, Y, and La[35] was subsequently reported (also in Table 1.3). A detailed neutron diffraction

study[74] for K-NH_3-GIC employing ND_3 (D = deuterium) and ^{15}N found that nitrogen atoms reside at the mid-plane of the interlayer region, with an intercalate tilt angle θ = 21.6º, whereas K^+ is situated not along the mid-plane, but closer to the graphene surfaces. Judging from the similar d_i values for other M-NH_3-GIC (~0.7 nm, Table 1.3), similar intercalate orientations can be assumed.

Table 1.3 Ternary GICs of metals and amine co-intercalates. All are stage 1 GICs unless a stage is indicated in parentheses.

GIC[a]	M	d_i/ nm	Ref.
$M(NH_3)_2C_{12}$	Li, Na, K, Rb and Cs	0.66	72
$M(NH_3)_{2\text{-}3}C_{28}$	Li, Na, K, Rb and Cs	0.66 (2)	72
$M(NH_3)_{2\text{-}3}C_{12}$	Ca, Sr and Ba	0.636-0.662	73
$M(NH_3)_{3\text{-}4}C_{27\text{-}30}$	Ca, Sr and Ba	0.644-0.660 (2)	73
$M(NH_3)_2C_{12\text{-}14}$	Be and Mg	0.623-0.636 (2)	73
$M(NH_3)_yC_z$	Al	0.550 [y = 2, z = 19] (3)	35
	Y	0.584 [y = 4.5, z = 28] (3)	
	La	0.583 [y = 4.0, z = 13] (3)	
$Sc(NH_3)_{4.5}C_{44}$	Sc	0.577 (4)	35
$Li(CH_3NH_2)_2C_{12}$	Li	0.666	72
$K(CH_3NH_2)_3C_{24}$	K	0.695	75
$Li(EN)C_{28}$	Li	0.850 (2)	73, 76
$K(TMEDA)_{0.7}C_{37}$	K	0.895	77
$K(NEt_3)_{0.43}C_{36}$	K	1.240	77

[a]EN = ethylenediamine, TMEDA = *N*,*N*,*N*',*N*'-tetramethylethylenediamine; NEt_3 = triethylamine

The use of other amine solvents yields their respective ternary GICs, the first of this type reported being $Li(CH_3NH_2)_2C_{12}$.[72] Additional examples are shown in

Table 1.3. The orientation of these organic co-intercalates can often be deduced by geometric consideration of the amine dimensions and the gallery expansion, Δd. The structure of K-CH_3NH_2-GIC[75] has perhaps been studied in greatest detail. Neutron diffraction of $K(CH_3NH_2)_3C_{24}$, $K(CD_3NH_2)_3C_{24}$, and $K(CD_3ND_2)_3C_{24}$ showed an approximately co-linear K^+, C and N at the gallery centers, indicating $\theta \sim 0^o$. Note that the K^+ in K-CH_3NH_2-GIC is at the gallery center, whereas it resides closer to the graphene sheet surfaces in K-NH_3-GIC.

The intercalation of amine guest species is common for many layered hosts.[1] Interestingly, despite the long history of GIC chemistry, the number of compounds containing amine co-intercalates remained fairly limited prior to this thesis work. The syntheses of such GICs will benefit our understanding of intercalation chemistry of graphite in relation to other host structures. We will report below a series of new ternary GIC containing alkali cations and nitrogen-containing organic bases. These include *n*-alkylamines (Chapter 2), branched alkylamines (Chapter 3), alkyldiamines (Chapters 4 and 5), and alkylpolyamines (Chapter 6). A detailed comparison of amine intercalation chemistry for graphite and other hosts will be provided in Section 1.4.

1.3.3.2 Etheric Co-intercalates

This class of GICs contains aliphatic ether co-intercalates, Table 1.4. In contrast to amine co-intercalates, an electron transfer agent such as anthracene, benzophenone, biphenyl, naphthalene, phenanthrene, *etc.*, appears to be required for these syntheses. This summary will focus on (i) compositional variations for a given guest; and (ii) the structural effect of the ethers on the GIC galleries.

Table 1.4 Ternary GICs of metals and ether co-intercalates. All are stage 1 GICs unless a stage is indicated in parentheses.

GIC[a]	d_i/ nm	Ref.
$M(DME)C_{28-31}$	0.732 (M = Li), 0.726 (M = Na), 0.728 (M = K)	81
$M(DME)_2C_{28}$	1.162 (M = Li), 1.177 (M = Na),	81
$K(DME)_3C_{31}$	1.194	81
Li-DEE-GIC	1.12	82, 83
$Li(THF)_yC_z$	1.253 [y = 1.4, z = 6], 1.244 [y = 2.3, z = 12],	84
	1.245 [y = 3.4, z = 18]	
$K(THF)C_{12n}$	0.716 (1), 0.721 (2), 0.717 (3)	85
$K(THF)_yC_z$	0.712 [y = 1, z = 36]	85
	0.89 [y = 2, z = 24]	86
M-MeTHF-GIC	0.738 (M = Rb), 0.722 (M = Cs)	87

[a]DME = 1,2-dimethoxyethane; DEE = 1,2-diethoxyethane; THF = tetrahydrofuran; MeTHF = 2-methyltetrahydrofuran. If reported, the compositions are listed in the table.

The ternary GICs with etheric co-intercalates have a wide range of compositions and interlayer structures. For example, a local tetrahedral arrangement around the metal M has been reported for $M(DME)_yC_z$ (see Table 1.4, M = Li, Na, y = 2, z = 28; M = K, y = 3, z = 31; d_i ~ 1.2 nm). Upon heating, a phase with the composition $M(DME)C_{28}$ (M = Li, Na, K; d_i ~ 0.73 nm) was obtained, with DME in a parallel orientation.

Beguin and Setton[85] reported the GICs containing potassium and THF with the composition $K(THF)C_{24}$ or $K(THF)C_{36}$, both with d_i ~ 0.7 nm. Although the ratio of intercalates to carbon is different, in both cases THF remains in a parallel orientation. A later report[86] indicated that GICs with different THF/K ratios are obtained depending on the synthetic conditions (d_i in nm in parenthesis): 1 (0.7), or 2 and 3 (0.9). From geometric considerations, the stage 2 and 3 GICs appear to have $\theta = 90^o$. Beguin *et al.*[84] also reported a stage 1 Li-THF-GICs with a wide range of co-intercalate/metal ratios, but all with d_i ~ 1.24 nm: $Li(THF)_{1.4}C_6$, $Li(THF)_{2.3}C_{12}$, and $Li(THF)_{3.4}C_{18}$. For these GICs, a T_d $Li(THF)_4^+$ intercalate complex was proposed.[84] Upon cooling[88] this T_d complex converts to a parallel bilayer structure, yielding a GIC with d_i = 1.063 nm. Lastly, $K(THF)_{2.5}C_{24}$ has a mean plane of THF molecules tilted with $\theta = 50\text{-}75^o$.[89]

Mizutani *et al.*[82,87,90,91] studied the effect of the etheric co-intercalate structures on the formation of M-ether-GICs (M = alkali metal). Ethers studied included THF, MeTHF, 2,5-dimethyltetrahydrofuran, tetrahydropyran, DME, DEE, 1,2-dibutoxyethane (DBE), 1-methoxypropane (MP), 1-methoxybutane (MB), and

diethylether. Important results include the findings by Tanaike and Inagaki[91] that, for compounds in the series Na-$[CH_2(OC_xH_{2x+1})]_2$-GIC (x = 1 for DME, x = 2 for DEE, and x = 4 for DBE), all have d_i ~ 1.2 nm. This indicates a parallel θ = 0 ° orientation regardless of the length of the alkyl chains. The tendency for an alkali metal to form ternary M-ether-GICs by this method increases from M = Li to Cs.[83]

1.3.3.3 Alkane Co-intercalates

In a series of publications, Pilliere *et al.* described the preparaion of M-alkane-GICs where the alkanes include methane,[92,93] *n*-butane,[92] *n*-pentane,[94] *n*-hexane,[95,96] cyclopentane[92] and cyclohexane,[92] Table 1.5. Due to the weak interaction of the alkane with the graphene sheets and alkali metal cations, the process was termed "physintercalation". Most of these GICs were synthesized by ternarization, allowing the gaseous alkane to interact with the preformed stage 2 M-GICs. For identified structures, the alkanes showed θ ~ 0º. In other cases[92] where the d_i values were not explicitly reported, as in Cs(*n*-butane)$_{0.56}C_{24}$ and Cs(cyclopentane)$_{0.58}C_{24,}$ the parallel orientation can be deduced from the data supplied.

Table 1.5 Ternary GICs of metals and alkane co-intercalates. All are stage 1 GICs unless a stage is indicated in parentheses.

GIC	d_i/ nm	Ref.
Cs(*n*-pentane)$_{0.60}$C$_{27}$	0.678	94
Cs(*n*-pentane)$_{0.97}$C$_{36}$	0.675 (2)	94
Cs(*n*-hexane)$_{0.9}$C$_{24}$	0.694	96
Cs(*n*-hexane)$_{0.59}$C$_{30}$	0.681 (2)	95

This family of GICs also presents interesting structural transformations. For example, starting from stage 2 CsC$_{24}$, ternarization leads to a stage 2 Cs(*n*-hexane)$_{0.59}$C$_{30}$ plus stage 1 binary CsC$_{8.}$[95] A similar reaction occurs for Cs-GIC with *n*-pentane.[94]

The ternarization of Cs-alkane-GICs can also lead to *disordered* heterostructures containing Cs^+ and Cs(alkane)$_y^+$ intercalates, where the I_c is the average of the stage 2 CsC$_{24}$ (I_c = 0.939 nm), or ordered ternary compounds (I_c = 1.013 nm for Cs-*n*-pentane-GIC; I_c = 0.986 nm for Cs-methane-GIC).[93, 94] Further discussion of heterostructures can be found in Section 1.3.3.7. For example, the disordered heterostructure stage 2 Cs-*n*-pentane-GIC (I_c = 0.972 nm ≈ (0.939 + 1.013)/2) was detected and explained as a phase boundary between the CsC$_{24}$ and the ordered ternary phase.[94] The linear dependence of I_c *vs* methane uptake was taken as evidence supporting the formation of the ordered Cs-methane-GIC.[93] Additionally, an order-disorder transition, as indicated by changes in the diffraction coherence lengths,

was also observed either by decreasing the temperature or by increasing the *n*-pentane pressure.[94]

1.3.3.4 Alkene Co-intercalates

The reaction of alkenes with donor-type binary GICs usually results in their polymerization, either (i) within GIC galleries, and/or (ii) on the graphite reactive edge surface. A third, relatively rare, case involves alkene intercalation without polymerization. Known examples include reacting stage 1 or 2 GICs with organic vapors including acrylonitrile,[97] ethylene,[98] 1-butene,[97] 1,3-butadiene,[97] isobutene,[97] isoprene,[99] styrene,[99] and tetracyanoethylene.[100]

In case (i), the starting binary GIC (*e.g.*, KC_8 or KC_{24}) expands along the c-direction once in contact with the organic vapor. In all cases, these products do not display sharp diffraction peaks, but are highly disordered, and are termed "composites". However, diffraction does indicate clearly that the binary GIC structures disappear after reaction with the alkene. The composite obtained from isoprene was elastic, like polyisoprene, whereas that from styrene was less elastic, like polystyrene.[99] The presence of polymer in the products was also supported through the detection of species with 5-20 carbon atoms by thermogravimetry-mass spectrometry (TG/MS) analysis of the pyrolyzed samples.[101]

In case (ii), diffraction patterns of the starting binary GICs are observed, and the samples do not show expansion. However, polymerization at the edge was deduced from the increased stability of the GIC in water and air as determined by

diffraction, electrical conductivity and Raman spectroscopy. This is the case for alkenes including acrylonitrile, 1-butene, and isobutene.[97]

An example of intercalation without polymerization is found in the reaction of KC_8 and KC_{24} with tetracyanoethylene [TCNE, $(NC)_2C=C(CN)_2$], which yields products of composition $K(TCNE)C_{24}$, $K(TCNE)_{0.25}C_8$, and $K(TCNE)_{0.4}C_8$.[100] In this report, the formation of ternary GICs was deduced from mass uptake, color, and the C ≡N (stretching) vibrational frequency. $K(TCNE)_{0.4}C_8$ was also obtained and reported with TCNE was in a parallel orientation.[100] However, this assignment does not agree well with the intercalate dimensions, and may require revision.

1.3.3.5 Aromatic Co-intercalates

There are numerous studies on ternary M-aromatic-GICs, and the orientation of aromatics in the GIC galleries.[70] Examples are shown in Table 1.6.

Table 1.6 Ternary GICs of metals and aromatic co-intercalates. All are stage 1 GICs unless a stage is indicated in parentheses.

GIC	d_i/ nm	Ref.
$K(benzene)_{0.8\text{-}1}C_{24}$	1.22-1.26 (2)	103
$K(benzene)_{2\text{-}3}C_{24}$	0.93	103, 104
$K(benzene)_3C_{24}$	1.22-1.26 (2)	103
$K(toluene)_1C_{24}$	1.23 (2)	105
$K(toluene)_3C_{24}$	0.91	70
K(*o*-xylene)$_2C_{24}$	1.06	105
$M(furan)_{0.76\text{-}0.90}C_8$	0.878 (M = K), 0.900 (M = Rb)	40

The ternary M-benzene-GICs show a wide variety of co-intercalate orientations observable by different d_i values. The first example is a full sandwich structure of the type benzene-M-benzene (d_i = 1.29 nm, K) with $\theta \sim 0^o$.[36,106] A second example is the half-sandwich structure (d_i = 0.755 nm for Li, 0.94 nm for K), $\theta \sim 0^o$, but with only one benzene intercalate per M^+.[36,106] The third case (d_i = 0.931 nm) also is ascribed to a full sandwich structure, with K^+ ions nestled between two benzene molecules, but with tilt angles $\theta_1 = 60^o$ or $\theta_2 = 120^o$.[107] Different orientations of *o*-xylene in K(*o*-xylene)$_2C_{24}$ were also proposed by Isaev *et al.*[105] Interesting only *o*-xylene forms GICs upon ternarization, whereas *m*-xylene, *p*-xylene, and mesitylene (1,3,5-trimethylbenzene) do not intercalate. Setton *et al.*[37] reported the ternarization of KC_8 or KC_{24} with a variety of aromatics. Merle *et al.*[36] reported the ternarization of

LiC_{12} with a solution of polystyrene in benzene to yield a product with d_i = 1.317 nm. They assigned this phase to a bilayer of polystyrene intercalate with polymers interconnected *via* –$CHCH_2CH$- linkages.

Schlögl and Boehm[40] reported the synthesis of stage 1 to 5 K-furan-GICs with d_i ~ 0.90 nm. The compositions found were $K(furan)_{0.76}C_8$ (stage 1), $K(furan)_{1.44}C_{24}$ (stage 2), and $K(furan)_{\sim 2}C_{12(x+1)}$ (x = 2-5). In these compounds, K^+ is off the gallery centers, and furan molecules are tilted at $\theta = 15^o$. Ternary Rb-furan-GICs with similar d_i values were also reported.[40]

1.3.3.6 Other Co-intercalates

Ternary M-DMSO-GICs (M = Li, K; DMSO = dimethysulfoxide) were prepared by the electrochemical reduction of graphite in DMSO solutions containing either $LiClO_4$ or KI.[108,109] The general composition found was $K(DMSO)_yC_{12x}$ ($x \geq 1$) with d_i = 1.15 nm[33] or 1.50 nm.[108] For these GICs, Besenhard *et al.*[33] have noted that Δd is close to the edge length of a hypothetical regular DMSO-octahedron, suggesting y = 6. Okuyama *et al.*,[108] however, reported y = 3.

Ginderow and Setton[110] synthesized the stage 1 GICs $Li(HMPT)C_{32}$ and $Na(HMPT)C_{27}$ (HMPT = hexamethylphosphoramide, $O=P(N(CH_3)_2)_3$) employing the direct reaction of graphite, alkali metal, and the amide. These appear to be the only amide-containing GICs reported. The observed d_i = 0.762 nm suggests that the P=O bond lies perpendicular to the graphene sheets.[110]

Beguin *et al.*[111] reported the structural study of the ternary K-N_2-GIC (d_i = 0.957 nm) and Rb-N_2-GIC (d_i = 0.946 nm). The differences in d_i were explained by $\theta \leq 15^o$ for M = K but $\theta \leq 10^o$ for M = Rb. These GICs, together with that of DME (Section 3.3.2) and 12DAP (Chapter 4), are examples of cation-directed orientation of co-intercalates in GICs. Setton *et al.*[112] synthesized the ternary K-K222-GIC [K222 = 4,7,13,16,21,24-hexaoxa-1,10-diazabicyclo[8.8.8]hexacosane, d_i = 1.550 nm, composition K(K222)C_{36}] through the ternarization of KC_{36} with a solution of K222 in THF. This is the only ternary GIC containing a macrocylic ligand reported to date.

1.3.3.7 Quaternary GICs of Organic Co-intercalates

The rich structural chemistry of ternary M-organic-GICs can be expanded further by employing two types of metal cations or organic co-intercalates, yielding quaternary GICs. There have been a limited number of donor-type quaternary GICs reported. Ginderow[113] prepared the compound $Li(THF)_{0.75}(BzN)_{0.25}C_{27}$ (d_i = 0.744 nm, BzN = benzonitrile) through the direct reaction of graphite, Li, and a mixture of organic co-intercalates. The quaternarization of $K(THF)_{1.2}C_{24}$,[114] or M-Hg-GICs (M = K, Rb)[115] by benzene, or of KC_8 by a mixture of benzene and THF was reported.[116] Unexpectedly, although no ternary GICs were formed by reacting KC_8 with either benzene or THF individually for up to 4 weeks, the reaction yielding the quaternary compound was complete in 3 h.[116] The orientation of co-intercalates were only indicated for K-(THF,benzene)-GIC,[114] with a tilt angle $\theta = 30^o$. Considering the reported d_i values, co-intercalates in other GICs appear to have $\theta = 0^o$.

There are two categories of quaternary GICs based on their d_i values. For the first type, d_i values fall between the ternary end members (if known). As an example (with d_i in nm in parenthesis), K-(THF,benzene)-GIC (0.900) has a d_i between $K(THF)_yC_{24}$ (0.800) and $K(benzene)_yC_{24}$ (0.924) (y = 2-3).[114] On the other hand, heterostructures are defined when different guest species intercalate between *different* graphene sheets in a regular manner. An example is $RbHg(benzene)_{0.65}C_8$,[115] where d_i = 2.02 nm is close to the sum of d_i values for Rb-benzene-GIC (0.93 nm) and Rb-Hg-GIC (1.065 nm). Therefore, a heterostructure with the sequence C-(Rb,benzene)-C-(Rb,Hg)-C was proposed. $KHg(benzene)_{0.65}C_8$ (d_i = 1.96 nm) can be obtained similarly.[115] The heterostructure arrangement can be contrasted with solid solutions that contain statistical distributions of two (or more) guests within each intercalate gallery (Section 1.3.1). It is also different from a polylayer structure, where the guests arrange themselves into multiple layers with a regular sequence, also within a single intercalate gallery (Section 1.3.2). We will present in Chapter 5 another example of a quaternary compound, Na-(EN,12DAP)-GIC (12DAP = 1,2-diaminopropane).

1.3.4 Binary R-GICs

In the binary compounds R-GICs (R = alkylammonium, imidazolium, *etc*), the organic cations provide the charge neutrality required by the reduced graphene sheets, Table 1.7. This is in contrast to the ternary GICs mentioned in Section 1.3.3.1, where neutral organic co-intercalates act as spacers between the metal cation. Besides those tabulated, there are reports on the intercalation of the following R^+ into graphite,

although no structural details were given: $(C_xH_{2x+1})_4N^+$ (x =1, 2, 4 and 8),[117] $(CH_3)_3(n\text{-}C_6H_{13})N^+$,[118,119] and a variety of ionic liquids based on imidazolium,[120,121] pyrrolidinium,[122] or piperidinium cation.[122, 123]

Table 1.7 Binary R-GICs. All are stage 1 GICs unless a stage is indicated in parentheses.

Cation	d_i/ nm
$(C_4H_9)_4N^+$ [6]	0.802
$(C_8H_{17})_4N^+$ [6]	0.775 (2)
$(CH_3)_4N^+$ (DMSO-solvated) [33]	1.59 (1-4)
1,2-dimethyl-3-*n*-butylimidazolium[124]	1.034
1-*n*-butyl-3-methylimidazolium[125]	1.038
1,2-dimethyl-3-*n*-propylimidazolium[125]	1.052

The electrochemical intercalation of graphite by R^+ has been widely studied, in part due to potential applications of graphitic electrodes in supercapacitors or in dual-intercalating molten electrolytes (DIME) cells.[120] The alkylammonium intercalates can be either unsolvated or solvated (by *e.g.*, DMSO[33]). The chemical synthesis of this GIC family has only been reported recently, and was accomplished by an ion exchange reaction with Na-EN-GIC.[6]

In electrochemical syntheses, the intercalation of R^+ was mainly deduced from a cathodic peak observed in cyclic voltammetry, supplemented by *e.g.*, *in situ* AFM to

observe a gallery expansion, or XPS to detect the surface composition of the electrodes after the reactions. PXRD patterns of the resulting GICs were rarely reported, or were inconclusive.[118, 122, 124-127]

1.4 COMPARISON: AMINES IN GRAPHITE AND IN OTHER HOST STRUCTURES

In this section the orientations of amines in GICs will be contrasted to those in other host structures. The alkyl chain(s) can be either parallel, perpendicular, or tilted to an angle θ relative to the sheets, Fig. 1.4. The intercalates can form mono-, bi-, or trilayers, or the overlap of those chains which is called *e.g.*, pseudotrilayer. Intercalation of more than three intercalate layers is not known.

As will be shown in Chapter 2, the amines in Na-nCx-GICs (nCx = *n*-alkylamine of x carbon atoms *e.g.*, $C_xH_{2x+1}NH_2$) show a parallel monolayer structure for x = 1-4, and a parallel bilayer structure for x = 6-14, with the x = 6 showing a transition between these structures.[79] This structure and the transition are reported in GICs for the first time. Similar amine orientations, however, are known in other hosts. For example, a parallel orientation for x = 1-4 for $FePS_3$,[126] and x = 2-8 in $BaC_6H_5PO_3$[127] has been reported. The perpendicular monolayer (x = 2-10 in $BaC_6H_5PO_3 \cdot 2H_2O$)[127] or the tilted bilayer (x = 4-12, $H_3Ti_3O_7$, 55º)[128] are known in the literature. Graphite oxide (GO),[10, 129] intercalates amines with both the monolayer and bilayer orientations (with tilt angles of 0º and 17-27º respectively) depending on the amine/GO ratio. Phases with different gallery expansions arising from amines of the same number of carbon

atoms are also known for other layered hosts. For example, the bilayer x = 12 and 16 in $HCaLaNb_2TiO_{10}$,[130] can show different tilt angles in the galleries depending on the drying conditions employed. Also of interest is birnessite, MnO_2, where amines with x = 10-18 unusually rearrange from an approximate monolayer perpendicular to bilayer perpendicular upon evacuation.[131]

The presence of α- (and to a lesser extent β–) branched intercalates has been reported to retard or inhibit intercalation reactions. In cases where intercalation does occur, however, the gallery expansions are similar regardless of the structure (linear *vs* branched) of intercalates, as in $(V_xNb_{1-x})OPO_4 \cdot yH_2O$.[132] In this case, Garcia-Ponce *et al.*[132] reported a bilayer with θ = 58º. Similar PXRD patterns were shown for the inclusion compound of *n*-butylamine and *iso*-butylamine with $[Cd(\mu_2\text{-}N,O\text{-}p\text{-}NH_2C_6H_4SO_3)_2(H_2O)_2]_n$,[133] implying a similar orientation although a structure model was not described. With Na-branched amine-GICs (Chapter 3), bilayers of branched amines intercalate with parallel orientations, in contrast to the monolayers obtained with the linear analogs.

As will be described in Chapter 5, for a variety of Li-diamine-GICs [diamine = EN, 12DAP, and *N*,*N*-dimethylethylenediamine (DMEDA)], more than one orientation can be obtained. In case of Li-EN-GIC, EN goes from perpendicular to parallel orientation during evacuation, with Li bonding to EN in a monodentate mode. Other host structures reported to show multiple orientations of EN include: TiOCl and VOCl (parallel monolayer),[134] $H_2Ti_4O_9$ (perpendicular monolayer and perpendicular bilayer),[135] $Ba(HO_3AsC_6H_5)_2 \cdot 2H_2O$ (tilted monolayer, 62º).[136] Intercalation of a series

of α,ω-diaminoalkane $H_2N(CH_2)_xNH_2$ with x = 2 (*i.e.*, EN)[137] or 4-10[138] into graphite oxide was reported, with the diamines in approximately parallel orientation.

The presence of functional groups at both ends of diamines together with the presence of a cation can involve binding of diamines to cations either as a monodentate (head-to-tail) or bidentate (chelation). This interaction is a topic of interest in computation chemistry of discrete molecules in the gas phase (*e.g.,* H^+, Li^+, and Na^+ with EN,[139] or H^+ and , Li^+ with $H_2N(CH_2)_xNH_2$ where x = 1-8[140]), but has not received as much attention in intercalation compounds. We will show in Chapter 5 that, for GICs, monodentate binding is observed for EN binding to Li^+, but the diamines 12DAP and DMEDA form chelates with Li^+ in a perpendicular orientation within the galleries. Interestingly, the perpendicular-to-parallel transition observed upon evacuation in Li-EN-GIC does not occur for Li-12DAP-GIC or Li-DMEDA-GIC.

Chapter 6 reports the synthesis and structure of M-polyamine-GICs, where a series of polyamines of increasing $–CH_2CH_2NH_x$ units was employed to investigate the structure-properties relationship. In addition to this work, publications on the intercalation of polyamines are relatively limited.[141,142] By reacting α-zirconium phosphate with diethylenetriamine (2E3N) at different reaction times, Nakayama *et al.*[141] obtained products with different gallery expansions, proposed as due to changing intercalate tilt angles. In the related Li-2E3N-GIC, the polyamine 2E3N shows a parallel orientation. Kijima *et al.*[143] reported the intercalation of tris(2-

aminoethyl)amine (3E4NS) into α- and γ-zirconium phosphates, with perpendicular orientation of 3E4NS. In Chapter 6, we propose a similar structure for K-3E4NS -GIC.

For completeness, the orientation of the perfluoroalkyl chain in the acceptor-type GICs should be described. For $C_xF_{2x+1}SO_3^-$ with x = 1 the fluoroalkyl chains have a parallel orientation. However, they form tilted bilayers when $x \geq 4$, with the SO_3^- head group orientated towards graphene sheets. Anions with more complex structure such as $C_{10}F_{21}SO_3^-$, $C_2F_5OC_2F_4SO_3^-$, and $C_2F_5(C_6F_{10})SO_3^-$ also form bilayer structures.[144]

1.5 CHAPTER SUMMARIES

In this thesis, the syntheses of ternary donor-type GICs containing alkali metal cations M^+ (M = Li, Na, K) and a variety of amines are reported. A limited number of quaternary GICs are also prepared. The goal is to explore new synthetic and structural chemistry in GICs through the use of amine co-intercalates. Several new intragallery structures, and structural transitions, are reported for the first time. Some of these were known in other layered hosts, but not with graphite.

Chapter 2 reports the synthesis of a homologous series of M-*n*-alkylamine-GICs with 3-14 carbon atoms. In all cases the alkyl chains lie parallel to the graphene sheets. However, the staging and number of amine layers depend on the specific amine employed. A novel bilayer-to-monolayer transition is also reported.

Chapter 3 compares the structures of the GICs containing *n*-alkylamine selected from Chapter 2 with those containing branched alkylamine. A notable

difference is observed for amines with 4 carbon atoms. While the linear amine forms parallel monolayers, the branched analogs instead form bilayers. This result contrasts with the general observation that more sterically-hindered intercalates tend to intercalate at lower concentrations. This structural difference is not observed, however, between linear and branched amines with 3 carbon atoms.

In addition to the structure-directing effect of amine intercalates, Chapter 4 describes a new series of GICs containing different cations and the same amine. The amine studied (12DAP) can orient with either a perpendicular, parallel, or tilted orientation. This is a rare example of cation-directed orientation in intercalation compounds. Interestingly, the gallery expansions increase as the cationic radii decrease.

Chapter 5 describes the synthesis and structure of M-diamine-GICs. A systematic study was performed employing amine analogs. These analogs include amines with different alkyl chain lengths, different positions of $–NH_2$ group, and the presence of $–CH_3$ substituents. Stage 1 and 2 Li-EN-GICs show the first example of a monolayer perpendicular-to-parallel transition. Another new example of cation-directed orientation of amines intercalates is also reported here by comparing Li-EN-GIC with Na-EN-GIC. Additionally, this works extends to the synthesis of the quaternary GICs containing mixed metal cations or mixed amines. Both solid solutions and the phase with fixed d_i are reported.

Chapter 6 explores ternary GICs containing polyamines (intercalates with more than two $–NH_2$ groups). Most of these new GICs have amines in parallel orientations,

though the GIC stage numbers depend on the size of the polyamine. In contrast, the star-shaped polyamine tris(2-aminoethyl)amine (3E4NS) has a perpendicular orientation. Similar structural modifications to the amines as in Chapter 5 are also examined in this chapter.

1.6 REFERENCES

1. Whittingham, M. S.; Jacobson, A. J. *Intercalation Chemistry;* Academic Press: New York, 1982.

2. Muller-Warmuth, W.; Schollhorn, R. *Progress in Intercalation Research;* Kluwer Academic Publishers: The Netherlands, 1994.

3. Ogawa, M.; Kuroda, K. *Bull. Chem. Soc. Jpn.* **1997,** *70*, 2593.

4. Osada, M.; Sasaki, T. *J. Mater. Chem.* **2009,** *19*, 2503.

5. Alberti, G.; Costantino, U. *J. Chromatogr.* **1974,** *102*, 5.

6. Sirisaksoontorn, W.; Adenuga, A. A.; Remcho, V. T.; Lerner, M. M. *J. Am. Chem. Soc.* **2011**, *133*, 12436.

7. Morlat-Therias, S.; Mousty, C.; Palvadeau, P.; Molinie, P.; Leone, P.; Rouxel, J.; Taviot-Gueho, C.; Ennaqui, A.; de Roy, A.; Besse, J. P. *J. Solid St. Chem.***1999,** *144*, 143.

8. Wang, B. S.; Dong, X. W.; Pan, Q. Y.; Cheng, Z. X.; Yang, Y. Z. *J. Solid St. Chem.* **2007,** *180*, 1125.

9. Komori, Y.; Sugahara, Y.; Kuroda, K. *Appl. Clay Sci.* **1999,** *15*, 241.

10. Matsuo, Y.; Miyabe, T.; Fukutsuka, T.; Sugie, Y. *Carbon* **2007,** *45,* 1005.

11. Zhang, Y. P.; Scott, K. J.; Clearfield, A. *Chem. Mater.* **1993,** *5,* 495.

12. Manthiram, A.; Kim, J. *Chem. Mater.* **1998,** *10,* 2895.

13. Rüdorff, W. *Adv. Inorg. Chem. Radiochem.* **1959,** *1,* 223.

14. Chung, D. D. L. *J. Mater. Sci.* **2002,** *37,* 1475.

15. Weller, T. E.; Ellerby, M.; Saxena, S. S.; Smith, R. P.; Skipper, N. T. *Nature Physics* **2005,** *1,* 39.

16. Elmakrini, M.; Guerard, D.; Lagrange, P.; Herold, A. *Physica B & C* **1980,** *99,* 481.

17. Safran, S. A. *Solid St. Phys.* **1987,** *40,* 183.

18. Noel, M.; Santhanam, R. *J. Power Sources* **1998,** *72,* 53.

19. Thomas, J. M.; Millward, G. R.; Schlogl, R. F.; Boehm, H. P. *Mater. Res. Bull.* **1980,** *15,* 671.

20. Solin, S. A. *Ann. Rev. Mater. Sci.* **1997,** *27,* 89.

21. Kirczenow, G., Staging and Kinetics. In *Graphite Intercalation Compounds I. Structure and Dynamics,* 1 ed.; Zabel, H.; Solin, S. A., Eds. Springer-Verlag: Germany, 1990; Vol. 14, pp 59-100.

22. Haynes, W. M., ed., *CRC Handbook of Chemistry and Physics,* 91st Edition (Internet Version 2011), CRC Press/Taylor and Francis, Boca Raton, FL, pp. 12-205 to 12-206. ΔH_{fusion} were listed in J/g and converted to kJ/mol, giving the following numbers: Li (3.0), Na (2.6), K (2.3), Rb (2.2 and Cs (2.1).

23. http://en.wikipedia.org/wiki/Enthalpy_of_vaporization accessed 09/09/2011 The following values of ΔH_{vap} were taken (in kJ/mol): Li (146), Na (97), K (80), Rb (72) and Cs (68).

24. Atkins, P.; Overton, T.; Rourke, J.; Weller, M.; Armstrong, F. *Shrivers & Atkins Inorganic Chemistry*. 4th ed.; Oxford University Press: 2006, pp. 771-772.

25. Setton, R. *Syn. Met.* **1989,** *34*, 279.

26. Boersma, M. A. M. *Catal. Rev. Sci. Eng.* **1974,** *10*, 243.

27. Charlier, A.; Setton, R.; Charlier, M. F. *Phys. Rev. B* **1997,** *55*, 15537.

28. Billaud, D.; Mareche, J. F.; McRae, E.; Herold, A. *Syn. Met.* **1980,** *2*, 37.

29. Ottmers, D. M.; Rase, H. F. *Carbon* **1966,** *4*, 125.

30. Jones, J. E.; Cheshire, M. C.; Casadonte, D. J.; Phifer, C. C. *Org. Lett.* **2004,** *6*, 1915.

31. Hick, S. M.; Griebel, C.; Blair, R. G. *Inorg. Chem.* **2009,** *48*, 2333.

32. Klein, H. F.; Gross, J.; Besenhard, J. O. *Angew. Chem. Int. Ed. Engl.* **1980,** *19*, 491-492.

33. Besenhard, J. O.; Mohwald, H.; Nickl, J. J. *Carbon* **1980,** *18*, 399.

34. Liu, D. R.; Yang, Z. H.; Li, W. X.; Qiu, S. L.; Luo, Y. T. *Electrochim. Acta* **2010,** *55*, 1013.

35. Stumpp, E.; Alheid, H.; Schwarz, M.; Janssen, J. J.; MullerWarmuth, W. *J. Phys. Chem. Solids* **1996,** *57*, 925.

36. Merle, G.; Rashkov, I.; Mai, C.; Gole, J. *Mater. Sci. Eng.* **1977,** *31*, 39.

37. Jegoudez, J.; Mazieres, C.; Setton, R. *Syn. Met.* **1983,** *7*, 85.

38. Jegoudez, J.; Mazieres, C.; Setton, R. *Carbon* **1986,** *24*, 747.

39. Bergbreiter, D. E.; Killough, J. M. *J. Am. Chem. Soc.* **1978,** *100*, 2126.

40. Schlogl, R.; Boehm, H. P. *Carbon* **1984,** *22*, 351.

41. Schlogl, R.; Boehm, H. P. *Carbon* **1984,** *22*, 341.

42. Isaev, Y. V.; Lenenko, N. D.; Gumileva, L. V.; Buyanovskaya, A. G.; Novikov, Y. N.; Stumpp, E. *Carbon* **1997,** *35*, 563.

43. Rida, H.; Cahen, S.; Herold, C.; Lagrange, P. *Carbon* **2010,** *48*, 3190.

44. Enoki, T.; Suzuki, M.; Endo, M. *Graphite Intercalation Compounds and Applications*. 1st ed.; Oxford University Press: New York, 2003.

45. Inagaki, M. *J. Mater. Res.* **1989,** *4*, 1560.

46. Inagaki, M.; Kang, F.; Toyoda, M. *Chem. Phys. Carbon* **2004,** *29*, 1.

47. Jang, B. Z.; Zhamu, A. *J. Mater. Sci.* **2008,** *43*, 5092.

48. Ogumi, Z.; Inaba, M. *Bull. Chem. Soc. Jpn.* **1998,** *71*, 521.

49. Shu, Z. X.; McMillan, R. S.; Murray, J. J. *J. Electrochem. Soc.* **1993,** *140*, 922.

50. Liang, M. H.; Zhi, L. J. *J. Mater.Chem.* **2009,** *19*, 5871.

51. Yin, S. Y.; Zhang, Y. Y.; Kong, J. H.; Zou, C. J.; Li, C. M.; Lu, X. H.; Ma, J.; Boey, F. Y. C.; Chen, X. D. *ACS Nano* **2011,** *5*, 3831.

52. Chung, D. D. L. *J. Mater. Eng. Perform.* **2000,** *9*, 161.

53. Toyoda, M.; Inagaki, M. *Carbon* **2000,** *38*, 199.

54. Setton, R. *Syn. Met.* **1988,** *23* (1-4), 467

55. Zhao, Y. F.; Kim, Y. H.; Simpson, L. J.; Dillon, A. C.; Wei, S. H.; Heben, M. J. *Phys. Rev. B* **2008,** *78*, 144102.

56. Han, S. S.; Jang, S. S. *Chem. Commun.* **2009,** 5427.

57. Yazami, R.; Guerard, D. *J. Power Sources* **1993,** *43*, 39.

58. Billaud, D.; McRae, E.; Mareche, J. F.; Herold, A. *Syn. Met.* **1981,** *3*, 21.

59. Billaud, D.; Henry, F. X.; Lelaurain, M.; Willmann, P. *J. Phys. Chem. Solids* **1996,** *57*, 775.

60. Billaud, D.; Henry, F. X. *Solid St. Commun.* **2002,** *124*, 299.

61. Billaud, D.; Herold, A. *Bull. Soc. Chim.* **1974,** *12*, 2715.

62. Solin, S. A.; Chow, P.; Zabel, H. *Phys. Rev. Lett.* **1984,** *53*, 1927.

63. Cullity, B. D.; Stock, S. R. *Elements of X-ray Diffraction*. 3rd ed.; Prentice Hall: USA, 2001.

64. Pruvost, S.; Herold, C.; Herold, A.; Lagrange, P. *Eur. J. Inorg. Chem.* **2004,** 1661.

65. Herold, C.; Pruvost, S.; Herold, A.; Lagrange, P. *Carbon* **2004,** *42*, 2122.

66. Herold, C.; Herold, A.; Lagrange, P. *Solid St. Sci.* **2004,** *6*, 125.

67. Edman, L.; Herold, A.; Jacobsson, P.; Lelaurain, M.; McRae, E.; Sundqvist, B. *J. Phys. Chem. Solids* **1999,** *60*, 475.

68. Herold, A.; Mareche, J. F.; Lelaurain, M. *Carbon* **2000,** *38*, 1955.

69. Solin, S. A.; Zabel, H. *Adv. Phys.* **1988,** *37*, 87.

70. Setton, R., Ternary Systems. In *Graphite intercalation compounds I. Structure and dynamics*, Zabel, H.; Solin, S. A., Eds. Springer-Verlag: Germany, 1990.

71. Rüdorff, W.; Schulze, E. *Angew. Chem.* **1954,** *66*, 305.

72. Rüdorff, W.; Schulze, E.; Rubisch, O. *Z. Anorg. Allg. Chem.* **1955,** *282*, 232.

73. Rüdorff, W. *Adv. Inorg. Chem. Radiochem.* **1959,** *1*, 223.

74. Walters, J. K.; Skipper, N. T.; Soper, A. K. *Chem. Phys. Lett.* **1999,** *300*, 444.

75. Skipper, N. T.; Walters, J. K.; Lobban, C.; McKewn, J.; Mukerji, R.; Martin, G. J.; de Podesta, M.; Hannon, A. C. *J. Phys. Chem. B* **2000,** *104*, 10969.

76. Rüdorff, W. *Chimia* **1965,** *19*, 489.

77. Merle, G.; Letoffe, J. M.; Rashkov, I. B.; Claudy, P. *J. Therm. Anal.* **1978,** *13*, 293.

78. Maluangnont, T.; Sirisaksoontorn, W.; Lerner, M. M. *Carbon* **2011,** *49*, 1040.

79. Maluangnont, T.; Bui, G. T.; Huntington, B. A.; Lerner, M. M. *Chem. Mater.* **2011,** *23*, 1091.

80. Maluangnont, M.; Lerner, M. M. *submitted to Inorg. Chem.*

81. Duc, C. M.; Gole, J.; Mai, C.; Riviere, R. *J. Chim. Phys.* **1972,** *69*, 991.

82. Abe, T.; Mizutani, Y.; Tabuchi, T.; Ikeda, K.; Asano, M.; Harada, T.; Inaba, M.; Ogumi, Z. *J. Power Sources* **1997,** *68*, 216.

83. Mizutani, Y.; Abe, T.; Inaba, M.; Ogumi, Z. *Syn. Met.* **2002,** *125*, 153.

84. Beguin, F.; Estradeszwarckopf, H.; Conard, J.; Lauginie, P.; Marceau, P.; Guerard, D.; Facchini, L. *Syn. Met.* **1983,** *7*, 77.

85. Beguin, F.; Setton, R. *Carbon* **1975,** *13*, 293.

86. Facchini, L.; Quinton, M. F.; Legrand, A. P.; Beguin, F.; Setton, R. *Physica B & C* **1980,** *99*, 525-530.

87. Mizutani, Y.; Ihara, E.; Abe, T.; Asano, M.; Harada, T.; Ogumi, Z.; Inaba, M. *J. Phys. Chem. Solids* **1996,** *57*, 799.

88. Goldmann, M.; Beguin, F. *Phase Transitions* **1991,** *30*, 91.

89. Schmidt, C.; Rosen, M. E.; Caplan, D. F.; Pines, A.; Quinton, M. F. *J. Phys. Chem.* **1995,** *99*, 10565-10572.

90. Mizutani, Y.; Abe, T.; Ikeda, K.; Ihara, E.; Asano, M.; Harada, T.; Inaba, M.; Ogumi, Z. *Carbon* **1997,** *35*, 61.

91. Tanaike, O.; Inagaki, M. *Syn. Met* **1998,** *96*, 109.

92. Beguin, F.; Pilliere, H. *Carbon* **1998,** *36*, 1759.

93. Pilliere, H.; Soubeyroux, J. L.; Beguin, F. *Phase Transitions* **1993,** *46*, 27.

94. Pilliere, H.; Goldmann, M.; Beguin, F. *J. Mater. Res.* **1993,** *8*, 2288.

95. Goldmann, M.; Pilliere, H.; Beguin, F. *Syn. Met.* **1990,** *34*, 59.

96. Pilliere, H.; Beguin, F. *Carbon* **1993,** *31*, 654.

97. Shioyama, H.; Tatsumi, K.; Iwashita, N.; Fujita, K.; Sawada, Y. *Syn. Met.* **1998,** *96*, 229.

98. Takahashi, Y.; Akuzawa, N.; Beguin, F. *Syn. Met.* **1995,** *73*, 45.

99. Shioyama, H. *Carbon* **1997,** *35*, 1664.

100. Prasad, B. L. V.; Radhakrishnan, T. P. *Syn. Met.* **1996,** *81*, 9.

101. Matsumoto, R.; Arii, T.; Oishi, Y.; Takahashi, Y. *Thermochim. Acta* **2005,** *431*, 53.

102. Matsumoto, R.; Takahashi, Y.; Akuzawa, N. *Mol. Cryst. Liq. Crys.* **2000,** *340*, 43.

103. Merle, G.; Beguin, F. *Carbon* **1980,** *18*, 371.

104. Isaev, Y. V.; Novikov, Y. N.; Volpin, M. E. *Syn. Met.* **1982,** *5*, 23.

105. Isaev, Y. V.; Novikov, Y. N.; Volpin, M. E.; Rashkov, I.; Panayotov, I. *Syn. Met.* **1983,** *6*, 9.

106. Merle, G.; Mai, C.; Gole, J.; Rashkov, I. *Carbon* **1977,** *15*, 243.

107. Beguin, F.; Setton, R.; Facchini, L.; Legrand, A. P.; Merle, G.; Mai, C. *Syn. Met.* **1980,** *2*, 161.

108. Okuyama, N.; Takahashi, T.; Kanayama, S.; Yasunaga, H. *Physica B & C* **1981,** *105*, 298.

109. Marcus, B.; Touzain, P. *J. Solid St. Chem.* **1988,** *77*, 223.

110. Ginderow, D.; Setton, R. *Carbon* **1968,** *6*, 81.

111. Moreh, R.; Pinto, H.; Finkelstein, Y.; Beguin, F. *J. Phys. Chem. Solids* **1996,** *57*, 909.

112. Setton, R.; Beguin, F.; Facchini, L.; Quinton, M. F.; Legrand, A. P.; Ruisinger, B.; Boehm, H. P. *J. Chem. Soc. Chem. Commun.***1983,** 36.

113. Ginderow, D. *Ann. Chim.* **1971,** *6*, 5-16.

114. Hamwi, A.; Touzain, P.; Bonnetain, L. *Comptes Rendus De L Academie Des Sciences Serie Ii* **1984,** *299*, 1385.

115. Isaev, Y. V.; Guerard, D.; Blumenfeld, A. L.; Lenenko, N. D.; Novikov, Y. N. *Carbon* **1996,** *34*, 97.

116. Beguin, F.; Setton, R. *J. Chem. Soc. Chem. Commun.* **1976,** 611.

117. Besenhar.Jo; Fritz, H. P. *J. Electroanal. Chem.* **1974,** *53*, 329.

118. Zheng, H. H.; Jiang, K.; Abe, T.; Ogumi, Z. *Carbon* **2006,** *44*, 203.

119. Katayama, Y.; Yukumoto, M.; Miura, T. *Electrochem. Solid St. Lett.* **2003,** *6*, A96.

120. Carlin, R. T.; Delong, H. C.; Fuller, J.; Trulove, P. C. *J. Electrochem. Soc.* **1994,** *141*, L73.

121. Carlin, R. T.; Fuller, J.; Kuhn, W. K.; Lysaght, M. J.; Trulove, P. C. *J. Appl. Electrochem.* **1996,** *26*, 1147.

122. Baranchugov, V.; Markevich, E.; Salitra, G.; Aurbach, D.; Semrau, G.; Schmidt, M. A. *J. Electrochem. Soc.* **2008,** *155*, A217.

123. Markevich, E.; Baranchugov, V.; Salitra, G.; Aurbach, D.; Schmidt, M. A. *J. Electrochem. Soc.* **2008,** *155*, A132.

124. Sutto, T. E.; Trulove, P. C.; De Long, H. C. *Electrochem. Solid St. Lett.* **2003,** *6*, A50.

125. Sutto, T. E.; Duncan, T. T.; Wong, T. C. *Electrochim. Acta* **2009,** *54*, 5648.

126. Joy, P. A.; Vasudevan, S. *Chem. Mater.* **1993,** *5*, 1182.

127. Benes, L.; Melanova, K.; Svoboda, J.; Zima, V. *J. Phys. Chem. Solids* **2010,** *71*, 530.

128. Papp, S.; Dekany, I. *Colloid Polym. Sci.* **2005,** *283*, 1116.

129. Bourlinos, A. B.; Gournis, D.; Petridis, D.; Szabo, T.; Szeri, A.; Dekany, I. *Langmuir* **2003,** *19*, 6050.

130. Gopalakrishnan, J.; Uma, S.; Bhat, V. *Chem. Mater.* **1993,** *5*, 132.

131. Wortham, E.; Bonnet, B.; Jones, D. J.; Roziere, J.; Burns, G. R. *J. Mater. Chem.* **2004,** *14*, 121.

132. Garcia-Ponce, L.; Moreno-Real, L.; Jimenez-Lopez, A. *Can. J. Chem.* **1990,** *68*, 592.

133. Zhou, J. S.; Cai, J. W.; Wang, L.; Ng, S. W. *Dalton Trans.* **2004,** 1493

134. Kargina, I.; Richeson, D. *Chem. Mater.* **1996,** *8*, 480.

135. Sugimoto, W.; Ohuchi, K.; Murakami, Y.; Takasu, Y. *Bull. Chem. Soc.Jpn.* **2005,** *78*, 633.

136. Lazarin, A. M.; Morales, G. C.; Sernaglia, R. L.; Andreotti, E. I. S.; Airoldi, C. *J. Phys. Chem. Solids* **2011,** *72*, 637.

137. Jimenez, P. V.; Martinez, M. I. A.; Rodriguez, A. M. *Carbon* **1985,** *23*, 473.

138. Herrera-Alonso, M.; Abdala, A. A.; McAllister, M. J.; Aksay, I. A.; Prud'homme, R. K. *Langmuir* **2007,** *23*, 10644.

139. Ikuta, S. *Chem. Phys.* **1986,** *108*, 441.

140. Kumar, M. K.; Rao, J. S.; Prabhakar, S.; Vairamani, M.; Sastry, G. N. *Chem. Commun.* **2005,** 1420.

141. Nakayama, H.; Hayashi, A.; Eguchi, T.; Nakamura, N.; Tsuhako, M. *J. Mater. Chem.* **2002,** *12*, 3093.

142. Danjo, M.; Hayashi, A.; Nakayama, H.; Kimira, Y.; Shimizu, T.; Mizuguchi, Y.; Yagita, Y.; Tsuhako, M.; Nariai, H.; Motooka, I. *Bull. Chem. Soc. Jpn.* **1999,** *72*, 2079.

143. Kijima, T.; Ohe, K.; Sasaki, F.; Yada, M.; Machida, M. *Bull. Chem. Soc. Jpn.* **1998,** *71*, 141.

144. Yan, W.; Lerner, M. M. *Carbon* **2004,** *42*, 2981.

CHAPTER 2

PREPARATION OF A HOMOLOGOUS SERIES OF GRAPHITE ALKYLAMINE INTERCALATION COMPOUNDS INCLUDING AN UNUSUAL PARALLEL BILAYER INTERCALATE ARRANGEMENT

Tosapol Maluangnont, Giao T. Bui, Benjamin A. Huntington, and Michael M. Lerner

Department of Chemistry

Oregon State University

Corvallis, OR 97331-4003, USA

Chem. Mater. **2011,** *23,* 1091-1095.

2.1 ABSTRACT

New ternary graphite intercalation compounds (GICs) containing Na^+ and linear alkylamines (Na-nC*x*-GIC) are reported. The following new GICs with indicated stages and intercalate arrangements are obtained: stage 1, monolayer (nC3, nC4); stage 1, bilayer (nC6, nC8); and stage 2 bilayer (nC12, nC14). Two features new to donor-type GICs found are (i) an intercalate bilayer arrangement with guest alkyl chains parallel to encasing graphene layers, and (ii) the transition from an intercalate bilayer to monolayer arrangement upon evacuation for nC6. Although there are many reports on the intercalation of short, medium, and long-chain alkylamines in layered hosts, this is the first example of a homologous compound series for GICs. The products obtained are characterized using powder X-ray diffraction, thermogravimetric analysis, and differential scanning calorimetry.

2.2 INTRODUCTION

Intercalation chemistry results in changes in both layered host and guest and allows the study of molecular confinement in two dimensions.[1] The properties and subsequent chemistry of intercalation compounds can be more clearly developed and controlled by understanding the intercalate composition and arrangement within the expanded galleries. Alkylamines and alkylammonium ions are among the most commonly employed intercalate guests. Details of complex transitions in intercalate arrangements have been obtained for some layered hosts. For example, the evolution of a hexadecylamine ($C_{16}H_{33}NH_2$) intercalate arrangement from parallel monolayer, to parallel bilayer, to perpendicular (or tilted) monolayer, to perpendicular (or tilted) bilayer, was observed with increasing intercalate content in bentonite.[2,3] Similar structural changes, with an added bilayer-to-trilayer transition, were reported for a R_4N^+-exchanged smectite clay.[4] These organoclays have several potential applications, including the adsorption of toxins, use as photo and electro-functional materials, and as precursors in the formation of clay-polymer nanocomposites with enhanced mechanical properties.[5]

Although the intercalation and exfoliation of layered materials using alkylamine intercalates (or the associated ammonium cations) is well known in the literature,[1,6] similar behavior has never been reported for graphite. In the donor-type graphite intercalation compounds (GICs), graphene sheets are reduced and cations intercalate between the carbon layers. Ternary GICs, in which the solvent molecules coordinate to the M cations and are co-intercalates, can be synthesized using either

direct or indirect methods. In the direct method, an alkali metal is dissolved in a polar, highly ionizing liquid such as liquid ammonia,[7-9] methylamine,[7] or ethylenediamine.[7] The electrons/radicals/anions thus generated reduce the graphene sheets, and the solvated cations intercalate to satisfy the charge neutralization. In the indirect method, a pre-formed binary GIC, *e.g.*, KC_{24} or KC_{36}, is further reacted with a co-intercalate in the liquid or gas phase, examples include the co-intercalation of *N,N,N',N'*-tetramethylethylenediamine (TMEDA),[10] triethylamine,[10] and the cryptand "K222".[11] In some cases, such as with methylamine, GIC's have been synthesized by both direct and indirect methods.[7,12] We recently reported the synthesis of the ternary GICs containing the alkali metal M (M = Li, Na, K) and 1,2-diaminopropane,[13] which provides an unusual example of cation-directed orientation of organic co-intercalates. However, no extended homologous series for alkylamines has been reported to date. This contrasts the extensive literature on amine intercalation for other layered hosts such as transition metal dichalcogenides and clays where homologous series of amines have been prepared and their structure-property relations evaluated.[1]

We report herein the synthesis of several new GICs containing Na^+ cations and a series of linear alkylamines with 3, 4, 6, 8, 12, 14 carbon atoms. These compounds exhibit two features new to donor-type GICs, an intercalate bilayer arrangement with guest alkyl chains parallel to encasing graphene layers, and a transition from an intercalate bilayer to monolayer arrangement. Both as prepared ("wet") and dried products were studied, as the intercalate arrangement can depend strongly on drying conditions. The GIC products are characterized using powder X-ray diffraction

(PXRD), thermogravimetric analysis (TGA), and differential scanning calorimetry (DSC).

2.3 EXPERIMENTAL

All synthesis and handling of the air-sensitive reagents and the resulting GICs were done under an inert atmosphere using a dry-box or septum-syringe techniques. In a typical synthesis, 0.25 g of graphite powder (SP-1, Union Carbide, average particle dia. 100 μm) was mixed with 0.06 g of Na metal (99.95%, Alfa Aesar) (mol C/mol Na = 8) and the amine (4 mL for *n*-propyl to *n*-octylamine, 0.75 g for *n*-dodecylamine and *n*-tetradecylamine). Anthracene (0.05g) was added as an electron transfer catalyst for the C12 and C14 amines. The reaction mixtures were continuously stirred for 1-7 days at the following temperatures: *n*-propylamine (nC3) and *n*-butylamine (nC4) 20 °C; *n*-hexylamine (nC6) 90 ºC; *n*-octylamine (nC8) 140 ºC, and *n*-dodecylamine (nC12) and *n*-tetradecylamine (nC14) 90 °C. For the nC12 synthesis, an additional experiment was performed using only 0.25 g of the amine. For some reactions, Li metal was used to prepare Li-nCx-GICs by the same methods. The liquid amines were removed by centrifugation immediately (nC3-nC8), or by washing with dry toluene followed by centrifugation (nC12, nC14). GIC products denoted “wet” were characterized after centrifugation without further processing, those denoted “dried” were placed under vacuum (<100 μm) at 20 ºC (nC3-nC4) or 50 ºC (nC6-nC14) for 6 h.

PXRD data were collected on a Rigaku MiniFlex II, using Ni-filtered Cu Kα radiation, with 0.02° 2θ steps from 3° to 60°. Sample holders were sealed with a

plastic tape window to prevent decomposition in air during the PXRD measurement. The *(00l)* reflections were indexed according to the relation $I_c = d_i + (n\text{-}1)(0.335\ \text{nm})$, where I_c is the identity period obtained directly by diffraction data, d_i is the gallery height, n is the GIC stage number, and 0.335 nm is the distance between two adjacent graphene sheets. The samples were digested in conc. HCl and the sodium content in the liquid was analyzed with ICP-AES using the Jobin Yvon Emission JY2000. TGA was performed using a Shimadzu TGA-50 under flowing Ar gas (20 mL/min) from RT to 800ºC at 5 ºC/min. DSC measurements were performed on a Shimadzu DSC-50, with samples (~5 mg) hermetically sealed in aluminum pans. The DSC samples were heated from ambient to 150 ºC at 5 ºC/min. Only the heating curves were recorded.

2.4 RESULTS AND DISCUSSION

2.4.1 Short to Medium Chain Amines

Fig. 2.1(a) shows the PXRD pattern of the blue stage 1 GIC product, Na-nC3-GIC (d_i = 0.701 nm), obtained with *n*-propylamine after RT drying under vacuum. The wet product shows the same PXRD pattern. This product has well-ordered galleries as evidenced by the presence of up higher order reflections. Neglecting the contribution of Na^+, which has a smaller diameter (≈0.2 nm) than the minimum amine dimension along any axis, the intercalate monolayer height within the graphene gallery is therefore 0.701 – 0.335 = 0.366 nm. The relationship between the orientation of alkyl chains and interactions with the Na^+ cation will be discussed later. This monolayer

height is similar to that reported previously for Li-methylamine-GIC (0.36 nm),[7] but smaller than those reported for Li-ethylenediamine-GIC (0.51 nm)[7] and K-TMEDA-GIC (0.56 nm).[10] The larger dimension for the TMEDA gallery is readily understood due to the increased steric requirement for the methyl group substituents on the amine.

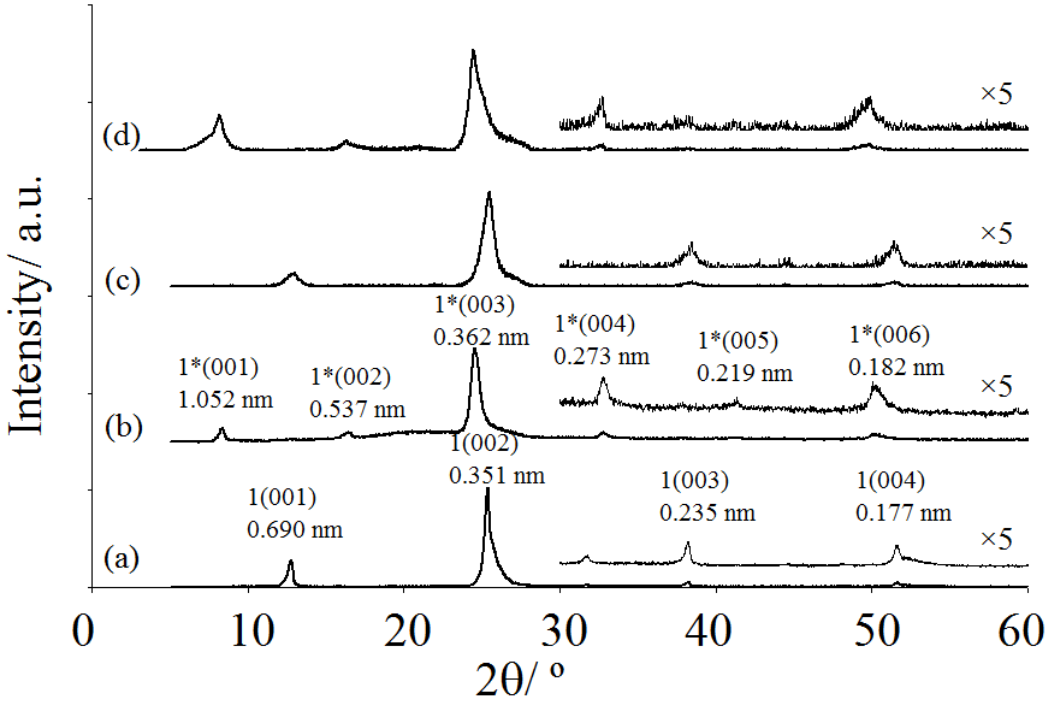

Figure 2.1 PXRD pattern of (a) Na-nC3-GIC, (b) Na-nC6-GIC (wet), (c) Na-nC6-GIC (dried), and (d) Na-nC8-GIC (dried). The number 1 and 1* indicate the stage 1 monolayer and bilayer respectively, with the assigned (00*l*) indices and the observed d values indicated. The PXRD patterns of Na-nC3-GIC and Na-nC8-GIC are the same for the wet and dry samples.

Na-nC4-GIC (d_i = 0.704 nm), Li-nC3-GIC (d_i = 0.700 nm), and Li-nC4-GIC (d_i = 0.697 nm) can all be prepared similarly, and the products have monolayer heights comparable to Na-nC3-GIC. From steric considerations, and the equivalent gallery heights for M-nC3-GIC and M-nC4-GICs (M = Li, Na), it is clear that these short chain alkylamine intercalates must form monolayers with long molecular axes lying parallel to the graphene sheets, as shown in Fig. 2.2(a). The synthesis of Cs-C*x*-GIC (for C4, C5, and C6 *alkane*) have also been previously reported through the reaction of CsC_{24} and the alkane vapor.[14] Although the d_i values of those GICs were not directly stated by the authors, the data included in the publication indicates that these GICs contained parallel alkane monolayers.

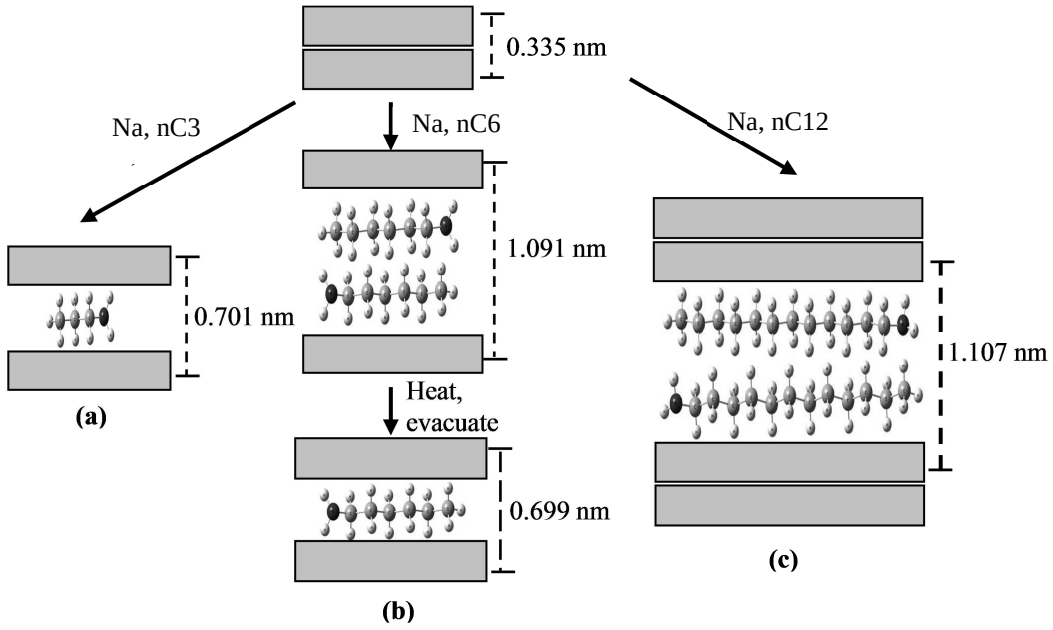

Figure 2.2 (a) The monolayer structure in Na-nC3-GIC, (b) the bilayer structure in wet Na-nC6-GIC and its transformation to the monolayer structure by drying, and (c) the bilayer structure in stage 2 Na-nC12-GIC. The gallery dimensions, d_i, are shown in each case. The locations of the Na^+ intercalates are not shown.

The wet Na-nC6-GIC product is a blue stage 1 GIC with d_i = 1.091 nm, corresponding to an intercalate dimension of 0.756 nm. As shown in Fig. 2.1(b), the presence of reflections up to *(006)* indicates well-ordered domains along the stacking direction. These galleries are assigned a bilayer arrangement, since the intercalate dimension is nearly twice that of the monolayer arrangement described above for M-nC3-GIC and M-nC4-GIC (M = Li, Na). After drying, a new nC6 monolayer GIC structure appears with d_i = 0.699 nm (Fig. 2.1(c)), indicating a transition to the

monolayer arrangement described above. This transition of bilayer-to-monolayer arrangement for alkyl-chain intercalates, indicated in the scheme in Fig. 2.2(b), is new for GICs. A bilayer structure is also observed in the wet product obtained with *n*-octylamine – the blue stage 1 Na-nC8-GIC (d_i = 1.093 nm). However, Na-nC8-GIC does not change structure after drying. The bilayer to monolayer transition was also not observed for the alkane-containing Cs-C5-GIC or Cs-C6-GIC.[14] The number of steps in the TGA mass loss curves further supports the monolayer and bilayer assignments (see below).

The formation of radicals/anions/solvated electrons through the reaction of alkali metal with liquid ammonia, ethylenediamine, and small chain amines is well established in the literature.[15] The analogous reactions with longer-chain amines have received less attention. However, the successful formation of Na-nC6-GIC and Na-nC8-GIC suggests that such reactive intermediates exist and can provide the strong reducing conditions necessary to form donor-type GICs. Since the highest Na content in a well-characterized binary Na-graphite is the stage 6 NaC_{48} (synthesized from the reaction of graphite and a molten Na-Ca alloy at 250-300 ºC),[16] it is unlikely that the indirect method is operative in these reactions. Much more likely, these GICs are formed by a direct method – coinsertion of cation and solvent. The intermediate formation of a binary alkali metal GIC has not been proposed in other reports of GICs containing amines.[7-9, 12]

2.4.2 Long Chain Amines

Preparation of the black Na-nC12-GIC product requires the addition of anthracene, possibly due to the low solubility of the sodium metal in the long chain amine. While the details of dissolution of alkali metals in liquid ammonia,[17] or small amines like ethylamine,[18] or ethylenediamine[19] are reported, we are not aware of similar experiments with long chain amines. Control experiments, where either anthracene or the amines were omitted, yielded only graphite, as evidenced by a strong and sharp *(002)* graphite reflection in the resulting PXRD (not shown). The use of electron transfer agents, including naphthalene and phenanthrene, has been reported previously in the synthesis of GICs containing alkali metals and ethers.[20, 21] Fig. 2.3(a) shows the PXRD obtained for Na-nC12-GIC, with reflections observed up to index *(008)*. Na-nC14-GIC is prepared under the same synthetic conditions, the product PXRD is shown in Fig. 2.3(c).

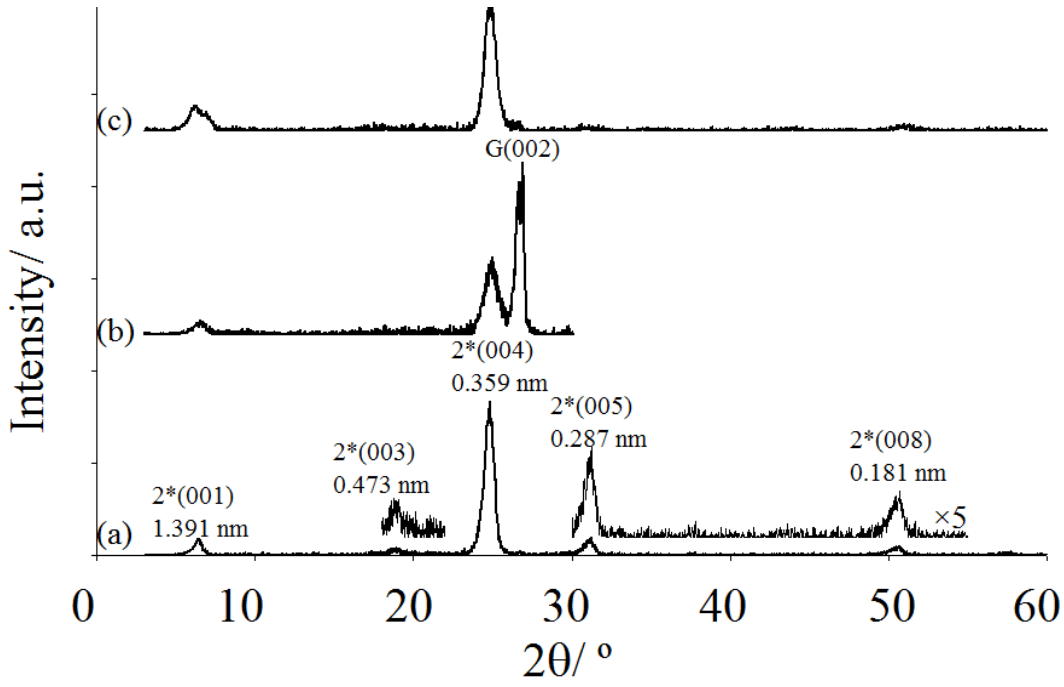

Figure 2.3 PXRD patterns of: (a) Na-nC12-GIC, (b) the mixture of Na-nC12-GIC and graphite obtained by decreasing the amine reactant (see text), and (c) Na-nC14-GIC. The 2*(00*l*) labels indicate reflections for the stage 2 parallel bilayer structure. The reflection from graphite is labeled G(002).

Na-nC12-GIC (d_i = 1.107 nm) and Na-nC14-GIC (d_i = 1.095 nm) are stage 2 compounds. These assignments give layer heights of 0.386 and 0.380 nm, respectively, consistent with a parallel oriented bilayer structure as described above. An alternate structure model, a stage 1 trilayer, would give intercalate layer heights around 0.37 nm, but was discarded due to the products black colors and TGA mass losses indicating organic content comparable to a bilayer arrangement (see Thermal

analysis, Section 2.4.3). Interestingly, the same stage 2 Na-nC12-GIC together with the unreacted graphite are obtained when the amount of nC12 reagent is reduced by 2/3, Fig. 2.3(b). These conditions favor the formation of mixed phases rather than higher-stage GIC products. The PXRD patterns of Na-nC12-GIC and Na-nC14-GIC do not change after drying.

Although the synthesis of intercalation compounds containing short, medium, and long chain alkylamine for other layered hosts is common in the literature,[1] we believe that this is the first report of such a series for GICs. A summary of the prepared GICs and structure assignments is provided in Table 2.1.

Table 2.1 Structural and compositional data of the prepared M-alkylamine-GICs

Amine	Stage number *n*	d_i / nm	Intercalate arrangement	Wt% amine	Wt% Na	Experimental composition
nC3	1	0.701 (0.700)[a]	Monolayer	15.4	9.3	$Na(nC3)_{0.7}C_{16}$
nC4	1	0.704 (0.697)[a]	Monolayer	(14.8)[a]	-	-
nC6 wet	1	1.091	Bilayer	-	-	-
nC6 dried	1	0.699	Monolayer	-	-	-
nC8	1	1.093	Bilayer	29.3	3.3	$Na(nC8)_{1.6}C_{40}$
nC12	2	1.107	Bilayer	18.0	-	-
nC14	2	1.095	Bilayer	14.5	-	-

[a] Values in parentheses indicate M = Li, all others are for M = Na.

A simple model for understanding the number of layers formed by the alkylamine intercalates can focus on the relative strength of alkyl chain hydrophobic interactions. The attractive forces between Na^+ cation intercalates and negatively charged graphene sheets strongly favors the formation of GICs with a minimum gallery height, in this case the parallel monolayer arrangement. However, interchain interactions grow in relative strength as the alkyl chain lengths increase. Thus, for Na-nC3-GIC and Na-nC4-GIC, only parallel monolayers are observed, whereas for Na-nC8-GIC, which has more significant interchain interactions, a bilayer arrangement is produced and is preserved even after the GIC is dried. An intermediate behavior is observed in Na-nC6-GIC, which undergoes the bilayer to monolayer transition upon drying. Unlike clay hosts where a trilayer structure has been reported for longer chain amines,[4] the bilayer structure persists for Na-nC12-GIC and Na-nC14-GIC. The change to stage 2 products rather than stage 1 for these GICs may also be associated with the retention of the bilayer arrangement.

2.4.3 Thermal and Elemental Analyses

Representative mass loss curves for the GIC products obtained are depicted in Fig. 2.4(a). All show mass losses from ~50-300 ºC that are absent in the graphite starting reagent. These losses are followed by a higher temperature mass loss with onset around 600-650°C, also seen in graphite, which is ascribed to the decomposition of the graphitic host lattice. A single mass loss region is observed for Na-nC3-GIC. Together with analysis of the sodium content, we can obtain a GIC composition of

$Na(nC3)_{0.7}C_{16}$. The Na to amine ratio (1/0.7) and the ~15% amine content of this phase are similar to previous reports for comparable GICs, namely K(*N*,*N*,*N'*,*N'*-tetramethylethylenediamine)$_{0.7}C_{37}$ (14.4% mass loss),[10] Cs(*n*-pentane)$_{1.0}C_{24}$ (14.6%),[14] Li(ethylenediamine)$_{1.0}C_{28}$ (14.9%),[7] Cs(*n*-hexane)$_{0.9}C_{24}$ (15.6%),[14] and Li(methylamine)$_2C_{12}$ (17.4%).[7]

For Na-nC8-GIC, the presence of two, rather than one, mass loss steps agrees with the assignment as a bilayer intercalate. The greater mass loss for the stage 1 bilayer Na-nC8-GIC (approx. 28%) supports also this assignment. However, we did not attempt to separate the intermediate phase monolayer Na-nC8-GIC by thermal decomposition of the bilayer Na-nC8-GIC. The obtained composition of $Na(nC8)_{1.6}C_{40}$ shows a significantly decreased Na/amine mole ratio as compared to the propylamine GIC (1/1.6 as compared to 1/0.7), but the amine/graphite ratio is similar in each case. The mass losses of the stage 2 bilayer Na-nC12-GIC and stage 1 monolayer Na-nC3-GIC are similar (Table 2.1). This appears reasonable considering the equivalent ratio of intercalate and graphene layers in the two structures. The determination of the amine content in the stage 2 bilayer structure may appear less reliable due to the overlap of the mass loss events (Fig. 2.4(a)). However, the same GICs prepared in separate experiments showed organic contents that agreed within 2%, and the Na contents in these cases agreed to within 0.6% for Na-nC3-GIC and 0.2% for Na-nC8-GIC.

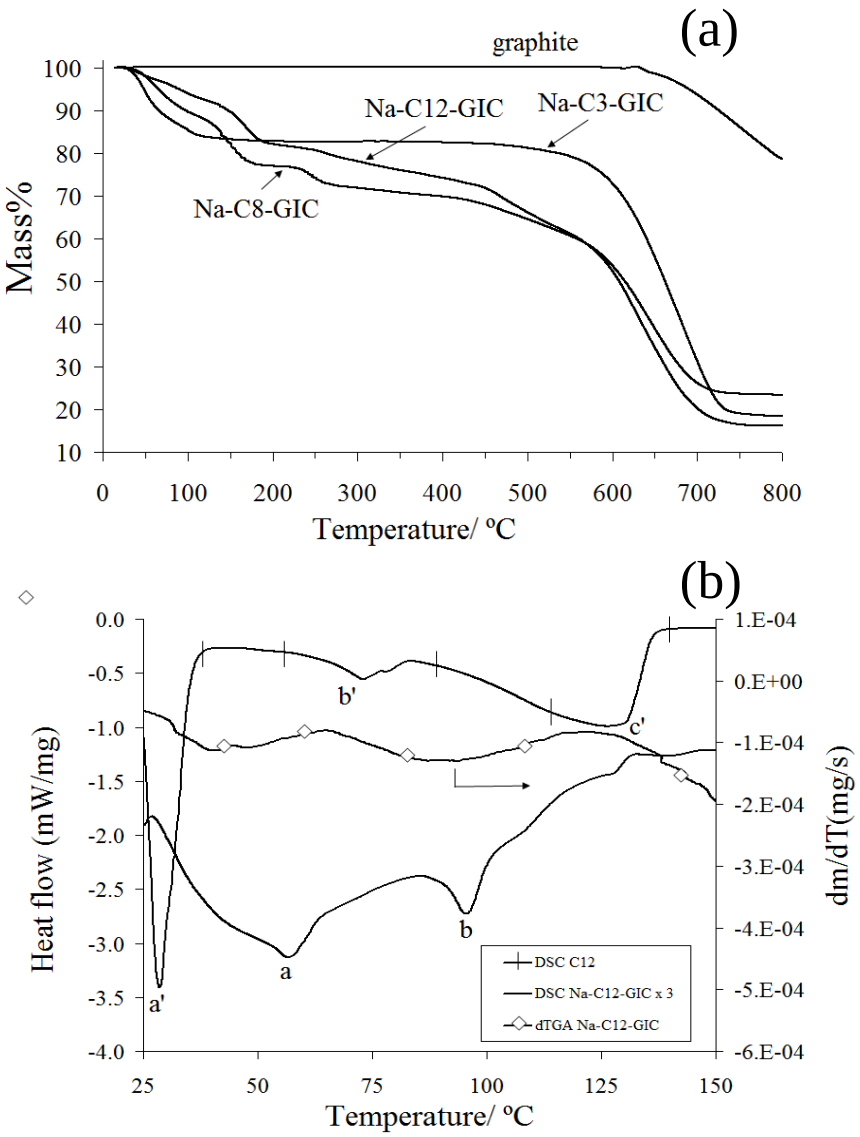

Figure 2.4 (a) Selected TGA mass loss data for GIC products, and (b) DSC curve for Na-nC12-GIC, nC12 amine, and the respective dTGA curve for Na-nC12-GIC.

We can determine the packing densities of the intercalate galleries by comparing the experimentally-obtained compositions and structural data of these Na-nC*x*-GICs with the known dimensions of the intercalates. For Na-nC3-GIC, the values required are the ionic volume of Na^+ (0.0060 nm^3), the van der Waals molecular volume of *n*-propylamine (0.0714 nm^3),[22] the surface area per carbon atom in a graphene layer (0.0261 nm^2), and the experimentally-determined composition and intercalate gallery expansion, $Na(nC3)_{0.7}C_{16}$ and 0.366 nm. The packing density, or ratio of intercalate molecular volumes to geometric volume available in the opened galleries is determined by the following ratio:

$$[(0.0060\ nm^3 + (0.7)(0.0714\ nm^3)]\ /\ (16)(0.0261\ nm^2)(0.366\ nm) = 0.98$$

The intercalate galleries in this GIC are efficiently packed. In contrast, a similar calculation for $Na(nC8)_{1.6}C_{40}$ using the molecular volume for *n*-octylamine (0.158 nm^3)[22] and the gallery expansion (0.758 nm) yields a much lower packing density of only 0.33. Two characteristics that may be associated with the very different packing efficiencies are the different intercalate volumes, and the arrangement of monolayer (for nC3) *vs* bilayer (for nC8).

The DSC heating curve for Na-nC12-GIC and the amine reagent are shown in Fig. 2.4(b). The amine reagent shows a strong, sharp melting endotherm at 29 ºC, and two additional endotherms at 74 and 130 ºC (labeled *a'-c'* respectively). The *n*-dodecylamine boiling point occurs at ~250 ºC and is beyond the temperature range studied. Endotherms for Na-nC12-GIC are observed at 58 ºC and 96 ºC (labeled as *a* and *b,* respectively). These coincide with peaks in the dTGA curve also shown in Fig.

2.4(b). The disappearance of the free amine melting endotherm, and appearance of two new endothermic transitions between 50 and 100 °C for amines intercalates confined in galleries are all consistent with previous observations on amine-intercalated montmorillonite.[2]

Surface studies of *n*-alkylamine (*e.g.*, nC8) on graphite show a parallel orientation of the amine long axis to the graphite basal plane,[23] similar to that described above for the GIC galleries. The adsorption of nC6-nC16 monolayers on graphite has also been reported.[24] In those cases, as in this study, the other orientation details, such as whether the H-C-H or H-N-H face orients towards the graphene layer, remain an unanswered and interesting question.

2.5 ACKNOWLEDGEMENT

TM thanks the OSU Whiteley Fellowship in Material Sciences for partial financial support. We thank Dr. Christine Pastorek for assistance with ICP analyses.

2.6 REFERENCES

1. Whittingham, M. S.; Jacobson, A. J.; ed, *Intercalation Chemistry;* Academic Press: New York, 1982.

2. Li, Y. Q.; Ishida, H. *Chem. Mater.* **2002**, *14*, 1398.

3. Li, Y. Q.; Ishida, H. *Langmuir* **2003,** *19,* 2479.

4. Chun, Y.; Sheng, G. Y.; Boyd, S. A. *Clays Clay Minerals* **2003**, *51*, 415.

5. Ogawa, M.; Kuroda, K. *Bull. Chem. Soc. Jpn.* **1997**, *70*, 2593.

6. Osada, M.; Sasaki, T. *J. Mater. Chem.* **2009**, *19*, 2503.

7. Rüdorff, W. *Chimia* **1965**, *19*, 489.

8. Stumpp, E.; Alheid, H.; Schwarz, M.; Janssen, J. J.; Müller-Warmuth, W. *J. Phys. Chem. Solids* **1996,** *57,* 925.

9. Scharff, P.; Alheid, H. *Phys. Stat. Sol. (a)* **2000,** *177,* 93.

10. Merle, G.; Letoffe, J. M.; Rashkov, I. B.; Claudy, P. *J. Therm. Anal.* **1978,** *13,* 293

11. Setton, R.; Beguin, F.; Facchini, L.; Quinton, M. F.; Legrand, A. P.; Ruisinger, B.; Boehm, H. P. *J. Chem. Soc. Chem. Commun.* **1983,** 36.

12. Skipper, N. T.; Walters, J. K.; Lobban, C.; McKewn, J.; Mukerji, R.; Martin, G. J.; de Podesta, M.; Hannon, A. C. *J. Phys. Chem. B* **2000**, *104*, 10969.

13. Maluangnont, T.; Gotoh, K.; Fujiwara, K.; Lerner M. M. *Carbon* **2011,** *49,* 1040.

14. Beguin, F.; Pilliere, H. *Carbon* **1998,** *36,* 1759.

15. Dye, J. L. *Acc. Chem. Res.* **1968,** *1,* 306.

16. Metrot, A.; Guerard, D.; Billaud, D.; Herold, A. *Syn. Met.* **1980,** *1,* 363.

17. Wasse, J. C.; Hayama, S.; Skipper, N. T.; Benmore, C. J.; Soper, A. K. *J. Chem. Phys.* **2000,** *112,* 7147.

18. Ottolenghi, M.; Bar-Eli, K.; Linschitz, H.; Tuttle, T. R. *J. Chem. Phys.* , **1964,** *40,* 729.

19. Dewald, R. R.; Dye, J. L. *J. Phys. Chem.* **1964,** *68,* 128.

20. Mizutani, Y.; Ihara, E.; Abe, T.; Asano, M.; Harada, T.; Ogumi, Z.; Inaba, M. *J. Phys. Chem. Solids* **1996,** *57,* 799.

21. Abe, T.; Mizutani, Y.; Tabuchi, T.; Ikeda, K.; Asano, M.; Harada, T.; Inaba, M.; Ogumi, Z. *J. Power Sources* **1997,** *68,* 216.

22. Zhao, Y. H.; Abraham, M. H.; Zissimos, A. M. *J. Org. Chem.* **2003,** *68,* 7368

23. Martin, D. S.; Weightman, P. *Surf. Sci.* **2000,** *450,* 171.

24. Cheah, N. P.; Messe, L.; Clarke, S. M. *J. Phys. Chem. B* **2004,** *108,* 4466.

CHAPTER 3

A COMPARATIVE STRUCTURAL STUDY OF TERNARY GRAPHITE INTERCALATION COMPOUNDS CONTAINING ALKALI METALS AND LINEAR OR BRANCHED AMINES

Tosapol Maluangnont, Weekit Sirisaksoontorn and Michael M. Lerner

Department of Chemistry

Oregon State University

Corvallis, OR 97331-4003, USA

Carbon, doi:10.1016/j.carbon.2011.09.018

3.1 ABSTRACT

New donor-type ternary graphite intercalation compounds (GICs) containing alkali metals and branched amines are prepared by direct reaction of graphite with the alkali metal and amine. The new GICs include $M(iC3)_{0.4}C_{15\text{-}18}$ (M = Li, Na; iC3 = *iso*-propylamine; d_i = 0.76 nm) with a monolayer intercalate arrangement; and $Na(sC4)_{1.6}C_{18}$ (sC4 = *sec*-butylamine; d_i = 1.34 nm) and $Na(iC4)_{2.0}C_{28}$ (iC4 = *iso*-butylamine; d_i = 1.28 nm) with bilayer arrangements. Li-sC4-GIC and K-iC3-GIC are not formed using this reaction chemistry. M-iC3-GICs show galleries expanded by 0.06 nm more than that for $M(nC3)_{0.7\text{-}0.8}C_{16}$ (M = Li, Na; nC3 = *n*-propylamine). Unlike the case of rigid-sheet hosts where branched amines intercalate at a lower rate and with lower amine content, M-sC4-GICs and M-iC4-GICs readily form intercalate bilayers.

3.2 INTRODUCTION

Alkylamines and alkylammonium ions are among the most widely studied guests employed in intercalation chemistry.[1] Intercalation compounds containing these species are applied as adsorbents for toxic compounds, photo and electro-functional materials, and catalysts.[2] The insertion of large guests can generate microporosity within layered materials, and can contribute to the delamination of the layered hosts into individual sheets. The latter process, known as exfoliation, provides a route to reassembled materials with novel magnetic, optical and electronic properties.[3] Studies of the affect of intercalate geometry on reaction rate and product stucture have provided a better understanding of this chemistry.[1]

In donor-type graphite intercalation compounds (GICs), the graphene sheets are reduced and cations intercalate to maintain charge neutrality.[4] When the metal cation intercalate as solvated ions, ternary GICs are produced. Despite the long history of exploring GIC chemistry, the number of known GICs with amine intercalates or co-intercalates is surprisingly limited. The amine intercalates reported are ammonia or ammomium,[5-7] methylamine,[8] ethylenediamine,[5,6] *N,N,N',N'*-tetramethylethylenediamine (TMEDA),[9] triethylamine,[9] cryptand "K222" (4,7,13,16,21,24-hexaoxa-1,10-diazabicyclo[8.8.8]hexacosane),[10] and 1,2-diaminopropane (12DAP).[11] We recently added several new GICs to this list in reporting the synthesis of a homologous series of ternary GICs containing Na^+ solvated by *n*-alkylamines with *x* carbon atoms, Na-nC*x*-GIC (*x* = 3, 4, 6, 8, 12, and

14).[12] The smaller homologs (nC3 and nC4) intercalate with a parallel monolayer arrangement, whereas the larger homologs (nC8 to nC14) exhibit a parallel bilayer intercalate structure that is new to GICs. The intermediate length amine, nC6, can intercalate with either arrangement and can transition between the two.

In this report, we extend this work to study the intercalation of branched amines into graphite, and compare the resulting GIC structures and reaction chemistry of amines containing α or β subsituents with their linear homologs. Specifically, the new ternary GICs containing alkail metal cations Li, Na, or K and *iso*-propylamine (iC3), *iso*-butylamine (iC4), or *sec*-butylamine (sC4) are described and their reaction chemistries, structures, and compositions compared to GICs containing *n*-propylamine (nC3) and *n*-butylamine (nC4), Fig. 3.1. The results obtained help extend an understanding of the energetics of graphite intercalation, which should prove useful towards preparing GICs with large and complex galleries, and ultimately developing a rational synthesis of colloidal graphene dispersions.

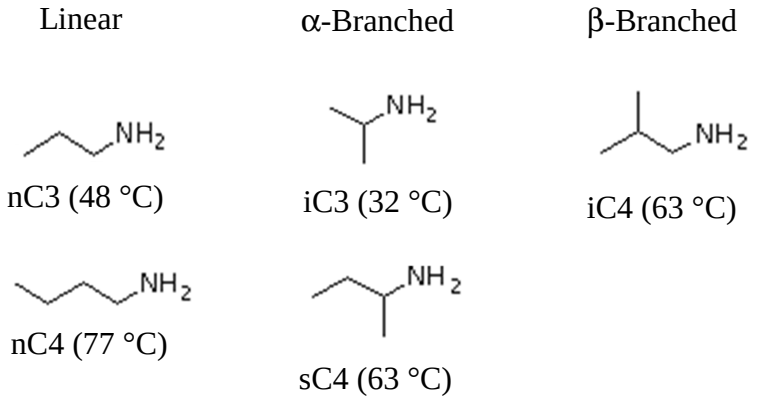

Figure 3.1 The amines studied and abbreviations (with normal boiling points)

3.3 EXPERIMENTAL

3.3.1 Synthesis

Reactions containing metallic Li were assembled in a Vac. Atm. PC-1 dry box under Ar (99.99+%). All other reagents and the obtained GICs were handled under N_2 (Vac. Atm. He-43-2 box, <5 ppm H_2O and O_2). In a typical synthesis, 0.25 g of polycrystalline graphite powder (SP-1, Union Carbide, avg particle dia. 100 μm) was mixed with 0.06 g of Na metal (99.95%, Alfa Aesar) (mol C/mol Na = 8) and the selected liquid amine (4 mL). Reactions using Li (m) and K (m) also used the same mole ratio of C/metal. ***Caution! Alkali metals are highly flammable when in contact with air and/or water and should be handle with care.*** The reaction mixtures were continuously stirred at ambient temperature under an inert atmosphere for 3 days (nC3, iC3 and nC4) or 7 days (sC4 and iC4). ***Caution! Pressure may increase and must be vented.*** The mixtures were then centrifuged and the liquid amine overlayer removed *via* syringe. GIC products were then dried *in vacuo* at 20°C for 6 h. Some products were subjected to different drying times (2-72 h), as described in the text.

3.3.2 Characterization

Powder X-ray diffraction (PXRD) data (Rigaku MiniFlex II, Ni-filtered Cu Kα radiation) were collected for a total time of 15 min per run using 0.02° 2θ steps, between 3° and 60° 2θ. A plastic film seal was sufficient to prevent decomposition in

air. This method provided sharp reflections without evidence of degradation for the much more reactive first-stage KC_8 at the same scan rate. PXRD (00*l*) reflections were indexed according to the relation $I_c = d_i + (n\text{-}1)(0.335\ \text{nm})$, where I_c is the unit cell repeat along the *c*-axis, d_i is the GIC gallery height, *n* is the GIC stage number, and 0.335 nm is the graphene sheet thickness. Thermogravimetric analyses (Shimadzu TGA-50) were performed under flowing Ar (20 mL/min) from RT to 800 ºC at a heating rate of 5 ºC/min. Elemental analyses for alkali metals were performed using Capillary Zone Electrophoresis (CZE). CZE analyses were performed on an HP ^{3D}CE instrument equipped with a UV detector, using a 50 µm inner diameter, 56 cm long fused-silica capillary (47.5 cm to the detection window). The new capillary was sequentially conditioned by flushing with methanol (30 min), Milli-Q water (5 min), 1.0 M NaOH (30 min), Milli-Q water (5 min) and finally the background electrolyte (BGE) for 30 min. In between runs, the capillary was flushed with 0.1M NaOH (2 min), Milli-Q water (3 min) and BGE (3 min). Separation was accomplished using an applied voltage of +15 kV. The capillary was thermostatted at 30 ^{o}C and solutions were injected hydrodynamically at 50 mbar for 5 s. Indirect detection was employed with the detection wavelength set at 210 nm. The background electrolyte used was 15mM imidazole, pH adjusted to 5.2 with glacial acetic acid. GICs synthesized from different batches and separately analzed showed amine contents agreeing within 2% and the alkali metal contents within 0.5%. The amine co-intercalate structures were optimized using the hybrid density functional method (B3LYP) with a 6-31+G(d,p) basis set and Gaussian 3.0 software.

3.4 RESULTS AND DISCUSSION

Except where noted, all the products obtained were first-stage GICs with intercalate galleries opened between all graphene sheets, *i.e.* no adjacent graphene sheets remain in the products. The first-stage compounds are all brilliant blue (see Fig. 3.3).

3.4.1 Intercalation of iC3

The PXRD patterns obtained for the blue M-iC3-GICs (M = Li, d_i = 0.760 nm; M = Na, d_i = 0.758 nm) are shown in Fig. 3.2. The presence of Bragg reflections up to (*004*) indicates an ordered GIC arrangement along the *c* direction. A blue product was also obtained from the reaction with M = K, but displayed only a broad PXRD pattern (not shown), indicating a disordered structure. After substracting the graphene sheet thickness of 0.335 nm, the expansion, Δd, related to intercalation of the M-iC3 complexes is ~0.43 nm. Because the Li and Na metal cation diameters (0.1-0.2 nm) are smaller than the minimum amine dimension, the cation contribution to gallery expansion is neglected (of course, the cations may indirectly be involved by affecting the orientation of the larger amine co-intercalates). For comparison, Fig. 3.2 also shows the PXRD pattern of the first stage Na-nC3-GIC (d_i = 0.701 nm, Δd = 0.37 nm), where the nC3 subsituent lies parallel to the adjacent graphene sheets.[12]

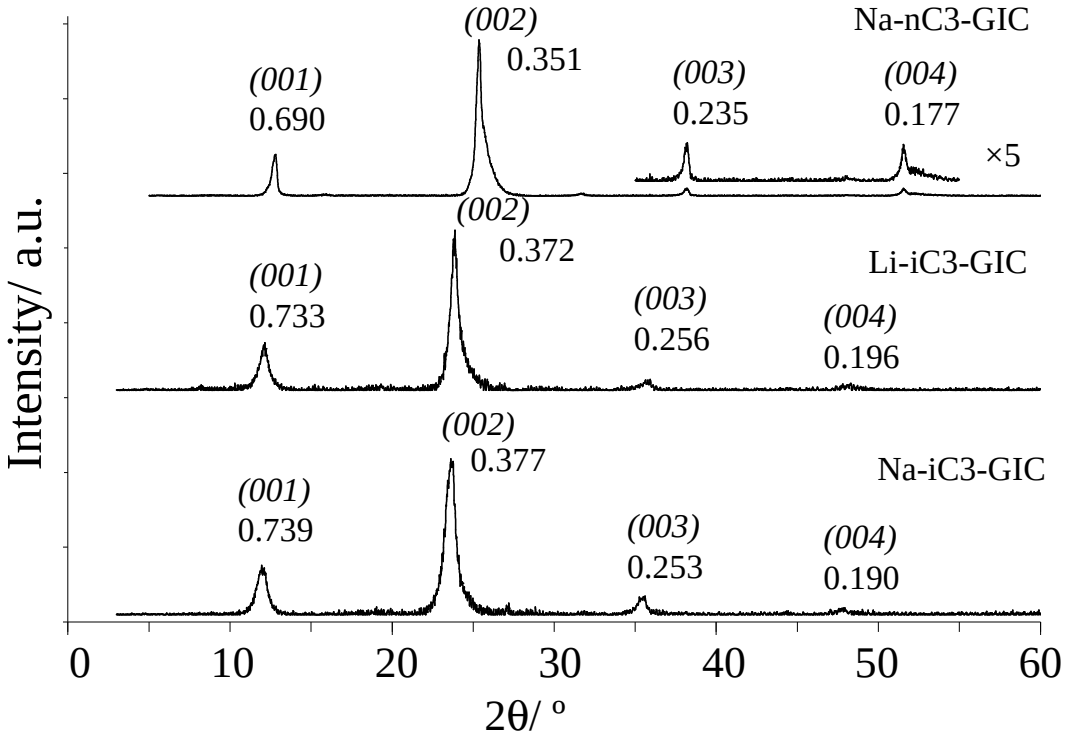

Figure 3.2 The PXRD patterns of Na-iC3-GIC, Li-iC3-GIC, and Na-nC3-GIC. The *d* values (in nm) and assigned Miller indices are indicated for each reflection.

The increased gallery expansion by 0.06 nm for iC3 *vs* nC3 co-intercalates conforms well with our calculated minumium dimensions (nC3 = 0.42 nm; iC3 = 0.49 nm) for these amines. To form these galleries, iC3 must therefore be oriented with either the C-C-C or N-C-C molecular axis parallel to the graphene sheets, leaving a $–NH_2$ or $–CH_3$ substituent, respectively, oriented towards the encasing graphene sheet. This branching is responsible for the increased gallery dimension relative to that of nC3, Fig. 3.3. PXRD data are not sufficient to locate alkali metal cation positions,

they are shown schematically at the gallery centers. An analogous gallery height increase in ternary GICs for substituted organic cointercalates has been observed by Isaev *et al.*[13] in comparing K-benzene-GIC (d_i = 0.895 nm) and K-1,2-dimethylbenzene-GIC (d_i = 1.06 nm). The additional steric requirements for the branched amine may also affect the GIC compositions, as discussed in Section 3.4.4, resulting in a lower packing density of iC3 than nC3.

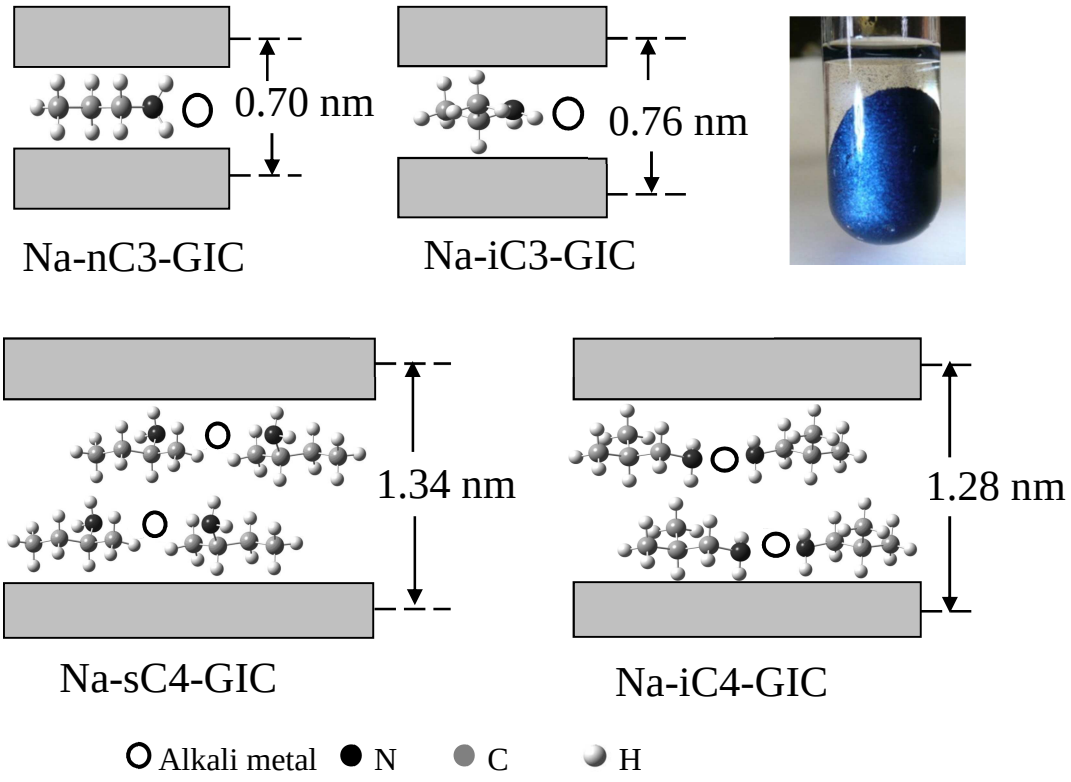

Figure 3.3 Schematic of intercalate orientations for Na-nC3-GIC, Na-iC3-GIC, Na-sC4-GIC, and Na-iC4-GIC. The inset shows the brilliant blue color of Na-sC4-GIC which is observed for all first-stage ternary GICs reported in this work.

3.4.2 Intercalation of sC4

Fig. 3.4 shows the PXRD pattern of the blue product M-sC4-GIC (M = Na, d_i = 1.341 nm; M = K, d_i = 1.335 nm). The gallery expansion due to the M-sC4 complex is ~1.00 nm. K-sC4-GIC is similar to the Na analog, with slightly broadened peaks indicating decreased structural ordering along the *c*-axis. Li-sC4-GIC was not obtained under similar conditions - a black product indicated only unreacted graphite (not shown). Comparing these PXRD patterns with that for Li-nC4-GIC[12] (d_i = 0.704 nm, Fig. 3.4) shows the dramatic effect of the α-CH_3 subsituent in sC4 on the resulting intercalate arrangement in the prepared GICs.

The large gallery height (1.34 nm) and high amine content (see section 3.4.4) indicate a parallel bilayer structure for the sC4 co-intercalate, Fig. 3.3. Again, the limited number of diffraction peaks observed prevents cation position evaluation, and the alkali cations in the model are shown schematically. Considering the full gallery expansion, each monolayer dimension is ~0.50 nm, somewhat greater than that observed for the iC3 monolayers (0.43 nm). Other known donor types GICs with comparable gallery dimensions include Na-nC8-GIC (d_i = 1.093 nm),[12] Li-DME-GIC (DME = dimethoxyethane, d_i = 1.162 nm),[15] and M-THF-GIC (M = Li, Na, K; THF = tetrahydrofuran, d_i = 1.245 nm).[16] The parallel bilayer structure was reported for Na-nC8-GIC, whereas a T_d co-intercalate geometry about the metal cation was suggested in the other cases. In the current example, we believe that the bilayer structure is more likely.

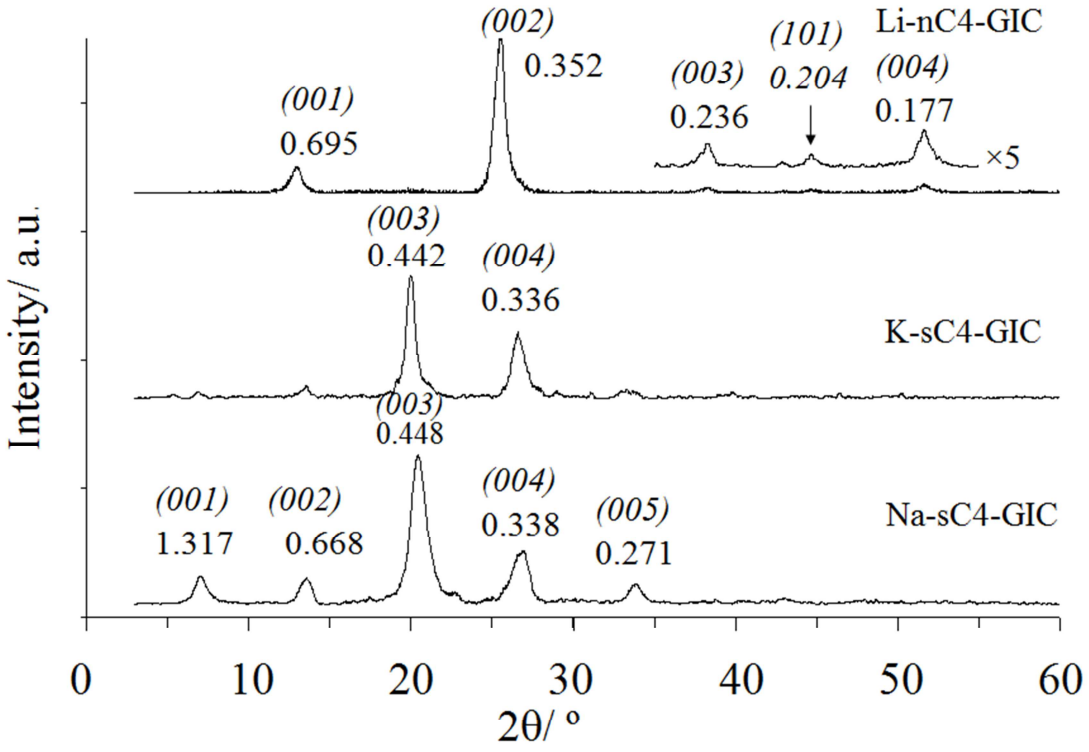

Figure 3.4 The PXRD patterns of Na-sC4-GIC, K-sC4-GIC, and Li-nC4-GIC. The *d* values (in nm) and assigned Miller indices are indicated for each reflection.

3.4.3 Intercalation of iC4

Fig. 3.5 shows the PXRD patterns of M-iC4-GICs (M=Li, Na, K). For the blue Na-iC4-GIC product, the observed d_i = 1.28 nm and Δd ~ 0.95 nm are similar to those for sC4 described above. Based on the similar gallery dimensions and amine contents (Secion 3.4.4), the intercalate galleries are also assigned a parallel bilayer structure similar to that shown in Fig. 3.3.

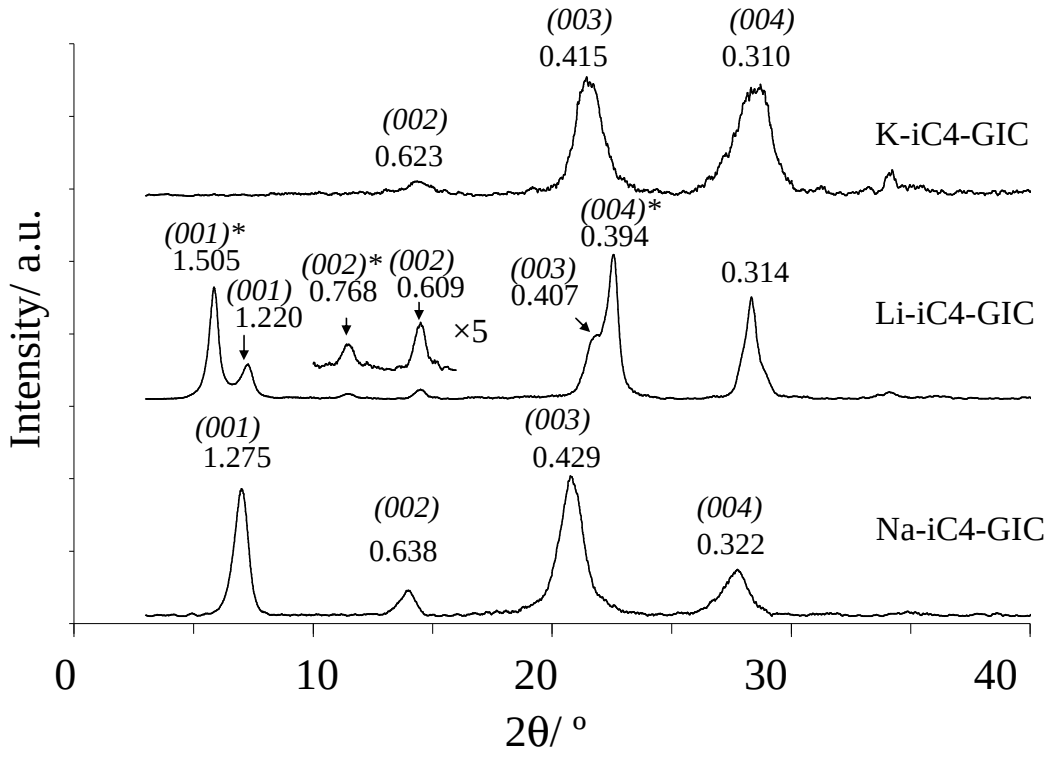

Figure 3.5 The PXRD patterns of Na-iC4-GIC, Li-iC4-GIC, and K-iC4-GIC. The *d* values (in nm) and assigned Miller indices are indicated for each reflection. The starred assignments indicate a stage 2 GIC, others are for stage 1.

Li-iC4-GIC is obtained as a blue, but notable darker, product than the Na analog. The PXRD pattern indicates a predominantly stage 2 GIC (I_c = 1.547 nm, d_i = 1.220 nm) with a small amount of a stage 1 present (d_i = 1.221 nm). Increasing the reaction time to 2 weeks resulted in a poorly-ordered first-stage product (d_i = 1.220 nm, PXRD not shown). Passivation of the Li(m) surface with nitride (due to an N_2 impurity in the Ar atmosphere) could account for the the higher stages obtained with Li(m). The broadened reflection at 0.314 nm is an overlap of the first-

stage *(004)* (calculated position = 0.305 nm) and the second-stage *(005)** (calculated at 0.312 nm). A similar overlap occurs for the first-stage *(003)* and second-stage *(004)** reflections, with the first-stage component on the low-angle side of the overlapping peak. A blue K-sC4-GIC (d_i = 1.244 nm) product can also be prepared, although the PXRD pattern indicates a poorly-ordered material that may also contain some stage 2 GIC. From the gallery dimensions and GIC compositions, all these M-iC4-GICs are assigned a parallel bilayer intercalate structure.

3.4.4 Compositional Analyses

Table 3.1 provides a summary of the structural and compositional data of the GICs prepared in this work. The ternary GICs show two mass loss regions in TGA, Fig. 3.6 The first mass loss (RT to 200 ºC) is ascribed to the volatilization of the amine intercalate; the higher temperature losses (>400 ºC) to the decomposition of the graphite host structure. This high temperature mass loss is also observed for a graphite control sample, and is due to the presence of trace O_2 in the flow gas.

Table 3.1 Structural and compositional data of first-stage ternary M-amine-GICs

Amine	Cation M	d_i / nm	Intercalate arrangement	Wt% M	Wt% amine	Composition	Packing fraction
nC3*	Li	0.700	Monolayer	2.9	19.0	$Li(nC3)_{0.8}C_{16}$	0.40
	Na	0.701	Monolayer	9.3	15.4	$Na(nC3)_{0.7}C_{16}$	0.37
iC3	Li	0.760	Monolayer	2.8	9.8	$Li(iC3)_{0.4}C_{18}$	0.16
	Na	0.758	Monolayer	10.1	9.9	$Na(iC3)_{0.4}C_{15}$	0.21
nC4	Li	0.704	Monolayer		14.8		
sC4	Na	1.341	Bilayer	6.6	32.9	$Na(sC4)_{1.6}C_{18}$	0.31
	K	1.335	Bilayer		21.7		
iC4	Li	1.221	Bilayer				
	Na	1.280	Bilayer	4.3	32.0	$Na(iC4)_{2.0}C_{28}$	0.27
	K	1.244	Bilayer		23.4		

* nC3 compositional data from ref.[12]

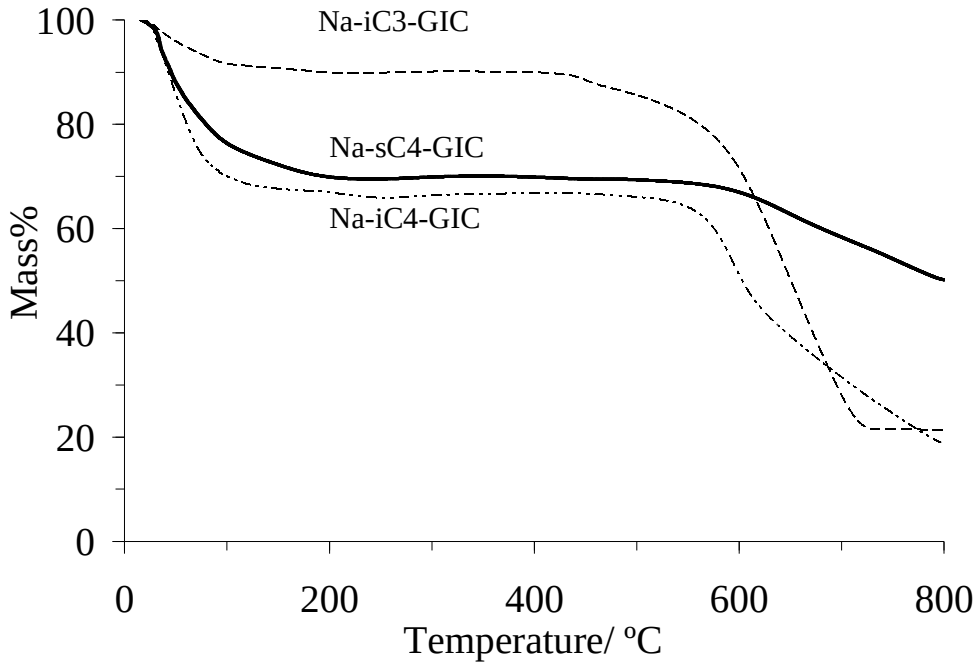

Figure 3.6 TGA mass loss curves for Na-iC3-GIC, Na-sC4-GIC, and Na-iC4-GIC.

The amine content in M-iC3-GIC (10%) is much lower than that of the linear isomer intercalate M-nC3-GIC (15-19%), and also lower than that observed in other ternary GICs with organic cointercalates of similar molecular size such as K-TMEDA-GIC (14.4%),[9] Cs-*n*-pentane-GIC (14.6%),[17] Li-ethylenediamine-GIC (14.9%),[5] Cs-*n*-hexane-GIC (15.6%),[17] and Li-methylamine-GIC (17.4%).[5] This lower packing fraction might relate to inefficient packing within the branched amine monolayer. A lower intercalate content due to the more rapid loss of the co-intercalate during drying (iC3 b.p. = 32 ºC; nC3 b.p. = 48 ºC) is unlikely and will be discussed below. There are other examples of decreased uptake of the iC3 amine isomer in intercalation reactions,

for example, Cai *et al.*[18] reported that [Cd(1,5-naphthalenedisulfonate)$(H_2O)_2$] intercalates 4 moles of nC3, but only 3 mols of iC3. Similarly [Cd(μ_2-*N,O-p*-$NH_2C_6H_4SO3)_2(H_2O)_2]_n$ intercalates 5 moles of nC3 but only 0.5 moles of iC3.[19]

The mass losses of the Na-sC4-GIC and Na-iC4-GIC are ~32%. These larger amine contents are consistent with the assigned bilayer structure, and are comparable to that for Na-nC8-GIC (29%) which was previously reported with a bilayer structure.[12] The lower amine contents observed for K-sC4-GIC and K-iC4-GIC (22-23%) might be related to their less ordered structures and some effect of packing with the larger cation.

The packing fraction, *i.e.* the volume of intercalates divided by the volume opened in the expanded galleries, are estimated in Table 3.1 from the known compositions, gallery dimension, the surface area per carbon atom in a graphene layer (0.0261 nm^2), and using intercalate volume (in nm^3): Li^+ (0.0016), Na^+ (0.0060), C3 (0.0714) and C4 (0.0887).[20] One notable result is that the monolayer arrangement with branched amines have much lower packing densities than the linear analogs (~0.2 vs 0.4) The bilayer arrangements show an intermediate value (~0.3). The packing fractions of other ternary GICs show a wide range, from about 0.1-0.7. Examples include $K(NEt_3)_{0.43}C_{36}$ (NEt_3 = triethylamine) (0.08),[21] $K(TMEDA)_{0.7}C_{37}$ (0.2),[9] $K(CH_3NH_2)_3C_{24}$ (0.55),[8] and $Li(CH_3NH_2)_2C_{12}$ (0.68).[5]

When comparing these compositions and structures, it is important to consider the possible variation in composition, especially that of the amine co-intercalates, due

to preparative conditions. Perhaps most significant is evacuation time, these GICs lose amine co-intercalate during evacuation. In order to evaluate these changes, mass losses of several Li-amine-GICs were recorded as a function of evacution time. Fig. 3.7 shows the normalized GIC mass as a function of evacuation time. Masses were normalized to the 2 h evacuated product (where no liquid phase co-exists) to avoid complications where excess liquid phase exists in the as-prepared sample. All samples show an approximately exponentially decreasing mass loss with time under vacuum. The rate of mass loss is lowest for Li-nC3-GIC and Li-nC4-GIC, and much greater for Li-iC4-GIC.

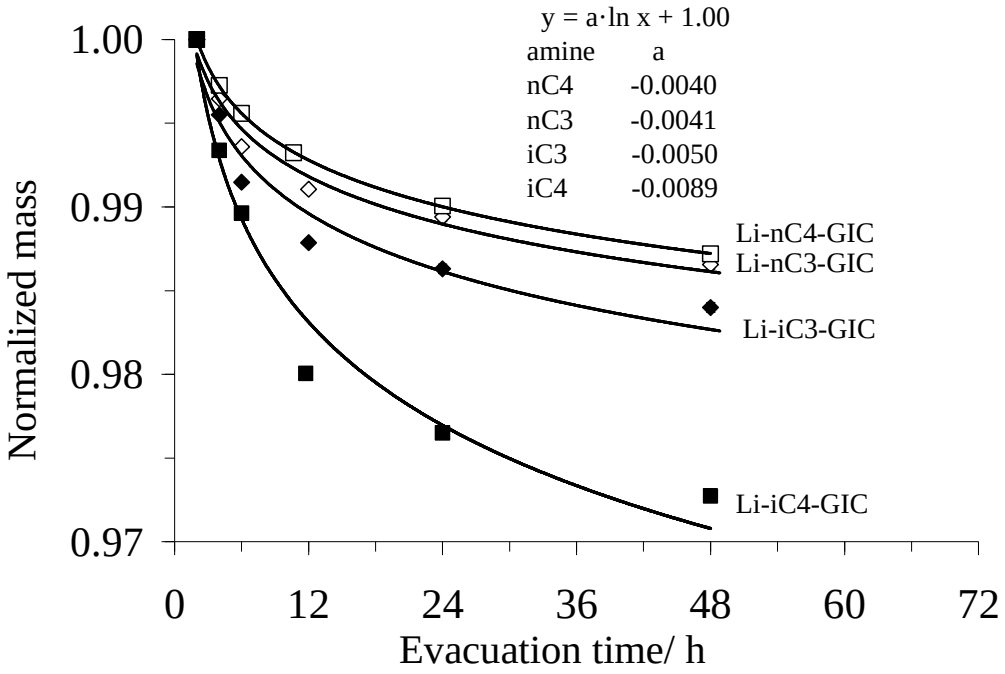

Figure 3.7 Normalized mass loss as a function of evacuation time. Lines are exponential fits to the data, with equations shown in the inset.

These loss rates do not correspond to the volatilities of the liquid amines (as indicated by their normal boiling points), and should result from different relative binding energies of amines in the GICs, or to the different co-intercalate diffusion rates for different gallery arrangements. The greater expansion in Li-iC4-GIC may facilite more rapid diffusion of the intercalates out of the intercalate galleries. We are studying these effects and will report conclusions more fully elsewhere. However, the magnitude of mass losses observed provide a useful result. Our standard evacuation time in preparations of 6 h corresponds, at most, to mass loss change of <0.5%. The

amine contents reported in Table 3.1 are therefore not variable with evacuation time above this extent, and the observations on packing fractions reported above remain valid despite different mass loss rates. Thus, we conclude that the lower amine content for iC3 (~10%) as compared to nC3 (16-19%) is associated with intercalate energetics or sterics rather than experimental conditions.

The intercalate mole ratios nC3 / M are in the range of 0.7-0.8 whereas those for iC3 / M are ~0.4. On the other hand, the branched C4 amine / M ratios are much larger, 1.6-2.0 (Table 3.1). These ratios are similar to others reported in the literature: 0.56 for Cs-*n*-butane-GIC,[17] 0.7 for Na-nC3-GIC,[13] 1.2 for Cs-acrylonitrile-GIC,[22] 1.6-2.2 for M-NH_3-GICs (M = Li, Na, K, Rb, Cs),[23] and 2 for Li-methylamine-GIC.[5] For the M-amine-GICs reported in this work, the metal cations seem to play an only relatively minor role in determining GIC orientation or arrangement, in contrast to the M-12DAP-GIC series (M = Li, Na, K) we have reported previously.[11] On the other hand, the amine properties may be related to the formation of bilayer or monolayer intercalate structures. In this work, the amines with higher dipole moment, sC4 (1.28 D) and iC4 (1.27) formed bilayer GICs, whereas those with lower dipole moments formed monolayers - nC3 (1.17 D), iC3 (1.19), and nC4 (~1).[24]

3.4.5 Graphite *vs* other hosts

Previous studies have reported on the affect of intercalate isomer type on reactivities or product structures for graphite or other hosts. Mizutani *et al.*[25] reported the synthesis of Li-1,2-diethoxyethane-GIC (d_i = 1.12 nm) *vs* Li-1,2-dimethoxyethane-GIC (d_i = 1.17 nm). Neither the Li / ether ratio nor the orientation of the ether co-intercalates are reported. The same group[26] also reported the synthesis of a ternary M-tetrahydrofuran-GIC, whereas only the binary M-GICs were formed when 2-methyltetrahydrofuran or 2,5-dimethyltetrahydrofuran (M = alkali metal) were present. Similarly Isaev *et al.*[13] reported the ternarization study of KC_{24} with aromatic compounds, where the ternary GICs were obtained with benzene and 1,2-dimethylbenzene, but not with 1,3-dimethylbenzene, 1,4-dimethylbenzene, or 1,3,5-trimethylbenzene.

For other layered hosts, the presence of α-branched intercalates has been reported to retard or inhibit guest intercalation much more significantly than for β–, γ-, or no-branching. Examples include the intercalation of amines into $Zn(O_3PC_6H_5)\cdot H_2O$,[27] $M^{II}(O_3PCH_3)$ (M = Co and Zn),[28] $Cd(O_3PCH_3)$,[29] and $(V_xNb_{1-x})OPO_4\cdot yH_2O$,[30] as well as the intercalation of branched alcohols into $VOPO_4$.[31] The intercalation of branched amines into rigid hosts such as metal phophonates can be limited by the requirement that guests occupy specific sites on the host surface, resulting in what has been termed ”selective intercalation”. For example, $Zn(O_3PC_6H_5)\cdot H_2O$ rapidly intercalates *n*-alkylamine, but require 1-3 weeks to form

corresponding compounds with an α-branched amine.[27] Similarly, $M^{II}(O_3PCH_3)$ (M = Co and Zn) intercalates nC4 (no branching) and iC4 (β-branching), but not sC4 or *tert*-butylamine (α-branching);[28] and $Cd(O_3PCH_3)$ intercalates 2-methylbutylamine (β-branching) and 3-methylbutylamine (γ-branching), but not 1-methylbutylamine (α-branching).[29]

However, as described above, GICs present a contrasting reaction chemistry for branched amines. The delocalized and somewhat variable charge on the graphene host, and perhaps the greater mechanical flexibility of graphene sheets, leads to the adoption of different intercalate arrangements for branched *vs* linear guests, moreso than a selectivity for different intercalate species.

3.5 ACKNOWLEDGEMENT

We thank Adeniyi Adenuga and Prof. Vincent T. Remcho (OSU Chemistry) for assistance in CZE analysis. TM thanks Khomson Suttisintong for help with the illustrations.

3.6 REFERENCES

1. Whittingham, M. S.; Jacobson, A. J. I*ntercalation Chemistry;* Academic Press: New York, 1982.

2. Ogawa, M.; Kuroda, K. *Bull. Chem. Soc. Jpn.* **1997,** *70*, 2593.

3. Osada, M.; Sasaki, T. *J. Mater. Chem.* **2009,** *19*, 2503.

4. Solin, S. A.; Zabel, H. *Adv. Phys.* **1988,** *37,* 87.

5. Rüdorff, W. *Chimia* **1965,** *19,* 489.

6. Stumpp, E.; Alheid, H.; Schwarz, M.; Janssen, J. J.; Müller-Warmuth, W *J. Phys. Chem. Solids* **1996,** *57,* 925.

7. Scharff, P.; Alheid, H. *Phys. Status Solidi A* **2000,** *177,* 93.

8. Skipper, N. T.; Walters, J. K.; Lobban, C.; McKewn, J.; Mukerji, R.; Martin, G. J.; de Podesta, M.; Hannon, A. C. *J. Phys. Chem. B* **2000,** *104,* 10969.

9. Merle, G.; Letoffe, J. M.; Rashkov, I. B.; Claudy, P. *J. Therm. Anal.* **1978,** *13,* 293.

10. Setton, R.; Beguin, F.; Facchini, L.; Quinton, M. F.; Legrand, A. P.; Ruisinger, B.; Boehm, H. P. *J. Chem. Soc. Chem. Commun.* **1983,** 36.

11. Maluangnont, T.; Gotoh, K.; Fujiwara, K.; Lerner, M. M. *Carbon* **2011,** *49,* 1040.

12. Maluangnont, T.; Bui, G. T.; Huntington, B. A.; Lerner, M. M. *Chem. Mater.* **2011,** *23,* 1091.

13. Isaev, Y. V.; Novikov, Y. N.; Volpin, M. E.; Rashkov, I.; Panayotov, I. *Syn. Met* **1983,** *6,* 9.

15. Duc, C. M.; Gole, J.; Mai, C.; Riviere, R. *J. Chim. Phys.* **1972,** *69,* 991.

16. Goldmann, M.; Beguin, F. *Phase Transitions* **1991,** *30,* 91.

17. Beguin, F.; Pilliere, H. *Carbon* **1998,** *36,* 1759.

18. Cai, J. W.; Zhou, J. S.; Lin, M. L. *J. Mater. Chem.* **2003,** *13,* 1806.

19. Zhou, J. S.; Cai, J. W.; Wang, L.; Ng, S. W. *Dalton Trans.* **2004,** 1493.

20. Zhao, Y. H.; Abraham, M. H.; Zissimos, A. M. *J. Org. Chem.* **2003,** *68*, 7368.

21. Enoki, T.; Suzuki, M.; Endo, M. *Graphite Intercalation Compounds and Applications*; Oxford University Press: New York, 2003.

22. Matsumoto, R.; Takahashi, Y.; Akuzawa, N. *Mol. Cryst. Liq. Cryst.* **2000,** *340*, 43.

23. Rüdorff, W.; Schulze, E.; Rubisch, O. *Z. Anorg. Allg. Chem.* **1955,** *282*, 232.

24. Haynes, W. M., ed., *CRC Handbook of Chemistry and Physics;* 91st Edition (Internet Version 2011), CRC Press/Taylor and Francis: Boca Raton, FL, 2011.

25. Mizutani, Y.; Abe, T.; Inaba, M.; Ogumi, Z. , *Syn. Met.* **2002,** *125*, 153.

26. Mizutani, Y.; Abe, T.; Ikeda, K.; Ihara, E.; Asano, M.; Harada, T.; Inaba, M.; Ogumi, Z. *Carbon* **1997,** *35*, 61.

27. Zhang, Y. P.; Scott, K. J.; Clearfield, A. *J. Mater. Chem.* **1995,** *5*, 315.

28. Cao, G.; Mallouk, T. E. *Inorg. Chem.* **1991,** *30*, 1434.

29. Cao, G.; Lynch, V. M.; Yacullo, L. N. *Chem. Mater.* **1993,** *5*, 1000.

30. García-Ponce, L.; Moreno-Real, L.; Jiménez-López, A. *Can. J. Chem.* **1990,** *68*, 592.

31. Benes, L.; Zima, V.; Melanova, K. *Eur. J. Inorg. Chem.* **2001,** 1883.

CHAPTER 4

CATION-DIRECTED ORIENTATION OF AMINES IN TERNARY GRAPHITE INTERCALATION COMPOUNDS

Tosapol Maluangnont,[a] Kazuma Gotoh,[b] Kazuya Fujiwara,[b] and Michael M. Lerner[a]

[a] Department of Chemistry

Oregon State University

Corvallis, OR 97331-4003, USA

[b] Graduate School of Natural Science and Technology

Okayama University

Okayama 700-8530, Japan

Carbon, **2011,** *49,* 1040-1042.

4.1 ABSTRACT

1,2-Diaminopropane (12DAP) provides an unusual example of an organic co-intercalate where graphite intercalation compounds (GICs) show intra-gallery orientation dependant on the identity of the alkali metal cation intercalate (Li^+, Na^+, or K^+). The GIC gallery heights, K-12DAP-GIC = 0.697 nm and Li-12DAP-GIC = 0.782 nm, indicate 12DAP long axis orientations that are parallel or perpendicular to the graphene sheets, respectively.

4.2 INTRODUCTION

Donor-type graphite intercalation compounds (GICs) have been widely studied for their unique chemical and physical properties, and their technological importance - especially LiC_6 in battery anodes.[1] Binary GICs of this type MC_x (M = alkali, alkaline earth, and a few other metals) have been studied extensively, and R_4NC_x has been reported. Many ternary GICs are known, typically where alkali metal cations intercalate along with co-intercalates that include H, N_2, Hg, Tl, pnictinides, chalcogenides, and organic molecules such as amines, ethers, benzene, and dimethylsulfoxide. For an overview of these GICs see ref[1]. The gallery heights (d_i) of the ternary GICs containing organic co-intercalates, *i.e.* the separation of carbon sheet centers along the stacking direction, are generally independent of the specific metal cation intercalate. In other words, the orientation and therefore steric height requirement of the organic co-intercalate is independent of the identity of the alkali metal cation. Examples of this include GICs (d_i in parentheses) with co-intercalates NH_3 (0.658-0.662 nm), 1,2-dimethoxyethane (1.16-1.20 nm), 2-methyltetrahydrofuran (0.722-0.738 nm), and furan (0.878-0.900 nm).[2] We report herein the synthesis of several new GICs, abbreviated as M-12DAP-C where M = Li, Na, or K, and 12-DAP = 1,2-diaminopropane. These new GICs show a cation-dependent orientation of the organic co-intercalates. In contrast to the trend of increasing alkali cation radii and corresponding gallery heights for LiC_x to KC_x,[1] the M-12DAP-GIC compounds have decreasing gallery heights from M= Li to K.

4.3 EXPERIMENTAL

In a typical reaction, 0.25 g of graphite powder (SP-1 grade, Union Carbide, average particle size 100 μm) and metallic Li, Na, or K (mol C / mol M = 8) were added to 4 mL of 12DAP under Ar (Li) or N_2 (Na, K). The reactants were stirred at 90 ºC for 1-3 days, after which the sample was centrifuged and top liquid phase removed, leaving a wet powder product. Samples were dried for 6 h at 60 ºC under vacuum. Powder XRD (PXRD) patterns (recorded on a Rigaku MiniFlex II, Ni-filtered CuKα radiation, 3-60° at 0.02° 2θ steps) were collected on the wet powder products. Thermogravimetric analyses (TGA) (Shimadzu TGA-50) were performed on the dried samples at 5 ºC/min under Ar flow (20 mL/ min). Solid state ^{7}Li NMR spectra (Varian Inova 300, 116.6 MHz) were recorded at ambient temperature (referenced to saturated LiCl solution at 0 ppm) using a single pulse sequence with pulse delay = 5 s and a $\pi/2$ pulse = 5 μs. Structure calculations were determined using the hybrid density functional method (B3LYP) with a 6-31G+(d,p) basis set and Gaussian 3.0 software.

4.4 RESULTS AND DISCUSSION

The blue solids isolated in each case show PXRD patterns with several diffraction peaks, all are indexed for stage 1 GIC products (Fig. 4.1). The GIC gallery heights (d_i) found are Li-12DAP-GIC (d_i = 0.782 nm), Na-12DAP-GIC (d_i = 0.749 nm), and K-12DAP-GIC (d_i = 0.697 nm). Subtracting the thickness of one graphene layer (0.335 nm) gives expansions due to intercalation of 0.447, 0.414, and 0.362 nm,

respectively. These expansions relate to the dimension of 12DAP along the stacking direction in the GICs. The different dimensions indicate a change in the orientations of 12DAP.

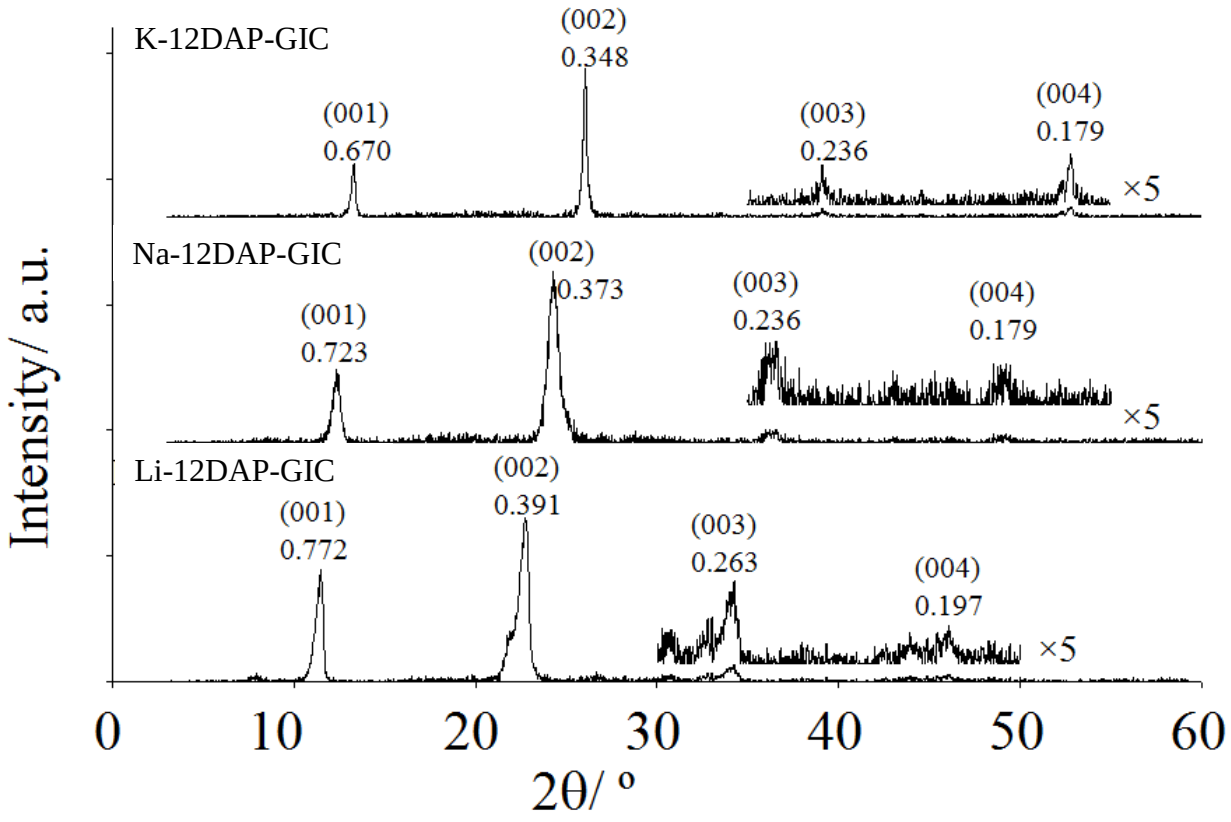

Figure 4.1 PXRD patterns with assigned (*hkl*) indices and d-spacing values (nm) added for M-12DAP-GIC products.

For K-12DAP-GIC, the smaller expansion of 0.362 nm sterically requires a 12DAP orientation with the CH_2CH_2 bond axis parallel to the graphene sheets; a similar expansion and orientation has been reported previously for $SnS_2(12DAP)_{0.45}$.[3] A structure model for this product is provided in Fig. 4.2(a). The structure model shows the required 12DAP orientation, and has the amine chelating the K^+ intercalate. Fig. 4.2(b) shows a structure model for Li-12DAP-GIC. Since the maximum calculated dimension for a Li^+-12DAP chelate complex of 0.447 nm is close to the observed co-intercalate dimension (0.476 nm), the 12DAP co-intercalate is most likely oriented with long axis perpendicular to the encasing graphene surfaces. Other 12DAP conformations that do not allow formation of the chelation complex are also possible, but would be much less energetically favorable. For Na-12DAP-GIC, the intermediate gallery height suggests an intermediate 12DAP orientation.

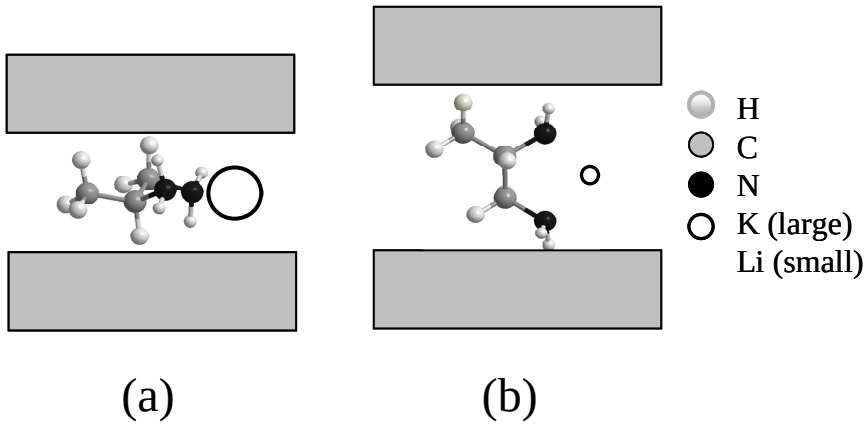

Figure 4.2 Structure models for (a) K-12DAP-GIC and (b) Li-12DAP-GIC, showing the different orientations of 12DAP intercalates and the chelation of cations by 12DAP.

These GICs show the mass loss from RT to 250 °C (23.9% for Li-12DAP-GIC, 19.3% for Na-12DAP-GIC) ascribed to the loss of amine intercalate. Values from different batches agree within 2%. K-12DAP-GIC was not stable after drying and the amine content could not be established by TGA. Assuming an amine-to-cation ratio of 1 as in ref [4,5] yields x = 19 for M = Li, and x = 24 for M = Na for the general formula M(12DAP)C_x. These ratios are much lower than those reported for other amine GICs where x = 53 for a GIC containing K and *N,N,N',N'*-tetramethylethylenediamine (calc from 14.4% amine wt pct),[5] [4], and x = 28 for a GIC containing Li and ethylenediamine (calc from 14.9% amine wt pct).[4]

Fig. 4.3 shows the ^{7}Li NMR spectra of Li-12DAP-GIC. The spectra show a broad peak at 0-6 ppm in both the static and MAS modes. The peak position indicates that Li is present as ionic Li^+ and interacting with the amine co-intercalate; in contrast stage 1 or 2 LiC_x, where Li strongly interacts with graphene layers, show NMR shifts of 42-43 ppm, and quasi-metallic Li in amorphous carbon is observed at over 80 ppm.[6,7] NMR peaks and sidebands remain broad in the MAS spectrum, indicating some distribution of chemical environments or an anisotropic Li environment. Although satellite peaks have been reported for a GIC containing Li and THF,[7] they are not present here, also implying a distribution in Li environments.

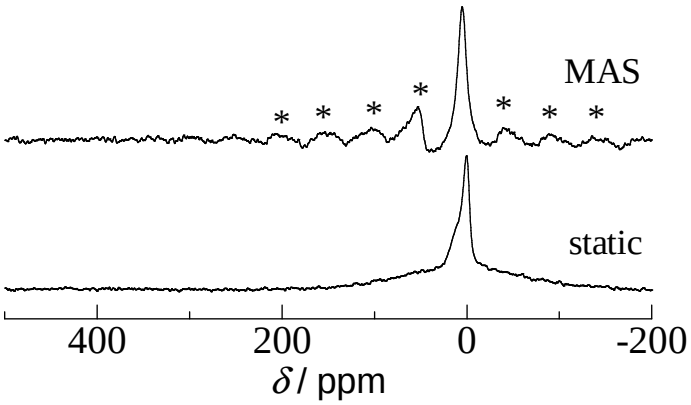

Figure 4.3 The ^{7}Li MAS- and static-NMR spectra of Li-12DAP-GIC. (*) indicates spinning side bands.

The cation-dependent orientation of the organic co-intercalates observed here is not common for ternary GICs. The few examples of ternary GICs that do show a strong cation effect include M-THF-GIC (M = Cs, d_i = 0.71 nm; M = K, d_i = 0.89 nm),[8] and M-N_2-GIC (M = K, d_i = 0.957 nm; M = Cs, d_i = 0.901-0.903 nm).[9] It is notable that in all these cases, counter to any expectation for a trend related to the size of the alkali cations, the larger cations all result in smaller gallery heights for GICs.

We are currently exploring additional GIC chemistry with amines co-intercalates. Due to the wide range in number and type of substituents possible, amines provide a diverse range of co-intercalate candidates. Diamines and polyamines further broaden the potential chemistry of this class of compounds.

4.5 ACKNOWLEDGEMENT

TM thanks the financial support from Whiteley Fellowship in Material Sciences for summer 2010 during which the manuscript was prepared.

4.6 REFERENCES

1. Enoki, T.; Suzuki, M.; Endo, M. *Graphite Intercalation Compounds and Applications*; 1st ed.; Oxford University Press: New York, 2003.

2. Jegoudez, J.; Mazieres, C.; Setton, R. *Carbon* **1986,** *24*, 747.

3. Morales, J.; Santos, J.; Barrado, J. R. R.; Espinos, J. P.; Gonzalez-Elipe, A. R. *J. Solid St. Chem.* **2000,** *150*, 391.

4. Rüdorff, W. *Chimia* **1965,** *19*, 489.

5. Merle, G.; Letoffe, J. M.; Rashkov, I. B.; Claudy, P. *J. Therm. Anal.* **1978,** *13*, 293.

6. Beguin, F.; Gonzalez, B.; Conard, J.; Estradeszwarkopf, H.; Guerard, D. *Syn. Met.* **1985,** *12*, 187.

7. Tatsumi, K.; Zaghib, K.; Sawada, Y.; Abe, H.; Osaki, T. In *Rechargeable lithium and lithium-ion batteries*, Megahed, S.; Barnett, B. M.; Xie, L., Eds. The Electrochemical Society: 1994; pp 97-109.

8. Schmidt, C.; Rosen, M. E.; Caplan, D. F.; Pines, A.; Quinton, M. F. *J. Phys. Chem.* **1995,** *99*, 10565.

9. Moreh, R.; Pinto, H.; Finkelstein, Y.; Beguin, F. *J. Phys. Chem. Solids* **1996,** *57*, 909.

CHAPTER 5

SYNTHESIS OF TERNARY AND QUATERNARY GRAPHITE INTERCALATION COMPOUNDS CONTAINING ALKALI METAL CATIONS AND DIAMINES

Tosapol Maluangnont and Michael M. Lerner

Department of Chemistry

Oregon State University

Corvallis, OR 97331-4003, USA

Inorg. Chem., submitted

5.1 ABSTRACT

A series of ternary graphite intercalation compounds of alkali metal cations (M = Li, Na, K) and diamines [EN (ethylenediamine), 12DAP (1,2-diaminopropane), and DMEDA (*N*,*N*-dimethylethylenediamine)] are reported. These include stage 1 and 2 M-EN-GIC (M = Li, d_i = 0.68-0.84 nm; M = Na, d_i = 0.68 nm), stage 2 Li-12DAP-GIC (d_i = 0.83 nm), and stage 1 and 2 Li-DMEDA-GIC (d_i = 0.91 nm), where d_i is the gallery height. For M = Li a perpendicular-to-parallel transition of EN is observed upon evacuation, whereas for M = Na the EN remains in parallel orientation. Li-12DAP-GIC and Li-DMEDA-GIC show chelation of Li^+ instead of the head-to-tail bonding, and the inhibition of the perpendicular-to-parallel transition. We also report the quaternary compounds of mixed cations (Li,Na)-12DAP-GIC and mixed amines Na-(EN,12DAP)-GIC, with d_i values in both cases between the ternary end members. However, (Li,Na)-12DAP-GIC is a solid solution with lattice dimensions dependent on composition, whereas for Na-(EN,12DAP)-GIC the lattice dimension does not change with relative amine contents.

5.2 INTRODUCTION

Intercalation chemistry is the insertion of guest species into layered host materials. This results in changes in both structures and properties of the layered host and guest.[1] Intercalation compounds have numerous applications, including the adsorption of toxins, the use as photo and electro-functional materials, or are precursors in the formation of clay-polymer nanocomposites with enhanced mechanical properties.[2] The insertion of large guests can generate microporosity within layered materials, and can contribute to the delamination of the layered hosts into individual sheets. The latter process, known as exfoliation, provides a route to reassembled materials with novel magnetic, optical and electronic properties.[3,4] Graphene is an example of a single-sheet material that has received much attention,[5] and for which there is much interest in developing an exfoliation method for large-scale synthesis.[6,7] A fundamental understanding of intercalation energetics, as well as intercalate composition and arrangement, is essential to design materials with new properties and new routes to expanded or exfoliated sheet materials.

α,ω-Diamines $H_2N(CH_2)_xNH_2$ have been widely employed as intercalate guests. Several host structures are known to incorporate diamines, including the layered metal (hydrogen/oxo)phosphates, metal chalcogenides, metal oxychloride, metal oxides and clays.[1] The incorporation of diamines into a 3-dimensional host structures such as zeolite ZSM-5 and Y[8] is also known. In addition to the parallel or perpendicular orientations that are observed with monoamine analogs, the presence of functional groups at both ends of diamines can result in more complex intragallery

arrangements. For example, different bonding modes of diamines intercalated into graphite oxide (GO) have been proposed.[9] These include (i) bridging two different layers, (ii) looping the two active sites on the same layer, and (iii) tailing where only one side is bonded and the other side is free.

In donor-type graphite intercalation compounds (GICs), the graphene sheets are reduced and cations intercalate to maintain charge neutrality.[10-12] Ternary GICs are produced when the metal cations intercalate as solvated ions. The number of GICs prepared containing diamines is surprisingly limited. The stage 2 compound Li-EN-GIC (EN = ethylenediamine) was reported by Rüdorff *et al.*[13] through the direct reaction of graphite, EN, and Li metal. However the orientation of EN within the intercalate galleries was not discussed in that report. Later, Merle *et al.*[14] prepared K-TMEDA-GIC (TMEDA = *N*,*N*,*N'*,*N'*-tetramethylethylenediamine) by the ternarization of KC_{24} with TMEDA. More recently, we reported that M-12DAP-GICs (M = Li, Na, K; 12DAP = 1,2-diaminopropane)[15] can be prepared and show cation-directed orientation of the amine co-intercalate. The GIC containing the macrocylic cyptand "K222" (4,7,13,16,21,24-hexaoxa-1,10-diazabicyclo[8.8.8]hexacosane)[16] with both oxygen and nitrogen donor atoms has also been reported. In addition to these diamine intercalates, there are several known GICs containing monoamines, including ammonia,[17-19] methylamine,[20] and triethylamine.[14] We added several new GICs to this list, reporting the synthesis of a homologous series of ternary GICs containing Na^+ solvated by *n*-alkylamines with *x* carbon atoms, Na-nC*x*-GIC (*x* = 3, 4, 6, 8, 12, and 14).[21] A more recent study also compared the structure of the ternary GICs of alkali

metals and linear *vs* branched amines.[22] In this article, we describe several new GICs containing alkali metal cations (M = Li, Na, K) with diamines. We will describe the intragallery structure and composition for the different cations as well as varying (i) diamine carbon chain lengths, *i.e. x* in $H_2N(CH_2)_xNH_2$, (ii) methyl substitution at the amine, *i.e.* $–NH_2$ *vs.* $–N(CH_3)_2$, and (iii) structural isomerism such as in $H_2N(CH_2)_3NH_2$ *vs* $H_2NCH_2CH(NH_2)CH_3$.

The rich structural chemistry of ternary M-amine-GICs can be expanded by employing the mixture of alkali metal cations or of the mixed amines, resulting in the quaternary compounds. The only donor-type quaternary GICs containing two metal cations and organic co-intercalate that we are aware of is $MHg(benzene)_2C_8$ (M = K, Rb),[23] which display a heterostructure of the sequence C-M-Hg-M-C-benzene-C along the stacking direction. Quaternary GICs with two organic intercalates include Li-(THF,BzN)-GIC[24] and K-(THF,Bz)-GIC[25] (THF = tetrahydrofuran, Bz = benzene, Bz = benzonitrile). We report herein the synthesis, structural features, and kinetics of the quaternary compounds (Li,Na)-12DAP-GIC and Na-(EN,12DAP)-GIC.

5.3 EXPERIMENTAL

All synthesis and handling of the air-sensitive reagents and the resulting GICs were performed under an inert atmosphere (N_2 for Na, K; Ar for Li) using a dry-box or septum-syringe techniques. Diamines were dried over molecular sieve 4A prior to use. The structures of the diamines employed, including their abbreviations, are shown in Fig. 5.1. In a typical synthesis of stage 1 compounds, 0.25 g (21 mmol) of

polycrystalline graphite powder (SP-1, Union Carbide, average particle dia. 100 μm) was mixed with 0.060 g of Na metal (99.95%, Alfa Aesar) (2.6 mmol) and the amine (2 mL). ***Caution! Alkali metals are highly flammable when in contact with air and/or water and should be handled with care.*** The reaction mixtures were *vigorously* stirred at 70 ºC for the following period: Na-EN-GIC (1 d), Na-12DAP-GIC (3 d), Li-12DAP-GIC (6 h), and Li-DMEDA-GIC (12 h). The stage 1 Li-EN-GIC is more reproducibly produced using 0.030 g (4.3 mmol) of Li (3 d). ***Caution! Pressure may increase and must be vented, especially for Li-12DAP-GIC.*** To synthesize stage 2 compounds, the above-mentioned conditions were optimized as follows: Na-EN-GIC (0.010 g of Na, 0.4 mmol, 3 d), Li-EN-GIC (0.010 g Li, 1.4 mmol, 3 d), Li-12DAP-GIC (5 mL of 12DAP, *occasionally* stirred), Li-DMEDA-GIC (7 d). The synthesis of Li-DMEDA-GIC is poorly reproducible. The quaternary (Li,Na)-12DAP-GIC was synthesized by employing 2.6 mmol of *each* metal to react with graphite and 12DAP. The quaternary Na-(EN,12DAP)-GIC was synthesized starting from 0.25 g of dry stage 2-Na-EN-GIC with 2.6 mmol of Na and 2mL of 12DAP. The mixtures were reacted for 0.5-72 h. The liquid amines were removed by centrifugation immediately, and the GIC products were rinsed briefly with the amine. GIC products denoted “as prepared” were characterized after centrifugation and brief washing without further processing, other samples were placed under vacuum (<100 μm) at 60 ºC for 6 h. Different drying conditions were applied for Li-EN-GIC (as described below).

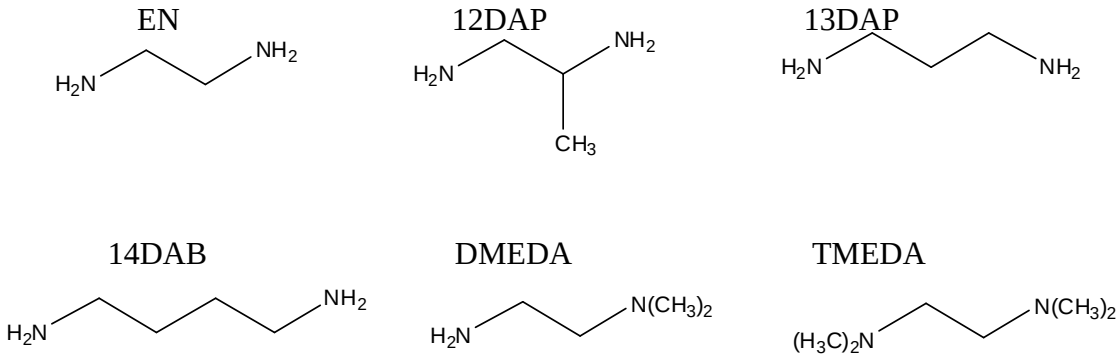

Figure 5.1 Structure of the diamines and abbreviations used in this work.

Powder X-ray Diffraction (PXRD) data were collected on a Rigaku MiniFlex II, using Ni-filtered Cu Kα radiation, with 0.02° 2θ steps from 5° to 35°. Sample holders were sealed with a plastic tape window to prevent decomposition in air during the PXRD measurement. The *(00l)* reflections were indexed according to the relation $I_c = d_i + (n\text{-}1)(0.335\text{ nm})$, where I_c is the identity period obtained directly from diffraction data, d_i is the gallery height, n is the GIC stage number, and 0.335 nm is the distance between two adjacent graphene sheets. The gallery expansion, Δd, is defined as $\Delta d = d_i - 0.335$ nm. Figure 5.2(a) illustrates these dimensions schematically. Thermogravimetric analysis (TGA) was performed using a Shimadzu TGA-50 under flowing Ar gas (20 mL/min) from RT to 800 ºC at 5 ºC/min. Elemental analyses for alkali metals were performed using Capillary Zone Electrophoresis (Agilent Technologies HP^{3D}CE equipped with a UV detector) with an indirect detection mode at 210 nm, after alkali cations in GICs were extracted into the liquid phase by a gentle

boiling in 3/1 (v/v) HCl/HNO_3 as described previously.[22] GICs synthesized from different batches and separately analyzed showed amine contents agreeing within 2%, and the alkali metal contents within 0.1% (Na) and 3% (Li). The amine co-intercalate structures were optimized using the hybrid density functional method (B3LYP) with a 6-31+G(d,p) basis set and Gaussian 3.0 software.

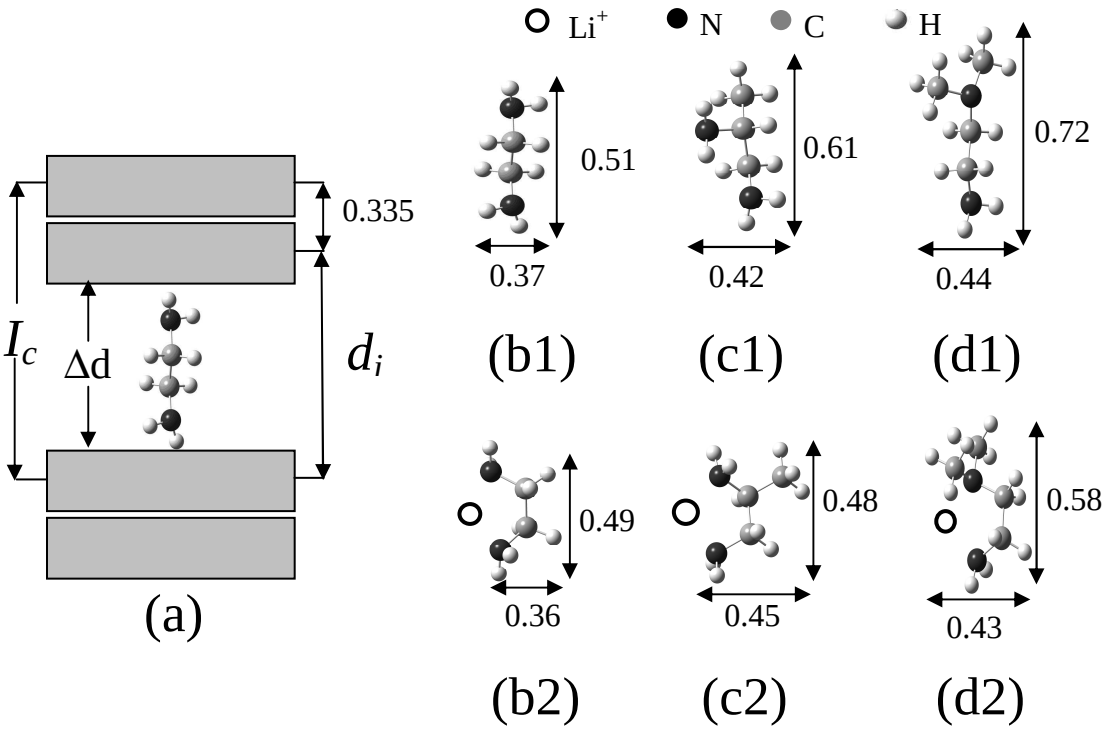

Figure 5.2 (a) Structural parameters used to describe GICs, shown here as stage 2, and calculated dimensions in nm of (b) EN, (c) 12DAP, and (d) DMEDA. The labels 1 and 2 indicate bonding in the head-to-tail (monodentate) and chelation (bidentate) modes, respectively.

5.4 RESULTS AND DISCUSSION

5.4.1 GICs of Ethylenediamine

Fig. 5.3(a,d) show PXRD patterns of wet blue/black products obtained by reacting graphite with Li(m) and EN. Following Rüdorff *et al.*,[13] these products can be assigned as stage 2 Li-EN-GIC (I_c = 1.176 nm, d_i = 0.841 nm *vs* the reported d_i of 0.85 nm[13]) and stage 1 (d_i = 0.855 nm, not reported previously). The stage 1 Li-EN-GIC is prepared by employing 4.3 mmol of Li (instead of 1.4 mmol for stage 2) while fixing the amount of graphite at 21 mmol. The gallery expansions for both stages, Δd ~ 0.5 nm, agree with the calculated dimension of EN (Fig. 1(b1)) with a perpendicular orientation relative to the graphene sheets with EN bonding to Li^+ in head-to-tail fashion, *i.e.*, a monodentate interaction.

Following evacuation at 60 ºC, the stage 1 and 2 phases undergo a structural change and transform into phases with smaller gallery dimensions (d_i = 0.676 and 0.684 nm respectively, Δd ~ 0.35 nm), as shown in Figure 2(b,c,e). From the diamine steric requirements, these phases must have the EN oriented parallel to the graphene sheets. The head-to-tail and chelate structures have similar dimensions with this orientation and either fits well with the observed dimensions. The expansion for the parallel orientation also agree well with the known monolayer thickness of amines in related GICs such as Na-*n*-alkylamine-GIC,[21] and in other host structures such as TiOCl and VOCl,[26] or TaS_2.[27] In the case of graphite oxide (GO),[9] EN is also in parallel orientation, and by varying x in $H_2N(CH_2)_xNH_2$, the interlayer distance of graphite oxide increases slowly from 0.64 nm (pristine GO) to 0.84 nm (x = 4) to 0.99

nm (x = 10). GO and amines interact via functional groups on GO, which is different from the redox intercalation in donor-type GICs.

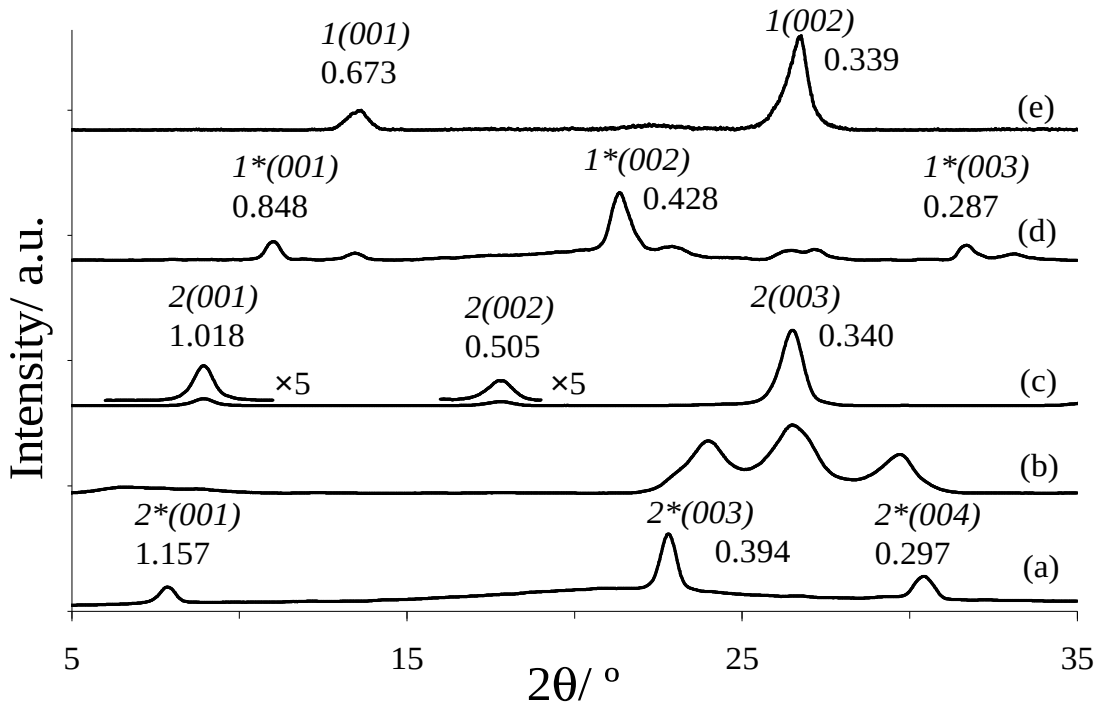

Figure 5.3 PXRD patterns of Li-EN-GICs: (a) stage 2 as prepared; (b) after 3 h and (c) 6 h evacuation at 60°C; (d) stage 1 as prepared; and (e) after 6 h evacuation at 60°C. Perpendicular phase reflections are indicated with an asterisk. The *d* values (in nm) and assigned Miller indices *n(00l)* are indicated for each reflection, where *n* is the stage number.

In comparing the related ternary GICs, Li-$H_2NCH_2CH_2X$-GICs with X = CH_3 (*n*-propylamine),[21] X = CH_2CH_3 (*n*-butylamine),[21] and X = NH_2 (EN), only the latter

shows the perpendicular-to-parallel transition after evacuation. The other GICs always retain a parallel intercalate orientation.

The cation plays a significant role in directing the orientation of the organic co-intercalates in M-EN-GIC. Fig. 5.4(a,b) shows the PXRD pattern of the stage 1 (d_i = 0.691 nm) and stage 2 (d_i = 0.676 nm) Na-EN-GIC. The as-prepared and evacuated GICs both show Δd ~ 0.36 nm, indicating a parallel EN orientation.

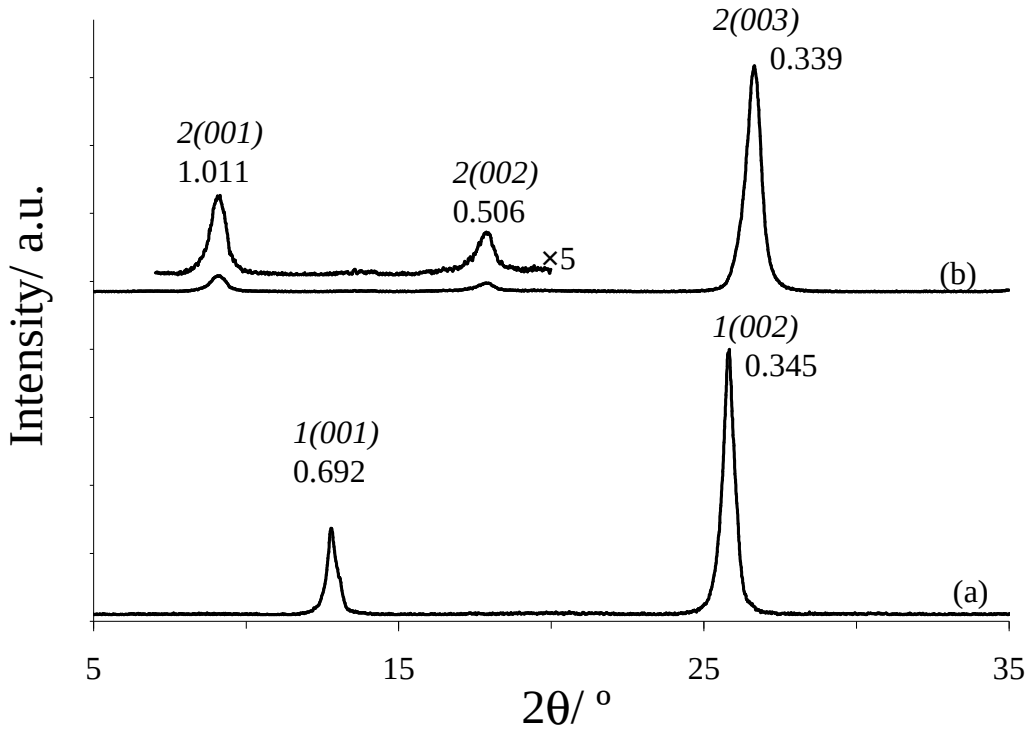

Figure 5.4 The PXRD patterns of (a) stage 1, and (b) stage 2 Na-EN-GIC. The *d* values (in nm) and assigned Miller indices *n(00l)* are indicated for each reflection, where *n* is the stage number.

These M-EN-GIC (M = Li, Na) provide another example where a strong cation directing effect occurs, the other reported cases are for M-THF-GIC[28] [d_i = 0.89 nm (M = K); 0.71 nm (M = Cs)], M-N_2-GIC[29] [d_i = 0.957 nm (M = K); 0.946 nm (M = Cs)], and M-12DAP-GIC[15] [d_i = 0.78 nm (M = Li); 0.75 nm (M = Na); 0.70 nm (M = K)]. In all these cases, counter to the relative cation radii, the gallery dimensions decrease from Li^+ to K^+.

Reaction of graphite, K and EN produces a blue solid product at RT and a black product at 70 ºC. In both cases, the product shows only the *weak (002)* of graphite (not shown). The presence of EN is deduced from TGA mass loss (not shown). It appears that the highly reactive K metal leads to an unstable or amorphous product. Schlögl and Boehm[30] reported that K-THF-GIC decomposed in the mother liquor upon prolonged contact. Alternately, the formation of the EN-solvated K^+ complexes, while known,[31] is less favorable than for Li^+ or Na^+, and this may prevent the formation of an ordered GIC product.

5.4.2 GIC of Substituted Ethylenediamine

The PXRD pattern of Li-12DAP-GIC stage 2 (d_i = 0.827 nm) is shown in Fig. 5.5(a). The stage 1 of this GIC was previously reported with a similar gallery dimension.[15] The gallery expansion Δd of 0.48-0.49 nm is in agreement with the calculated dimension of 12DAP perpendicular to the graphene sheets and chelating the cation, Fig. 5.3(c2).[15] The calculated dimension of 12DAP without chelation (*i.e.*,

along the N-C-C-C backbone), 0.61 nm, is too large. The as-prepared and evacuated products are similar, thus the added methyl group on the amine (Li-12DAP-GIC compared to Li-EN-GIC) prevents intercalate re-orientation. On the other hand, the observed dimensions for K-12DAP-GIC (d_i = 0.697 nm) require that the 12DAP lie parallel to the graphene sheets, whereas in Na-12DAP-GIC (d_i = 0.749 nm) the diamine displays an intermediate orientation.[15]

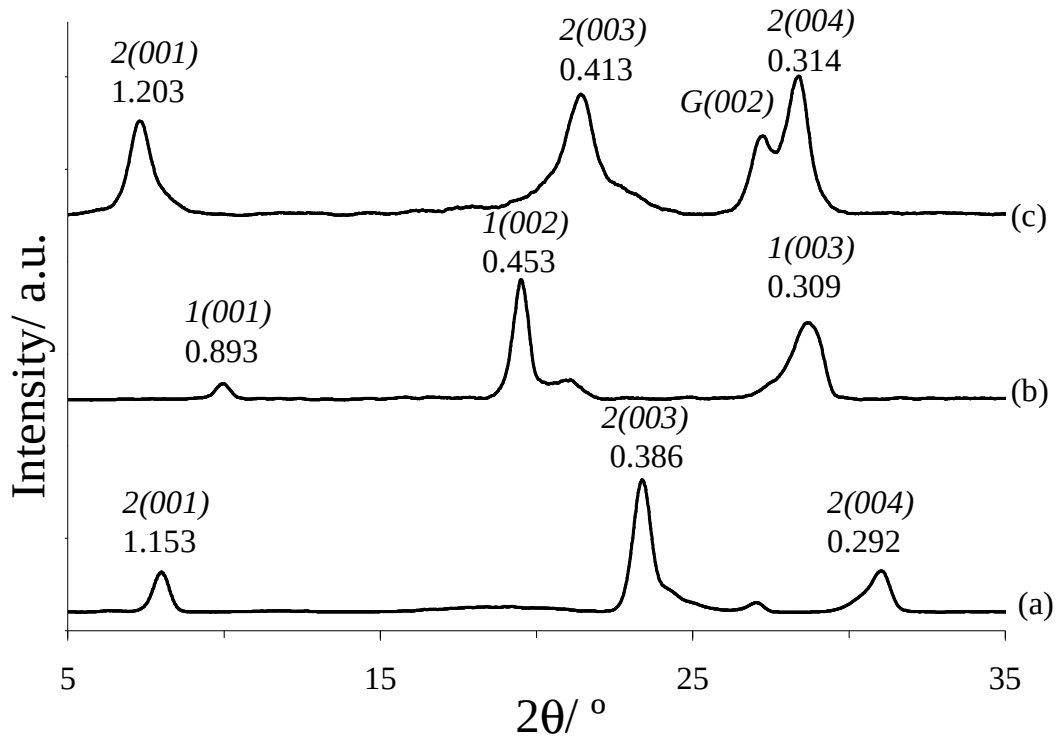

Figure 5.5 PXRD patterns of (a) stage 2 Li-12DAP-GIC, and (b) stage 1 and (c) stage 2 Li-DMEDA-GIC. The *d* values (in nm), stage *n* and assigned Miller indices *n(00l)*, are indicated for each reflection. *G(002)* indicates the graphite *(002)* reflection.

Ternary GICs of alkali metals with 13DAP and 14DAB are not obtained by these methods; in all trials only the *(002)* reflection from graphite is observed after reaction (PXRDs not shown). This underlines the necessity of $-NH_2$ groups in 1,2-position (*i.e.*, vicinal) for intercalation to proceed. Li(m) does not appear to react with and dissolve into 13DAP and 14DAB, whereas Na(m) and K(m) react but do not generate reactive free radicals. The formation of $M^+H_2N(CH_2)_3NH^-$ from 13DAP was reported in the presence of ultrasound (M = Na) or ammonia gas (M = K).[32] Further, Laszlo *et al.*[33] showed by ^{23}Na NMR that the preference for Na^+ solvation by the diamines was in the order 14DAB < 13DAP < EN. Ternary GIC formation is, in part, driven by the solvation enthalpy of co-intercalates, and this provides another explanation for the instability of GICs containing these diamines.

Fig. 5.5(b) shows the PXRD pattern of the product assigned as a stage 1 Li-DMEDA-GIC, d_i = 0.910 nm. As-prepared and evacuated products are similar. DMEDA is structurally related to EN with two additional methyl groups substituted for the two hydrogen atoms on the same amine group, Fig. 5.1. The gallery expansion of $\Delta d \sim 0.58$ nm indicates a perpendicular and chelating DMEDA orientation, similar to that observed for EN and 12DAP, Fig. 5.3(d2). Stage 2 Li-DMEDA-GIC [d_i = 0.916 nm, Fig. 5.5(c)], again with perpendicular, chelating DMEDA was obtained at longer reaction times. Thus, methyl substitution on EN to form 12DAP or DMEDA results in chelation of Li^+ within the GICs and the inhibition of the perpendicular-to-parallel transition.

Although the solvation of Na^+ by DMEDA is known in the solid state,[34] the Na and K analogs of M-DMEDA-GIC were not obtained. The PXRD pattern from the reaction of graphite, Na metal, and DMEDA shows only the unreacted graphite and Na(m) remaining in the reaction tube. A similar result was obtained for K(m), though the DMEDA turned brown, indicating solvent decomposition.

The synthesis of a stage 1 K-TMEDA-GIC (d_i = 0.894 nm) by the ternarization of the KC_{24} with TMEDA is known.[14] Assuming the parallel arrangement of TMEDA, the reported Δd = 0.559 nm is close to that observed (0.563 nm) for intercalation compounds of VOCl and TMEDA.[26] We found that the direct reaction of graphite, K(m), and TMEDA yields a blue product with I_c = 0.855 nm (PXRD not shown), and this phase is assigned as K-TMEDA-GIC following Merle *et al.*[14] Li(m) and Na(m) do not dissolve in TMEDA and do not form GICs by this method. The addition of electron transfer agents (*e.g.,* anthracene, biphenyl, naphthalene) known to assist the formation of ternary GICs of alkali metal cations and ether,[35, 36] does not result in GIC products. The synthetic obstacles for M-TMEDA-GIC (M = Li, Na, K) by the direct method are not due to the instability of metal TMEDA complexes; many known crystal structures show TMEDA solvating Li^+,[37-41] Na^+,[41-43] or K^+.[44, 45]

The formation of radicals/anions/solvated electrons through the reaction of alkali metal with liquid ammonia or small chain amines is well-established in the literature.[46] After reaction with *n*-butyl lithium, free radicals were detected by electron paramagnetic resonance (EPR) for EN and 12DAP, whereas 13DAP and DMEDA were EPR-silent.[47] This is in line with the production of ternary GICs of alkali metals

with EN and 12DAP, but non-reaction of 13DAP. DMEDA does intercalate, contrary to this model, this discrepancy might be related to the use of Li metal as a reducing agent rather than *n*-butyl lithium.

5.4.3 Compositional Analyses

Representative mass loss curves for the GIC products obtained are shown in Fig. 5.6. All show mass losses from 50−150 °C, followed by a higher temperature mass loss with an onset around 600 °C. The lower temperature loss is ascribed to intercalate volatilization, and the latter to the decomposition of the graphitic host lattice. This high temperature mass loss is also observed for a graphite control sample (not shown), and is due to the presence of trace O_2 in the flow gas. GIC compositions obtained from TGA mass losses and elemental analyses are provided in Table 5.1.

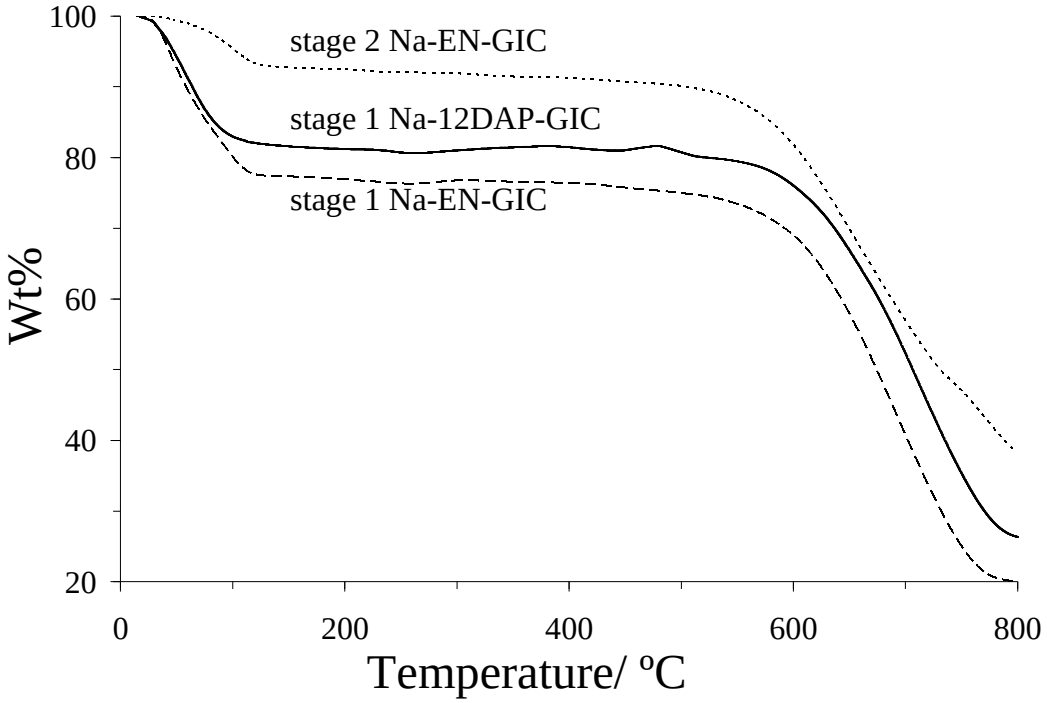

Figure 5.6 TGA mass loss data for GIC products.

Table 5.1 Compositional data for ternary M-diamine-GICs

Diamine	Cation M	Stage no.	Wt% M	Wt% diamine	Composition	Packing fraction
EN	Li	2	1.72	14.9	$Li_1(EN)_{1.0}C_{28}$[a]	0.35
	Li	2	1.95	11.2	$Li_1(EN)_{0.7}C_{26}$	0.28
	Li	1	2.96	20.8	$Li_1(EN)_{0.8}C_{15}$	0.40
	Na	2	6.50	10.0	$Na_1(EN)_{0.6}C_{25}$	0.40
	Na	1	8.66	21.7	$Na_1(EN)_{1.0}C_{15}$	0.51
12DAP	Li	1	2.82	28.7	$Li_1(12DAP)_{0.95}C_{14}$	0.45
	Li	2	1.76	17.7	$Li_1(12DAP)_{0.94}C_{26}$	0.47
	Na	1	5.70	24.2	$Na_1(12DAP)_{1.3}C_{24}$	0.44

[a] reference 13

The diamine/M molar ratios are generally close to 1/1 similar to *e.g.,* Na-*n*-propylamine-GIC[21] and others.[48] The composition of the stage 2 perpendicular $Li_1(EN)_{0.7}C_{26}$ found is similar to the reported $Li_1(EN)_{1.0}C_{28}$.[13] The T_d geometry around solvated Li^+ is documented in other GICs such as Li-THF-GIC[49] or Li-DME-GIC.[50] However, the mole ratios found above indicate lower coordination numbers for GICs with diamine intercalates. For most products obtained, the compositions of these ternary GICs are close to one metal cation for 15 (or 26) for stage 1 (or stage 2) graphene C atoms.

The packing fractions within the intercalate galleries are obtained by comparing the experimentally obtained compositions and structural data. For example, with Li-EN-GIC, the values required are the volume of Li^+ (0.0016 nm^3), the van der Waals molar volume of EN (0.0651 nm^3),[51] the surface area per C atom in a graphene layer (0.0261 nm^2), and the experimentally determined GIC composition, stage number, and intercalate gallery expansion. The packing density, or fraction of volume in the expanded galleries occupied by intercalates, can then be determined as:

$$[(0.0016\ nm^3 + (0.7)(0.0651\ nm^3)) / [(26/2)(0.0261\ nm^2)(0.505\ nm)] = 0.28$$

The calculated packing fractions are shown in Table 4.1, and fall in the range ≈0.2-0.5. These values show a wide range for other ternary GICs, from about 0.1-0.7.[14, 17, 20-22] Recently Han *et al.*[52] proposed Li-THF-GIC as a new hydrogen storage material based on the porous galleries. Several new ternary GICs synthesized in this work could be interesting materials to test for H_2 storage.

5.4.4 Quaternary GIC with Two Metal Cation Co-intercalates

Solid solutions of Li,Na-amine-GIC can be prepared directly by reaction of graphite with two alkali metals and the amine. PXRD patterns of products from different reaction times are shown in Fig. 5.7 and compositional results in Table 5.2. In all cases, quaternary stage 1 GICs are obtained. A gradual shift in d_i (in nm) with reaction time is observed: 0.806 (0.5 h), 0.802 (1.5 h), 0.775 (3.25 h), 0.768 (6 h), 0.766 (10 h), and 0.743 (24 h). The shorter reaction times show gallery dimensions

closer to that of Li-12DAP-GIC (d_i = 0.816 nm), whereas long reaction times show dimensions more similar to Na-12DAP-GIC (d_i = 0.749 nm). As shown in Table 5.2, Li content decreases, and Na content increases, as the reaction proceeds.

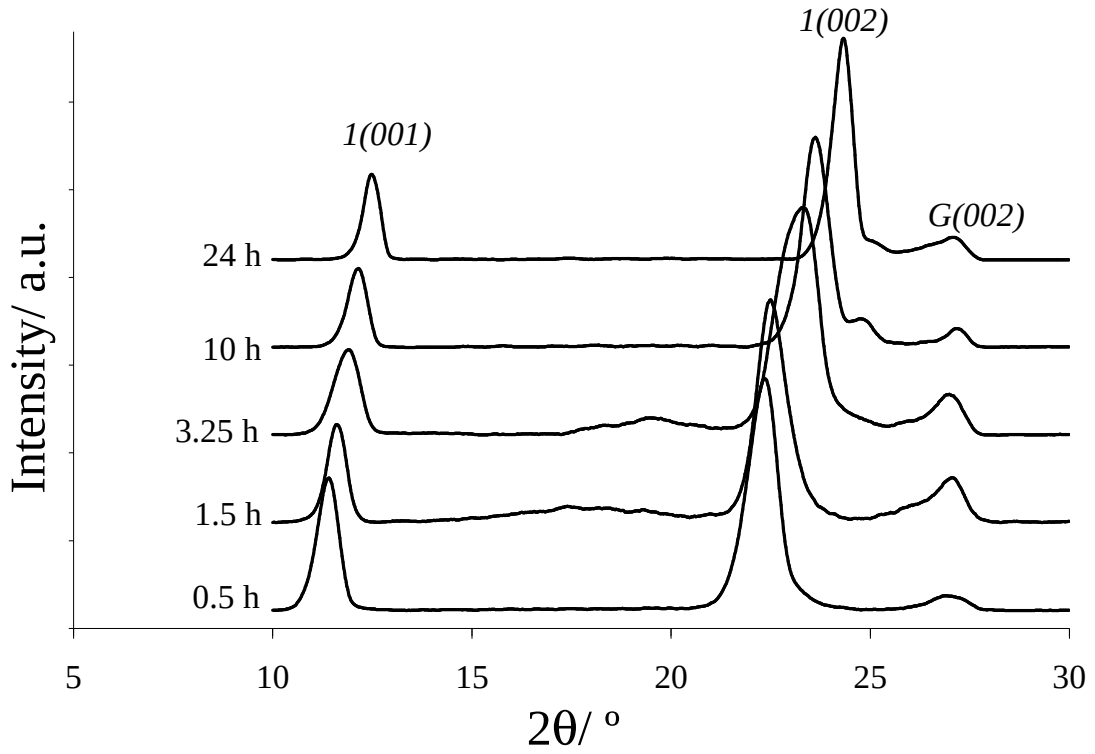

Figure 5.7 Selected PXRD patterns of the first stage (Li,Na)-12DAP-GIC made by direct synthesis at different reaction times. *G(002)* indicates the *(002)* reflection from graphite.

Table 5.2 Structural and compositional data of the quaternary (Li,Na)-12DAP-GIC.

Time/ h	Wt% (Metal)	Wt% diamine	Derived composition
0.5	3.12 (Li), not detected (Na)	29.8	$Li_1(12DAP)_{0.9}C_{12}$
1.5	3.52 (Li), 0.24 (Na)	28.5	$(Li_{0.98}Na_{0.02})(12DAP)_{0.7}C_{11}$
6	2.75 (Li), 0.66 (Na)	25.2	$(Li_{0.93}Na_{0.07})(12DAP)_{0.8}C_{15}$
10	2.05 (Li), 0.53 (Na)	26.7	$(Li_{0.93}Na_{0.07})(12DAP)_{1.1}C_{19}$
24	2.18 (Li), 3.79 (Na)	24.2	$(Li_{0.66}Na_{0.34})(12DAP)_{0.7}C_{12}$

The continuous change in lattice dimension *vs* the Li content [*x*, in $Li_xNa_{1-x}(12DAP)_yC_z$] follows Vegard's law for solid solutions, Figure 5.8. Composition-dependent lattice variations, either linear or with anomaly, were reported for the compound $K_{1-x}Rb_xC_8$.[53-55] In the present case, Li metal reacts with 12DAP rapidly, forming the Li^+-12DAP complexes that intercalate first (Note the optimized reaction times are 6 h *vs* 3 days for Li- and Na-12DAP-GIC respectively, see Experimental.) Some Li^+ complexes are more slowly displaced by Na^+-12DAP as reaction times increase. Li^+-12DAP can also displace the Na^+ complexes in a prepared Na-12DAP-GIC sample (data not shown), suggesting there is little thermodynamic preference for either complex, and that reaction kinetics plays a dominant role. In addition to

$M(12DAP)_y^+$ (M = Li, Na) complexes, the $Na(EN)_y^+$ complexes can also be exchanged with tetraalkylammonium cations,[56] resulting in a new route to novel GICs.

The only other quaternary GIC of this type that we are aware of, $MHg(benzene)_2C_8$ (M = K, Rb),[23] forms ordered heterostructures as opposed to the solid solutions observed here.

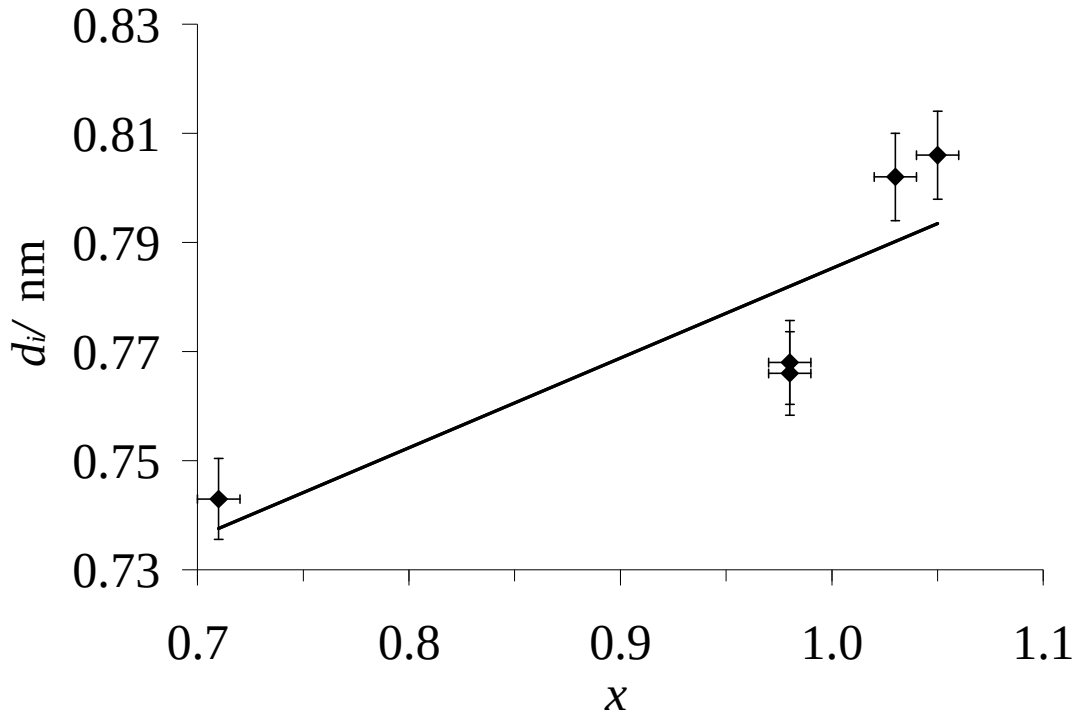

Figure 5.8 A plot of d_i of the first stage (Li,Na)-12DAP-GIC *vs* the Li content *x* as in $(Li_xNa_{1-x})(12DAP)_yC_z$. The y-error bars for d_i show ± one standard deviation. The x-error bars are ± 0.01.

5.4.5 Quaternary GICs with Two Amine Co-intercalates

When stage 2 Na-EN-GIC [d_i = 0.678 nm, Fig. 5.9(a)] reacts with Na(m) and 12DAP, the solid changes from black/blue to intense blue. The PXRD patterns for the obtained products are shown in Fig. 5.9(b) to (d). A stage 1 quaternary Na-(EN,12DAP)-GIC (d_i = 0.716 nm) is observed with a gallery dimension intermediate between Na-EN-GIC (0.691) and Na-12DAP-GIC (0.749). At long reaction times, Na-12DAP-GIC appears in addition to Na-(EN,12DAP)-GIC.

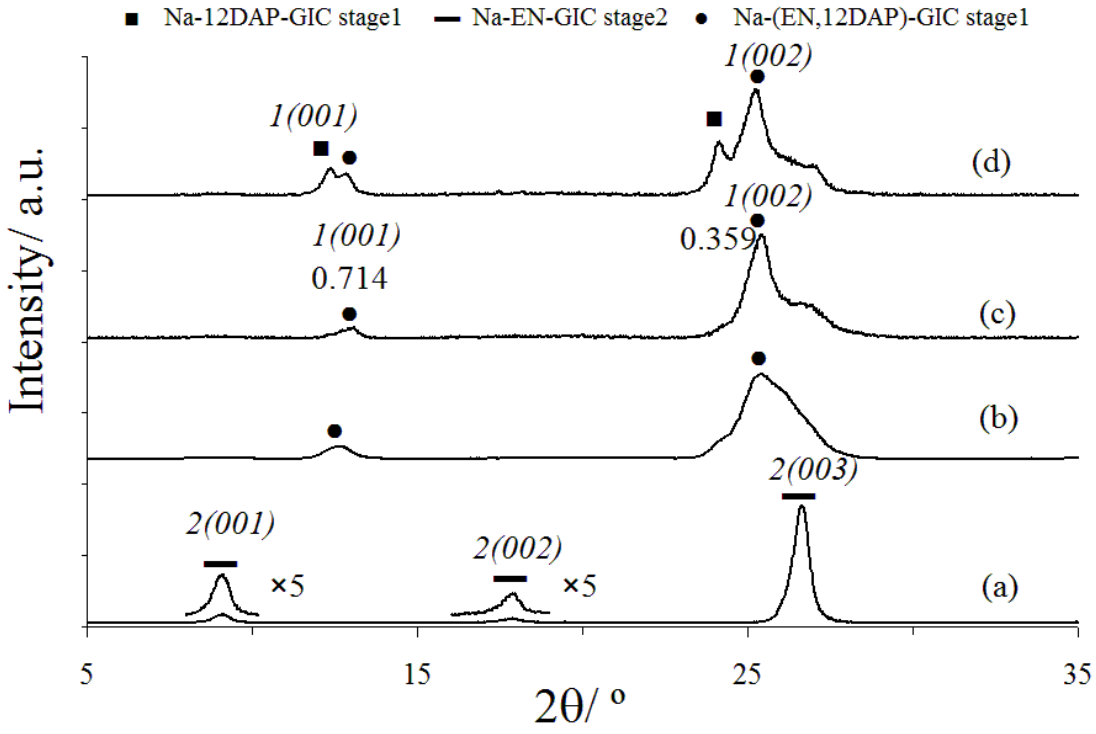

Figure 5.9 The PXRD patterns of (a) stage 2 Na-EN-GIC, and the product from its reaction with Na(m) and 12DAP at (b) 6, (c) 24, and (d) 72 h. The *d* values (in nm) and assigned Miller indices *n(00l)* are indicated for each reflection, where *n* is the stage number.

There is no diffraction evidence for an ordered heterostructure where the EN-solvated Na^+ intercalates into alternate galleries. We propose that $Na(12DAP)_y^+$ complexes intercalate into both the empty layer and the layer already occupied by $Na(EN)_y^+$. The displacement reaction occurs more slowly than the opening of new galleries, accounting for the formation of a quaternary compound followed by appearance of the Na-12DAP-GIC phase. Attempts to prepare quaternary GICs by reaction of graphite with Na and a mixture of EN and 12DAP (at several different ratios) yielded disordered materials as indicated by broad PXRD patterns.

From the previously reported d_i values for Li-(BzN,THF)-GIC (d_i = 0.744 nm)[24] and K-(THF,Bz)-GIC (d_i = 0.9 nm),[25] organic co-intercalates can form solid solutions. There have also been reports of ordered heterostructures for acceptor-type GICs, where the second guest species intercalates into the empty gallery easily without displacing the initial guest species.[57]

5.5 ACKNOWLEDGEMENT

Part of this work was presented at 2010 Solid State Chemistry Gordon Research Conference. TM thanks OSU Chemistry and the Gordon Research Conference for financial support.

5.6 REFERENCES

1. Whittingham, M. S.; Jacobson, A. J. *Intercalation Chemistry;* Academic Press: New York, 1982.
2. Ogawa, M.; Kuroda, K. *Bull. Chem. Soc. Jpn.* **1997,** *70*, 2593.
3. Osada, M.; Sasaki, T. *J. Mater. Chem.* **2009,** *19*, 2503.
4. Inagaki, M. *J. Mater. Res.* **1989,** *4*, 1560.
5. Novoselov, K. S.; Geim, A. K.; Morozov, S. V.; Jiang, D.; Zhang, Y.; Dubonos, S. V.; Grigorieva, I. V.; Firsov, A. A. *Science* **2004,** *306*, 666.
6. Gengler, R. Y. N.; Spyrou, K.; Rudolf, P. *J. Appl. Phys. D* **2010,** *43*, 374015.
7. Allen, M. J.; Tung, V. C.; Kaner, R. B. *Chem. Rev.* **2010,** *110*, 132.
8. Solache-Rios, M.; Garcia-Sosa, I.; Sosa-Reyes, S. *J. Radioanal. Nucl. Chem.* **1998,** *237*, 151.
9. Herrera-Alonso, M.; Abdala, A. A.; McAllister, M. J.; Aksay, I. A.; Prud'homme, R. K. *Langmuir* **2007,** *23*, 10644.
10. Dresselhaus, M. S.; Dresselhaus, G. *Adv. Phys.* **2002,** *51*, 1
11. Setton, R. Ternary Systems. In *Graphite intercalation compounds I. Structure and dynamics*; Zabel, H.; Solin, S. A. Springer-Verlag: Germany, 1990.
12. Solin, S. A.; Zabel, H. *Adv. Phys.* **1988,** *37*, 87.
13. Rüdorff, W. *Adv. Inorg. Chem. Radiochem.* **1959,** *1*, 223.
14. Merle, G.; Letoffe, J. M.; Rashkov, I. B.; Claudy, P. *J. Therm. Anal.* **1978,** *13*, 293.

15. Maluangnont, T.; Gotoh, K.; Fujiwara, K.; Lerner, M. M. *Carbon* **2011,** *49*, 1040.

16. Setton, R.; Beguin, F.; Facchini, L.; Quinton, M. F.; Legrand, A. P.; Ruisinger, B.; Boehm, H. P. *J. Chem. Soc., Chem. Commun.* **1983**, 36.

17. Rüdorff, W. *Chimia* **1965**, *19*, 489.

18. Stumpp, E.; Alheid, H.; Schwarz, M.; Janssen, J. J.; MullerWarmuth, W. *J. Phys. Chem. Solids* **1996,** *57*, 925.

19. Scharff, P.; Alheid, H. *Phys. Status Solidi A* **2000**, *177*, 93.

20. Skipper, N. T.; Walters, J. K.; Lobban, C.; McKewn, J.; Mukerji, R.; Martin, G. J.; de Podesta, M.; Hannon, A. C. *J. Phys. Chem. B* **2000,** *104*, 10969.

21. Maluangnont, T.; Bui, G. T.; Huntington, B. A.; Lerner, M. M. *Chem. Mater.* **2011,** *23*, 1091.

22. Maluangnont, T.; Sirisaksoontorn, W.; Lerner, M. M. submitted to *Carbon*.

23. Isaev, Y. V.; Guerard, D.; Blumenfeld, A. L.; Lenenko, N. D.; Novikov, Y. N. *Carbon* **1996,** *34*, 97.

24. Ginderow, D., *Ann. Chim.* **1971,** *6*, 5.

25. Hamwi, A.; Touzain, P.; Bonnetain, L., *Comptes Rendus De L Academie Des Sciences Serie Ii* **1984,** *299*, 1385.

26. Kargina, I.; Richeson, D. *Chem. Mater.* **1996,** *8*, 480.

27. Figueroa, E.; Brill, J. W.; Selegue, J. P. *J. Phys. Chem. Solids* **1996,** *57*, 1123.

28. Schmidt, C.; Rosen, M. E.; Caplan, D. F.; Pines, A.; Quinton, M. F. *J. Phys. Chem.* **1995,** *99*, 10565.

29. Moreh, R.; Pinto, H.; Finkelstein, Y.; Beguin, F. *J. Phys. Chem. Solids* **1996,** *57*, 909.

30. Schlogl, R.; Boehm, H. P. *Carbon* **1984,** *22*, 341.

31. Liau, Y. H.; Su, T. M. *J. Am. Chem. Soc.* **1992,** *114*, 9169.

32. Kimmel, T.; Becker, D. *J. Org. Chem.* **1984,** *49*, 2494.

33. Delville, A.; Detellier, C.; Gerstmans, A.; Laszlo, P. *Helv. Chim. Acta* **1981,** *64*, 556.

34. Rocher, N. M.; Frech, R.; Powell, D. R. *J. Phys. Chem. B* **2006,** *110*, 15117.

35. Mizutani, Y.; Ihara, E.; Abe, T.; Asano, M.; Harada, T.; Ogumi, Z.; Inaba, M. *J. Phys. Chem. Solids* **1996**, *57*, 99.

36. Abe, T.; Mizutani, Y.; Tabuchi, T.; Ikeda, K.; Asano, M.; Harada, T.; Inaba, M.; Ogumi, Z. *J. Power Sources* **1997,** *68*, 216.

37. Cousins, D. M.; Davidson, M. G.; Garcia-Vivo, D.; Mahon, M. F. *Dalton Trans.* **2010,** *39*, 8203.

38. Melero, C.; Guijarro, A.; Yus, M. *Dalton Trans.* **2009**, 1286.

39. Rhine, W. E.; Stucky, G. D. *J. Am. Chem. Soc.* **1975,** *97*, 737.

40. Mackenzie, F. M.; Mulvey, R. E.; Clegg, W.; Horsburgh, L. *Polyhedron* **1998,** *17*, 993.

41. Sanders, R. A.; Frech, R.; Khan, M. A. *J. Phys. Chem. B* **2003,** *107*, 8310.

42. Armstron, D. R.; Graham, D. V.; Kennedy, A. R.; Mulvey, R. E.; O'Hara, C. T. *Chem. Eur. J.* **2008,** *14*, 8025.

43. Bock, H.; Havlas, Z.; Hess, D.; Nather, C. *Angew. Chem. Int. Ed. Engl.* **1998,** *37,* 502.

44. Jordan, V.; Behrens, U.; Olbrich, F.; Weiss, E. *J. Organomet. Chem.* **1996,** *517,* 81.

45. Janiak, C. *Chemische Berichte-Recueil* **1993,** *126,* 1603.

46. Dye, J. L., *Acc. Chem. Res.* **1968,** *1,* 306.

47. Wotiz, J. H.; Barelski, P. M.; Hinckley, C. C.; Koster, D. F.; Kleopfer, R. D. *J. Org. Chem.* **1972,** *37,* 1758.

48. Beguin, F.; Pilliere, H. *Carbon* **1998,** *36,* 1759.

49. Goldmann, M.; Beguin, F. *Phase Transitions* **1991,** *30,* 91.

50. Duc, C. M. ; Mai, C.; Riviere, R. ; Gole, J. *Journal De Chimie Physique Et De Physico-Chimie Biologique* **1972,** *69,* 991.

51. Zhao, Y. H.; Abraham, M. H.; Zissimos, A. M. *J. Org. Chem.* **2003,** *68,* 7368.

52. Han, S. S.; Jang, S. S. *Chem. Commun.* **2009**, 5427.

53. Solin, S. A.; Chow, P.; Zabel, H. *Phys. Rev. Lett.* **1984,** *53,* 1927.

54. Medjahed, D.; Merlin, R.; Clarke, R. *Phys. Rev. B* **1987,** *36,* 9345.

55. Chow, P. C.; Zabel, H. *Phys. Rev. B* **1988,** *38,* 12837.

56. Sirisaksoontorn, W.; Adenuga, A. A.; Remcho, V. T.; Lerner, M. M. *J.Am. Chem. Soc.* DOI: 10.1021/ja2053539

57. Shioyama, H. *Syn. Met.* **2000,** *114,* 1.

CHAPTER 6

TERNARY GRAPHITE INTERCALATION COMPOUNDS OF ALKALI METALS AND POLYAMINES

Tosapol Maluangnont and and Michael M. Lerner

Department of Chemistry

Oregon State University

Corvallis, OR 97331-4003, USA

To be submitted

6.1 ABSTRACT

Ternary graphite intercalation compounds (GICs) of alkali metals and polyamines are reported. These include Li-2E3N-GIC (2E3N = diethylenetriamine, d_i = 0.74-1.13 nm), Li-3E4N-GIC (3E4N = triethylenetetramine; I_c = 1.43 nm, unknown stage), M-4E5N-GIC (M = Li, Na; 4E5N = tetraethylenepentamine, d_i = 0.75-0.76 nm), K-2E3NMe-GIC (2E3NMe = *N*,*N*,*N'*,*N'*,*N"*-pentamethyldiethylenetriamine; d_i = 0.86 nm), and K-3E4NS-GIC (3E4NS = tris(2-aminoethyl)amine; d_i = 1.06 nm), where d_i is the gallery height and I_c is the identity period. While Li-2E3N-GIC exhibits the parallel bilayer-to-monolayer transition of 2E3N, in Li-4E5N-GIC the larger polyamine 4E5N shows only the parallel monolayer orientation. Such a transition is absent in K-2E3NMe-GIC, where 2E3NMe is the pentamethylated analog of 2E3N. The structure and the stage number of Li-3E4N-GIC containing the intermediate size polyamine 3E4N are proposed yet not certain. On the contrary in K-3E4NS-GIC, where the star-shaped polyamine 3E4NS is the structural isomer of the linear analog 3E4N, the 3E4NS is perpendicular to the sheets. With these ternary metal-polyamine-GICs, we demonstrate that alkyl chains intercalate into GICs can exhibit a rich intragallery structure similar to intercalation compounds of clays.

6.2 INTRODUCTION

Graphite intercation compounds (GICs) have been extensively studied as they exhibit intereresting structural, electronic, optical and magnetic properties.[1,2,3] Upon reaction with reducing agents such as the alkali metal M, graphite is reduced and the alkali metal cation M^+ intercalates between graphene sheets, giving binary compounds M-GICs. Some of these compounds have found commercial use, *e.g.,* LiC_6 as the anode in lithium ion batteries.[4,5] Co-intercalation of neutral species, usually solvent molecules through either direct or post-synthesis (ternarization) method, results in the ternary M-solvent-GICs.[6,7] The first examples of such compounds were M-NH_3-GICs reported by Rüdorff and Schulze.[8] These compounds have received recent attention due to their potential use in energy-related applications. For example, Zhao *et al.,*[9] Han *et al.*[10] and Cheng *et al.*[11] have proposed their use as H_2-storage materials. Ternary GICs can also serve as precursors for the synthesis of graphene, as reported by Viculis *et al.,*[12] Widenkvist *et al.*[13] and Lee *et al.*[14]

In addition to ammonia, other amine co-intercalates reported to date are: methylamine,[15,16] ethylenediamine (EN),[16] *N,N,N',N'*-tetramethylethylenediamine (TMEDA),[17] and triethylamine.[17] The GIC containing a macrocylic cyptand "K222" (4,7,13,16,21,24-hexaoxa-1,10-diazabicyclo[8.8.8]hexacosane)[18] with both oxygen and nitrogen donor atoms has also been reported. Recently, our group added several new amine co-intercalates to this list, including a homologous series of *n*-alkylamines with 3-14 carbon atoms,[19] branched amines with $–CH_3$ substituent at α and β-positions,[20] and several diamines (*e.g.*, EN, 1,2-diaminopropane, *N,N*-

dimethylethylenediamine, and TMEDA) including their solid solutions.[21] Although the functionalization of graphene sheet surfaces by polyamines has been reported,[22,23] there is no previous report of the intercalation of polyamines *into* graphite to form GICs.

We report herein the preparation and characterization of ternary GICs of alkali metals and a homologous series of polyamines, with different numbers of $CH_2CH_2N(H)$ unit. The effect of methylation at the amine sites is also studied. Additionally, the intragallery structure of the linear *vs* star-shaped isomers will be compared. With these ternary metal-polyamine-GICs, we demonstrate that alkyl chains intercalate into GICs can exhibit a rich intragallery structure similar to *e.g.* intercalation compounds of clays.[24]

6.3 EXPERIMENTAL

All air-sensitive reagents and the obtained GICs were handled under Ar (for Li) or N_2 (for others). In a typical reaction, 0.25 g (20.8 mmol) of graphite powder (SP-1 grade, Union Carbide, average particle size 100 μm) was mixed with metallic Li (0.02 g, 2.9 mmol) and 3 mL of the neat polyamine whose the structures are shown in Fig. 6.1. All polyamine reagents were of 99+% purity, except 3E4N and 4E5N which were technical grade. In some cases, metallic Na or K were used, maintaining the graphite/metal mole ratio of ~ 7 as for Li. The reaction mixture was continuously stirred for 1 day at 90 ºC, after which the liquid phase was syringed out, leaving a wet powder product. GIC products denoted “wet” were characterized without further

processing, whereas those denoted “heat-treated” were subject to evacuation at 90ºC for 6h. Most of the GICs (except that containing 2E3N) cannot be dried under our experimental setup due to the high boiling point of the polyamines (> 250ºC). Washing the products with solvents such as toluene, *n*-hexane or ethanol, results in amorphous products. Upon heating to dryness, Li-2E3N-GIC became disordered (PXRD not shown). Structural calculations were performed using B3LYP method with 3-21G basis set and Gaussian 3.0 software.

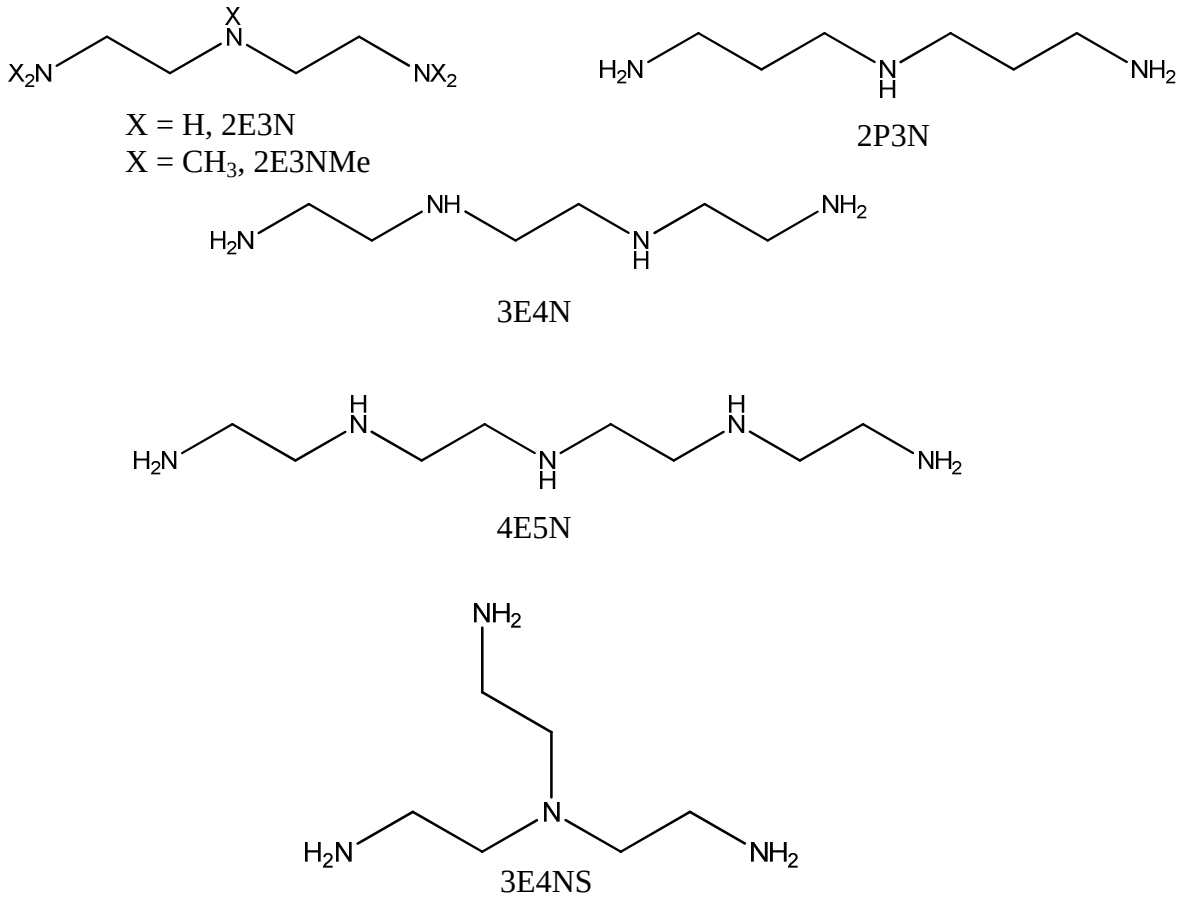

Figure 6.1 Structures and abbreviations of polyamines employed in this study

Powder X-ray Diffraction (PXRD) patterns were collected on the wet powder products using a Rigaku MiniFlex II, Ni-filtered CuKα radiation, 5-45° at 0.02° 2θ steps. Products were indexed following the relation $I_c = d_i + 0.335(n\text{-}1)$ nm, where I_c is the identity period read directly from the diffraction pattern, d_i is the gallery height, 0.335 nm is the distance between two graphene sheets, and n is the stage number, with the expansion due to intercalates $\Delta d = d_i - 0.335$ nm.

6.4 RESULTS AND DISCUSSION

6.4.1 Linear Polyamines

The products identified as GICs are all bright blue, except for the case of 3E4N, which forms a black/blue product. The reaction of graphite, Li, and 2E3N gives the product with d_i = 1.127 nm when wet [Fig. 6.2(a)] and d_i = 0.742 nm after heat treatment (but still wet) [Fig. 6.2(b)]. For the latter phase, the expansion Δd = 0.407 nm is close to 0.404-0.416 nm for TiOCl/3E4N and VOCl/3E4N intercalation compounds,[25] and is slightly larger than 0.35-0.37 nm for the intercalated *n*-alkylamine[19] or EN[21] in ternary Na-(di)amine-GICs. In the above cases[19,21,25] the amine intercalates are oriented parallel to the graphene sheets. Therefore, the heat-treated product is consistent with a 2E3N monolayer with parallel orientation. The metal-amine interaction cannot be defined because both bidentate (chelating) and monodentate interactions can show similar gallery expansions. White *et al.*[30] reported single crystal structures of the compounds LiX·*n*2E3N (X = Cl, Br; n = 1 and 1.5) where 2E3N coordinates to Li^+ either in a monodentate or bidentate mode.

Compositional studies might clarify this, although these data cannot be obtained currently due to the presence of residual polyamines. We reported similar assignment in ternary M-diamine-GICs.[21]

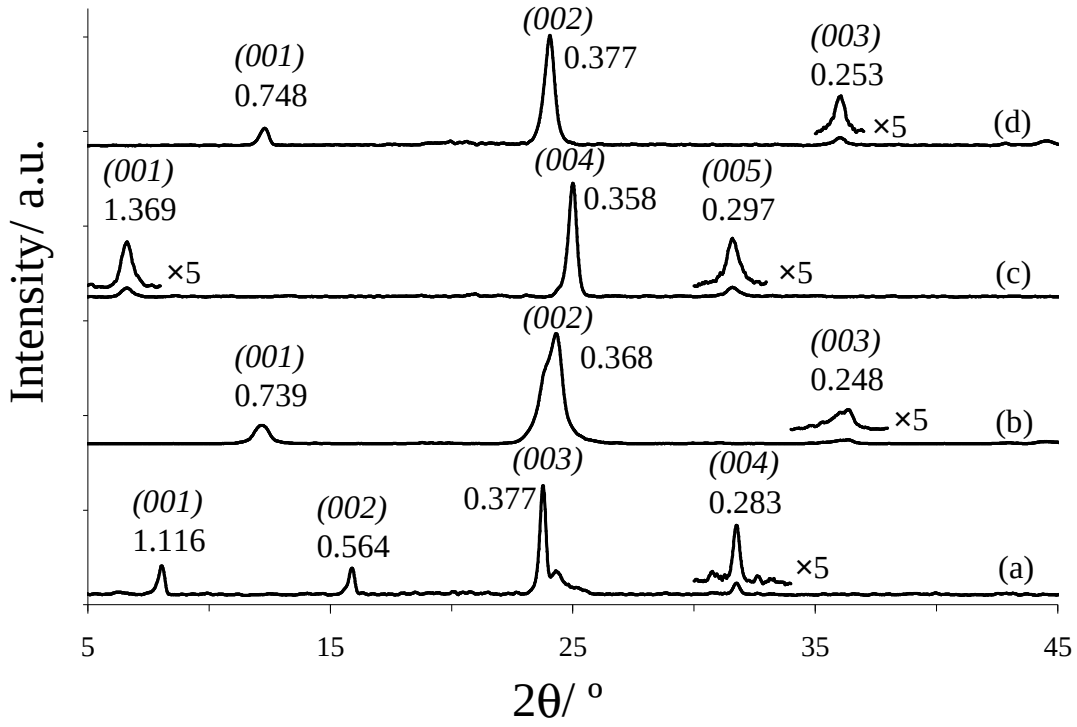

Figure 6.2 PXRD patterns of (a) wet and (b) dry Li-2E3N-GIC, (c) wet Li-3E4N-GIC, and (d) wet Li-4E5N-GIC. The *d* values (in nm) and the assigned Miller indices *(00l)* are indicated for each reflection.

We therefore ascribe the wet product to an intercalate bilayer with parallel orientation, where each layer is 0.407-nm thick. The parallel bilayer-to-monolayer transition in Li-2E3N-GIC is illustrated in Fig. 6.3(a). A similar transition was observed for Na-*n*-hexylamine-GIC.[19] In contrast, a perpendicular-to-parallel

monolayer transition is observed in a smaller homolog Li-EN-GIC[21] (EN = $H_2NCH_2CH_2NH_2$, or 1E2N in this present notation).

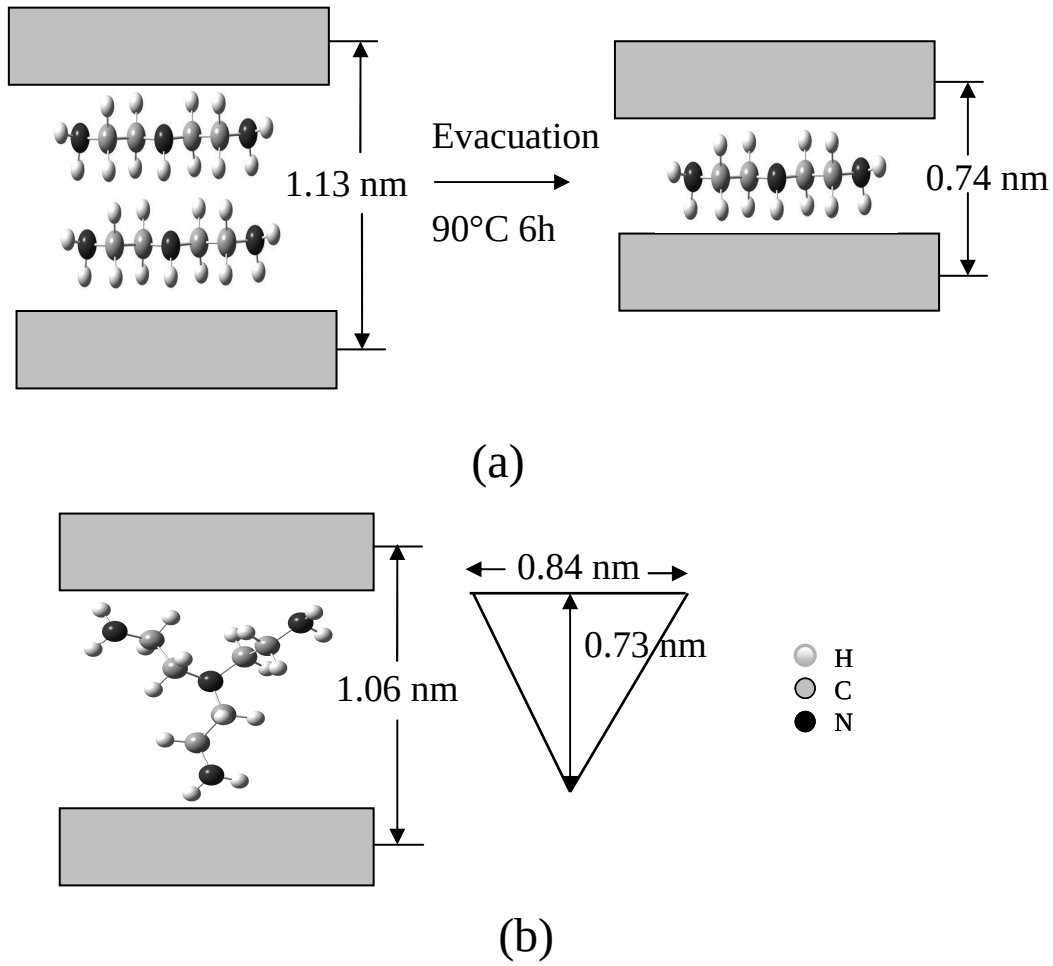

Figure 6.3 Illustration of (a) the parallel bilayer structure and the associate transition to the parallel monolayer structure in Li-2E3N-GIC, and (b) the perpendicular monolayer structure in K-3E4NS-GIC, where the shape of 3E4NS is approximated as an equilateral triangle. Cations are omitted for both illustrations.

A PXRD pattern of Li-3E4N-GIC (I_c = 1.428 nm, Δd = 1.094 nm) is shown in Fig. 6.2(c). Assuming the monomolecular thickness of 3E4N to be similar to that of 2E3N, ~0.40 nm, we compare the following three models describing the intragallery structures of this GIC. In the first two models 3E4N molecules are parallel to the graphene sheets. Model I is a stage 1 compound with the trilayer 3E4N, with predicted I_c = 0.335 + (3×0.40) = 1.54 nm. Although the trilayer structure of alkyl chains is well known for intercalation compounds of clays,[24] we are not aware of this structure in GICs. Next, model II is a stage 2 compound with the bilayer 3E4N, predicted I_c = (0.335×2) + (2×0.40) = 1.48 nm. Such an intercalate structure was reported for the first time by us in Na-*n*-alkylamine-GIC with amines containing long alkyl chains (12 and 14 carbon atoms).[19] The blue/black color of Li-3E4N-GIC suggests, though does not confirm, this intercalate structure. Lastly, we consider model III, which is a stage 1 compound with the long axis of the 3E4N tilted by $\sin^{-1}(1.10/1.26) \approx 60°$ to the underlying graphene sheets. (The 3E4N molecular length of ~1.26 nm was obtained by geometry optimization, Section 6.3). Tsukako *et al.*[26] also reported a tilt angle of 60° for 3E4N intercalates in α-zirconium phosphate. Considering that all other linear polyamines in this work show a parallel orientation, we believe that model III is less likely. Elemental analyses or structural refinements on high-quality samples may be required to elucidate the correct intragallery structure of 3E4N.

In contrast to 2E3N and 3E4N where a structural transition or a complex structure is observed, the intercalation of 4E5N surprisingly yields a GIC product parallel intercalate monolayer (d_i = 0.754 nm, Fig. 6.2(d)) (Na-4E5N-GIC with similar

d_i (0.763 nm) was also prepared.) The parallel orientation of 4E5N here is different from the 60°-tilted structure reported by Tsukako *et al.*[26] for 4E5N intercalates into α-zirconium phosphate. Interestingly in these Li-polyamine-GICs, the increased size of co-intercalates reduced the complexity of the intragallery structure. The opposite trend was reported for intercalation compounds of clays.[24] Whether or not the intra-gallery structure obtained is kinetically controlled, however, warrants further investigation.

Attempts to prepare GICs with a larger polyamine (5E6N, structure not shown) were unsuccessful as the metal (Li, Na or K) was found to be insoluble in the amine. Similarly, reactions using alkali metal M (M = Li, Na or K) and the polyamine 2P3N did not result in GIC formation. This polyamine has $–NH_2$ unit joined through the propylene group ($CH_2CH_2CH_2$), compared to the ethylene group (CH_2CH_2) in 2E3N, Fig. 6.1. This points to the importance of using amine co-intercalates where the $–NH_x$ (or $-N(CH_3)_x$, Section 6.4.2) is in a 1,2-position (*e.g.,* vicinal). We reported similar findings in the synthesis of ternary M-diamine-GICs,[21] which the GIC was obtained with 1,2-diaminopropane but not with 1,3-diaminopropane.

6.4.2 Methylated Polyamines

Fig. 6.4 shows the PXRD pattern of the stage 1 K-2E3NMe-GIC (d_i = 0.863 nm), which can be ascribed to a parallel polyamine monolayer. However, this synthesis was found to be poorly reproducible. The relatively large gallery expansion of ~0.5 nm, (calculated thickness of 2E3NMe = 0.491 nm) as compared to other

unsubstituted polyamines (Δd = 0.41-0.43 nm), can be attributed to the presence of the $-CH_3$ substituents.

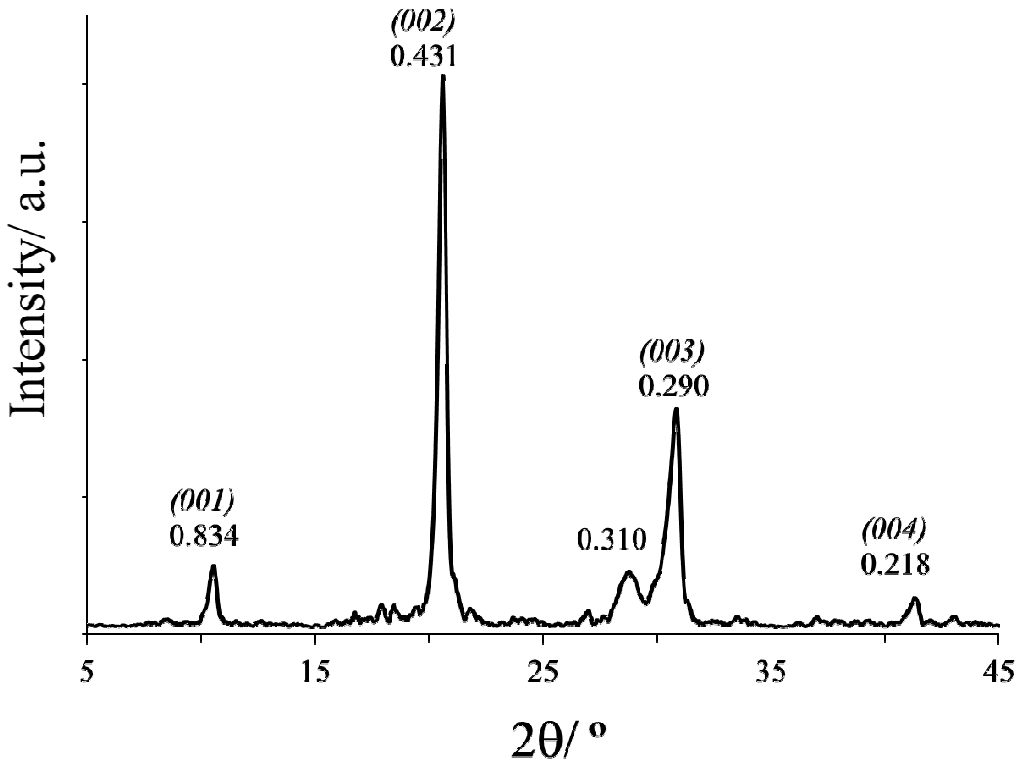

Figure 6.4 The PXRD pattern of K-2E3NMe-GIC. The *d* values (in nm) and the assigned Miller indices *(00l)* are indicated for each reflection. The peak at d = 0.310 nm is unidentified.

6.4.3 Star-Shaped Polyamine

Fig. 6.5 shows the PXRD pattern of the stage 1 K-3E4NS-GIC (d_i = 1.06 nm, Δd = 0.725 nm). Na-3E4NS-GIC with similar value of d_i can be prepared, although it is much less crystalline (PXRD not shown). Kijima *et al.*[28] reported an expansion of

0.72 nm for the intercalation compound of α-zirconium phosphate and 3E4NS. Roughly, this star-shaped polyamine can be described as an equilateral triangle, Fig. 6.3(b), which is 0.73 nm-high and whose side is 0.84 nm. The "thickness" of this triangle is ≈0.37 nm. (All dimensions are taken from the structure optimization.) The experimentally found Δd fits well to the calculated height of 3E4NS, suggesting that the molecular plane is nearly perpendicular to the graphene sheets. This orientation is also shown in Fig. 6.3(b). An alternate structure model has the amine 3E4NS tilted at an angel of $\sin^{-1}(0.73/0.84) = 60°$ (not shown).

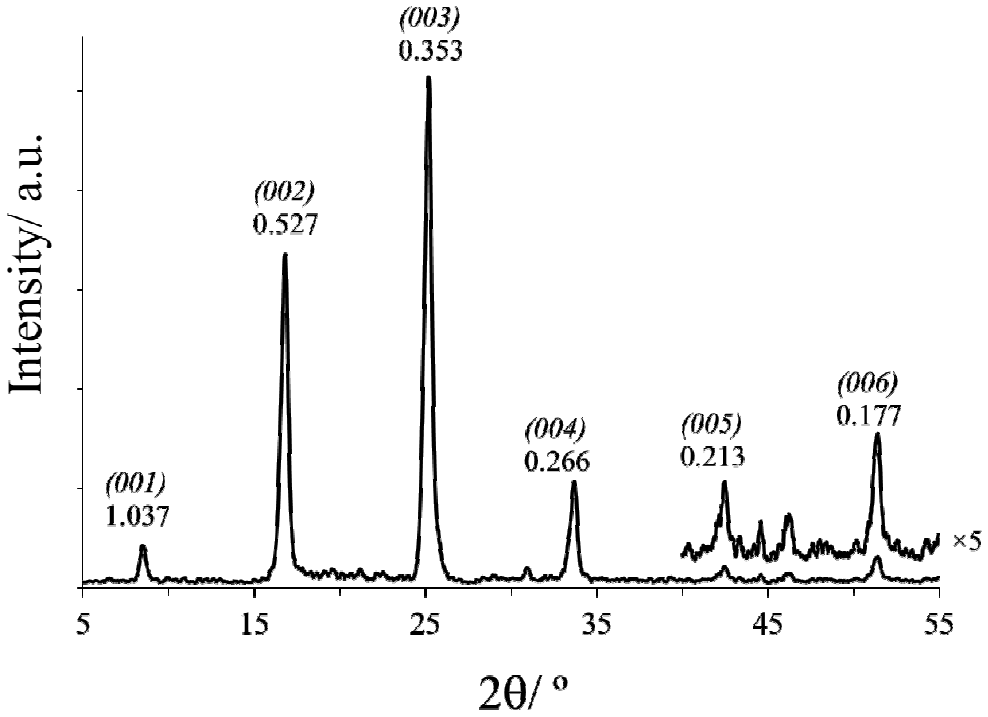

Figure 6.5 The PXRD pattern of K-3E4NS-GIC. The *d* values (in nm) and the assigned Miller indices *(00l)* are indicated for each reflection.

In addition to the assignments based on the (approximately) perpendicular orientation of 3E4NS, we now consider the following alternatives for the parallel orientation. We use the monolayer thickness of 0.42 nm (as found for 2E3N and 4E5N) in the calculation. The first is the stage 1 parallel bilayer structure [calculated d_i = 0.335 + (2×0.42) = 1.18 nm]. Another model is where K-3E4NS-GIC is the stage 2 parallel monolayer structure [calculated d_i = (0.335×2) + 0.42 = 1.09 nm]. This assignment is discarded due to the bright blue color of the compound, which is known[29] to be characteristics of stage 1 ternary M-solvent-GICs. However, similar to the case of Li-3E4N-GIC in Section 6.4.1, other analyses will be beneficial. The GICs reported in this chapter are summarized in Table 6.1.

Table 6.1 Ternary GICs of Li-polyamine-GIC reported in this work. All are stage 1 compounds except those of M-4E5N-GICs, where the value reported is I_c rather than d_i.

Polyamine	Cation	d_i/ nm	Intercalate arrangement
2E3N	Li	1.127	Parallel bilayer
	Li	0.742	Parallel monolayer
3E4N	Li	1.428	Unknown
4E5N	Li	0.754	Parallel monolayer
	Na	0.763	Parallel monolayer
2E3NMe	K	0.863	Parallel monolayer
3E4NS	K	1.057	Perpendicular monolayer

We note the following salient points from this study. Firstly, a sequence of intercalate orientation from bilayer (in 2E3N) to monolayer (4E5N) was observed as the molecular mass of polyamines increases. The orientation of polyamine with intermediate size (3E4N) is not yet certain. In these Li-polyamine-GICs, increasing size of co-intercalates reduces the complexity of the intragallery structure, opposed to what is known for intercalation compounds of clays.[24] However, the kinetics might play a role and this warrants further investigation. Secondly, in combination with our previous work on Na-*n*-alkylamine-GIC,[19] there seems to be a range of suitable molecular weight of the organic co-intercalates allowing the parallel bilayer-to-

monolayer transition. This is known for the *n*-alkylamine series (*n*-hexylamine, 101.19 g/mol) and the polyamine series 2E3N (103.17 g/mol). The low molecular mass intercalates show the monolayer structure, whereas the high molecular mass intercalates show the bilayer structure. Such a transition, however, is not observed for 2E3NMe which is the pentamethylated analog of 2E3N. We reported similar results[21] where the parallel-to-perpendicular monolayer transition was observed for 1E2N but not 1E2NMe. Thirdly, the van der Waals monomolecular thickness of polyamines (~0.42 nm) is bigger than that of *n*-alkylamine (0.37 nm),[19] possibly due to the larger number of lone pair electrons in the former. Lastly, the parallel monolayer structure as in Fig. 6.3(a), can be substituted by the structure where the polyamine chelates to metal cations. This will give the same Δd, as suggested previously for ternary M-diamine-GICs.[21]

6.5 REFERENCES

1. Zabel, H.; Solin, S. A. *Graphite Intercalation Compounds I. Structure and Dynamics*. 1 ed.; Springer-Verlag: Germany, 1990; Vol. 14.

2. Zabel, H.; Solin, S. A. *Graphite intercalation compounds II. Transport and electronic properties*. 1 ed.; Springer-Verlag: US, 1992; Vol. 18.

3. Dresselhaus, M. S.; Dresselhaus, G. *Adv. Phys.* **2002,** *51*, 1.

4. Shu, Z. X.; McMillan, R. S.; Murray, J. J. *J. Electrochem. Soc.* **1993,** *140*, 922.

5. Ohzuku, T.; Iwakoshi, Y.; Sawai, K. *J. Electrochem. Soc.* **1993,** *140*, 2490.

6. Setton, R., Ternary Systems. In *Graphite intercalation compounds I. Structure and Dynamics*, Zabel, H.; Solin, S. A., Eds. Springer-Verlag: Germany, 1990.

7. Solin, S. A.; Zabel, H. *Adv. Phys.* **1988,** *37*, 87.

8. Rüdorff, W.; Schulze, E. *Angew. Chem.* **1954,** *66*, 305.

9. Zhao, Y. F.; Kim, Y. H.; Simpson, L. J.; Dillon, A. C.; Wei, S. H.; Heben, M. J. *Phys. Rev. B* **2008,** *78*, 144102.

10. Han, S. S.; Jang, S. S. *Chem. Commun.* **2009,** 5427.

11. Cheng, H. S.; Sha, X. W.; Chen, L.; Cooper, A. C.; Foo, M. L.; Lau, G. C.; Bailey, W. H.; Pez, G. P. *J. Am. Chem. Soc.* **2009,** *131*, 17732.

12. Viculis, L. M.; Mack, J. J.; Kaner, R. B. *Science* **2003,** *299*, 1361.

13. Widenkvist, E.; Boukhvalov, D. W.; Rubino, S.; Akhtar, S.; Lu, J.; Quinlan, R. A.; Katsnelson, M. I.; Leifer, K.; Grennberg, H.; Jansson, U. *J. Phys. D Appl. Phys.* **2009,** *42*, 112003.

14. Lee, J. H.; Shin, D. W.; Makotchenko, V. G.; Nazarov, A. S.; Fedorov, V. E.; Kim, Y. H.; Choi, J. Y.; Kim, J. M.; Yoo, J. B. *Adv. Mater.* **2009,** *21*, 4383.

15. Skipper, N. T.; Walters, J. K.; Lobban, C.; McKewn, J.; Mukerji, R.; Martin, G. J.; de Podesta, M.; Hannon, A. C. *J. Phys. Chem. B* **2000,** *104*, 10969.

16. Rüdorff, W. *Adv. Inorg. Chem. Radiochem.* **1959,** *1*, 223.

17. Merle, G.; Letoffe, J. M.; Rashkov, I. B.; Claudy, P. *J. Therm. Anal.* **1978,** *13*, 293.

18. Setton, R.; Beguin, F.; Facchini, L.; Quinton, M. F.; Legrand, A. P.; Ruisinger, B.; Boehm, H. P. *J. Chem. Soc. Chem. Commun.* **1983,** 36.

19. Maluangnont, T.; Bui, G. T.; Huntington, B. A.; Lerner, M. M. *Chem. Mater.* **2011,** *23*, 1091.

20. Maluangnont, T.; Sirisaksoontorn, W.; Lerner, M. M. *submitted to Carbon*

21. Maluangnont, M.; Lerner, M. M. *submitted to Inorg. Chem.*

22. Pittman, C. U.; He, G. R.; Wu, B.; Gardner, S. D. *Carbon* **1997,** *35*, 317.

23. Geng, Y.; Li, J.; Wang, S. J.; Kim, J. K. *J. Nanosci. Nanotech.* **2008,** *8*, 6238.

24. Ogawa, M.; Kuroda, K. *Bull. Chem. Soc. Jpn.* **1997,** *70*, 2593.

25. Kargina, I.; Richeson, D. *Chem. Mater.* **1996,** *8*, 480.

26. Danjo, M.; Hayashi, A.; Nakayama, H.; Kimira, Y.; Shimizu, T.; Mizuguchi, Y.; Yagita, Y.; Tsuhako, M.; Nariai, H.; Motooka, I. *Bull. Chem. Soc. Jpn.* **1999,** *72*, 2079.

27. Leung, S. Y.; Underhill, C.; Dresselhaus, G.; Krapchev, T.; Ogilvie, R.; Dresselhaus, M. S. *Solid St. Commun.* **1979,** *32*, 635.

28. Kijima, T.; Ohe, K.; Sasaki, F.; Yada, M.; Machida, M. *Bull. Chem. Soc. Jpn.* **1998,** *71*, 141.

29. Eklund, P. C.; Doll, G. L., Effects of charge transfer on the optical properties of graphite intercalation compounds. In *Graphite Intercalation Compounds II. Transport and Electronic Properties*, Zabel, H.; Solin, S. A., Eds. Springer-Verlag: UA, 1992; Vol. 18, pp 105-162.

30. Buttery, J. H. N.; Plackett, N. C.; Skelton, B. W.; Whitaker, C. R.; White, A. H. *Z. für Anorg. Allg. Chem.* **2006,** *632*, 1856.

31. Strohmann, C.; Gessner, V. H. *Angew. Chem. Int. Ed. Engl.* **2007,** *46*, 4566.

CHAPTER 7

CONCLUSION

7.1 CONCLUSION

The syntheses and intragallery structure of ternary M-amine-GICs (M = Li, Na and K) are reported in this thesis. The amines studied include *n*-alkylamine, branched amines, and a systematic variation on the structure of diamines and polyamines. Selected samples of the quaternary compounds, either with mixed alkali metal cations or with mixed amines, are reported as well. Summaries of d_i, stage number *n*, composition of the GICs, and intragallery orientations for new compounds obtained are shown in Table 7.1 (*n*-alkylamine and branched amines), Table 7.2 (diamines), and Table 7.3 (polyamines).

Table 7.1 Summary of ternary M-*n*-alkylamine-GICs and M-branched amine-GICs reported in this thesis

M	Amine[a]	Composition	*n*	d_i/ nm	Intercalate arrangement
Li	nC3	$Li(nC3)_{0.8}C_{16}$	1	0.700	Parallel monolayer
Na	nC3	$Na(nC3)_{0.7}C_{16}$	1	0.701	Parallel monolayer
Li	nC4	-	1	0.697	Parallel monolayer
Na	nC4	-	1	0.704	Parallel monolayer
Na	nC6	-	1	1.091	Parallel bilayer
Na	nC6	-	1	0.699	Parallel monolayer
Na	nC8	$Na(nC8)_{1.6}C_{40}$	1	1.093	Parallel bilayer
Na	nC12	-	2	1.107	Parallel bilayer
Na	nC14	-	2	1.095	Parallel bilayer
Li	iC3	$Li(iC3)_{0.4}C_{18}$	1	0.760	Parallel monolayer
Na	iC3	$Na(iC3)_{0.4}C_{15}$	1	0.758	Parallel monolayer
Na	sC4	$Na(sC4)_{1.6}C_{18}$	1	1.341	Parallel bilayer
K	sC4	-	1	1.335	Parallel bilayer
Li	iC4	-	1	1.221	Parallel bilayer
Na	iC4	$Na(iC4)_{2.0}C_{28}$	1	1.280	Parallel bilayer
K	iC4	-	1	1.244	Parallel bilayer

[a]Cx is the amine with x carbon atoms, with the prefix indicating its structure: n = normal, i = *iso*, and s = *sec*.

Table 7.2 Summary of ternary M-diamine-GICs reported in this thesis

M	Amine[a]	Composition	*n*	d_i/ nm	Intercalate arrangement
Li	EN	-	1	0.855	Perpendicular monolayer
Li	EN	-	2	0.841	Perpendicular monolayer
Li	EN	$Li_1(EN)_{0.8}C_{15}$	1	0.676	Parallel monolayer
Li	EN	$Li_1(EN)_{0.7}C_{26}$	2	0.684	Parallel monolayer
Na	EN	$Na_1(EN)_{1.0}C_{15}$	1	0.691	Parallel monolayer
Na	EN	$Na_1(EN)_{0.6}C_{25}$	2	0.676	Parallel monolayer
Li	12DAP	$Li_1(12DAP)_{0.95}C_{14}$	1	0.808	Perpendicular (chelating) monolayer
Li	12DAP	$Li_1(12DAP)_{0.94}C_{26}$	2	0.827	Perpendicular (chelating) monolayer
Na	12DAP	$Na_1(12DAP)_{1.3}C_{24}$	1	0.749	Tilted
K	12DAP	-	1	0.697	Parallel monolayer
Li	DMEDA	-	1	0.910	Perpendicular (chelating) monolayer
Li	DMEDA	-	2	0.916	Perpendicular (chelating) monolayer

[a]EN = ethylenediamine; 12DAP = 1,2-diaminopropane; DMEDA = *N*,*N*-dimethylethylenediamine

Table 7.3 Summary of ternary M-polyamine-GICs reported in this thesis

M	Amine[a]	*n*	d_i/ nm	Intercalate arrangement
Li	2E3N	1	1.127	Parallel bilayer
Li	2E3N	1	0.742	Parallel monolayer
Li	3E4N	Unknown	1.428	Unknown
Li	4E5N	1	0.754	Parallel monolayer
Na	4E5N	1	0.763	Parallel monolayer
K	2E3NMe	1	0.863	Parallel monolayer
K	3E4NS	1	1.057	Perpendicular monolayer

[a]2E3N = diethylenetriamine; 3E4N = triethylenetetramine; 4E5N = tetraethylenepentamine; 2E3NMe = *N,N,N',N',N"*-pentamethyldiethylenetriamine; 3E4NS = tris(2-aminoethyl)amine

After the first report on M-NH_3-GIC (M = Li, Na, K, Rb and Cs) by Rüdorff *et al.*,[1] there followed similar GICs with M = Ca, Sr, Ba[2] and M = Be, Mg, Al, Sc, Y, and La.[3] Early extensions to amine co-intercalates included methylamine,[4,5] ethylenediamine (EN),[2] *N,N,N',N'*-tetramethylethylenediamine (TMEDA),[6] triethylamine,[6] and "K222" (4,7,13,16,21,24-hexaoxa-1,10-

diazabicyclo[8.8.8]hexacosane).[7] This thesis significantly expands the number of known ternary GICs of alkali metal cations and amines.

The GICs synthesized show many interesting and/or novel structural features. Examples include (i) a parallel bilayer arrangement of *n*-alkylamines (with x carbon atoms, nCx) as observed in Na-nCx-GIC; (ii) a parallel bilayer-to-monolayer transition in Na-nC6-GIC and Li-2E3N-GIC; (iii) formation of intercalate bilayers in sterically-demanding branched amines; (iv) the cation-directed orientation in diamine co-intercalates EN and 12DAP; and (v) a perpendicular-to-parallel transition in Li-EN-GIC. This thesis also attempts to provide new insights into how the diamine and polyamine co-intercalate structures direct the intragallery arrangements of the prepared GICs.

7.2 REFERENCES

1. Rüdorff, W.; Schulze, E. *Angew. Chem.* **1954,** *66*, 305

2. Rüdorff, W. *Adv. Inorg. Chem. Radiochem.* **1959,** *1*, 223.

3. Stumpp, E.; Alheid, H.; Schwarz, M.; Janssen, J. J.; Müller-Warmuth, W. *J. Phys. Chem. Solids* **1996,** *57*, 925.

4. Walters, J. K.; Skipper, N. T.; Soper, A. K. *Chem. Phys. Lett.* **1999,** *300*, 444.

5. Skipper, N. T.; Walters, J. K.; Lobban, C.; McKewn, J.; Mukerji, R.; Martin, G. J.; de Podesta, M.; Hannon, A. C. *J. Phys. Chem. B* **2000,** *104*, 10969.

6. Merle, G.; Letoffe, J. M.; Rashkov, I. B.; Claudy, P. *J. Therm. Anal.* **1978,** *13*, 293.

7. Setton, R.; Beguin, F.; Facchini, L.; Quinton, M. F.; Legrand, A. P.; Ruisinger, B.; Boehm, H. P. *J. Chem. Soc. Chem. Commun.***1983,** 36.

BIBLIOGRAPHY

Abe, T.; Mizutani, Y.; Tabuchi, T.; Ikeda, K.; Asano, M.; Harada, T.; Inaba, M.; Ogumi, Z. *J. Power Sources* **1997,** *68*, 216.

Alberti, G.; Costantino, U. *J. Chromatogr.* **1974,** *102*, 5.

Allen, M. J.; Tung, V. C.; Kaner, R. B. *Chem. Rev.* **2010,** *110*, 132.

Armstron, D. R.; Graham, D. V.; Kennedy, A. R.; Mulvey, R. E.; O'Hara, C. T. *Chem. Eur. J.* **2008,** *14*, 8025.

Atkins, P.; Overton, T.; Rourke, J.; Weller, M.; Armstrong, F. *Shrivers & Atkins Inorganic Chemistry.* 4th ed.; Oxford University Press: 2006, pp. 771-772.

Baranchugov, V.; Markevich, E.; Salitra, G.; Aurbach, D.; Semrau, G.; Schmidt, M. A. *J. Electrochem. Soc.* 2008, *155*, A217.

Beguin, F.; Estradeszwarckopf, H.; Conard, J.; Lauginie, P.; Marceau, P.; Guerard, D.; Facchini, L. *Syn. Met.* **1983,** *7*, 77.

Beguin, F.; Gonzalez, B.; Conard, J.; Estradeszwarkopf, H.; Guerard, D. *Syn. Met.* 1985, *12*, 187.

Beguin, F.; Pilliere, H. *Carbon* **1998,** *36*, 1759.

Beguin, F.; Setton, R. *Carbon* **1975,** *13*, 293.

Beguin, F.; Setton, R. *J. Chem. Soc. Chem. Commun.* **1976,** 611.

Beguin, F.; Setton, R.; Facchini, L.; Legrand, A. P.; Merle, G.; Mai, C. *Syn. Met.* **1980,** *2*, 161.

Benes, L.; Melanova, K.; Svoboda, J.; Zima, V. *J. Phys. Chem. Solids* **2010,** *71*, 530.

Benes, L.; Zima, V.; Melanova, K. *Eur. J. Inorg. Chem.* **2001,** 1883.

Bergbreiter, D. E.; Killough, J. M. *J. Am. Chem. Soc.* **1978,** *100*, 2126.

Besenhard, J. O.; Fritz, H. P. *J. Electroanal. Chem.* **1974,** *53*, 329.

Besenhard, J. O.; Mohwald, H.; Nickl, J. J. *Carbon* **1980,** *18*, 399.

Billaud, D.; Henry, F. X. *Solid St. Commun.* **2002,** *124,* 299.

Billaud, D.; Henry, F. X.; Lelaurain, M.; Willmann, P. *J. Phys. Chem. Solids* **1996,** *57*, 775.

Billaud, D.; Herold, A. *Bull. Soc. Chim.* **1974,** *12,* 2715.

Billaud, D.; Mareche, J. F.; McRae, E.; Herold, A. *Syn. Met.* **1980,** *2*, 37.

Billaud, D.; McRae, E.; Mareche, J. F.; Herold, A. *Syn. Met.* **1981,** *3*, 21.

Bock, H.; Havlas, Z.; Hess, D.; Nather, C. *Angew. Chem. Int. Ed. Engl.* **1998,** *37*, 502.

Boersma, M. A. M. *Catal. Rev. Sci. Eng.* **1974,** *10,* 243.

Bourlinos, A. B.; Gournis, D.; Petridis, D.; Szabo, T.; Szeri, A.; Dekany, I. *Langmuir* **2003,** *19,* 6050.

Buttery, J. H. N.; Plackett, N. C.; Skelton, B. W.; Whitaker, C. R.; White, A. H. *Z. für Anorg. Allg. Chem.* **2006,** *632,* 1856.

Cai, J. W.; Zhou, J. S.; Lin, M. L. *J. Mater. Chem.* **2003,** *13,* 1806.

Cao, G.; Lynch, V. M.; Yacullo, L. N. *Chem. Mater.* **1993,** *5*, 1000.

Cao, G.; Mallouk, T. E. *Inorg. Chem.* **1991,** *30*, 1434.

Carlin, R. T.; Delong, H. C.; Fuller, J.; Trulove, P. C. *J. Electrochem. Soc.* **1994,** *141*, L73.

Carlin, R. T.; Fuller, J.; Kuhn, W. K.; Lysaght, M. J.; Trulove, P. C. *J. Appl. Electrochem.* **1996,** *26*, 1147.

Charlier, A.; Setton, R.; Charlier, M. F. *Phys. Rev. B* **1997,** *55*, 15537.

Cheah, N. P.; Messe, L.; Clarke, S. M. *J. Phys. Chem. B* **2004,** *108,* 4466.

Cheng, H. S.; Sha, X. W.; Chen, L.; Cooper, A. C.; Foo, M. L.; Lau, G. C.; Bailey, W. H.; Pez, G. P. *J. Am. Chem. Soc.* **2009,** *131*, 17732.

Chow, P. C.; Zabel, H. *Phys. Rev. B* **1988,** *38*, 12837.

Chun, Y.; Sheng, G. Y.; Boyd, S. A. *Clays Clay Minerals* **2003,** *51,* 415.

Chung, D. D. L. *J. Mater. Eng. Perform.* **2000,** *9*, 161.

Chung, D. D. L. *J. Mater. Sci.* **2002,** *37,* 1475.

Cousins, D. M.; Davidson, M. G.; Garcia-Vivo, D.; Mahon, M. F. *Dalton Trans.* **2010,** *39,* 8203.

Cullity, B. D.; Stock, S. R. *Elements of X-ray Diffraction*. 3rd ed.; Prentice Hall: USA, 2001.

Danjo, M.; Hayashi, A.; Nakayama, H.; Kimira, Y.; Shimizu, T.; Mizuguchi, Y.; Yagita, Y.; Tsuhako, M.; Nariai, H.; Motooka, I. *Bull. Chem. Soc. Jpn.* **1999,** *72*, 2079.

Delville, A.; Detellier, C.; Gerstmans, A.; Laszlo, P. *Helv. Chim. Acta* **1981,** *64*, 556.

Dewald, R. R.; Dye, J. L. *J. Phys. Chem.* **1964,** *68,* 128.

Dresselhaus, M. S.; Dresselhaus, G. *Adv. Phys.* **2002,** *51*, 1.

Duc, C. M.; Gole, J.; Mai, C.; Riviere, R. *J. Chim. Phys.* **1972,** *69*, 991.

Dye, J. L., *Acc. Chem. Res.* **1968,** *1*, 306.

Facchini, L.; Quinton, M. F.; Legrand, A. P.; Beguin, F.; Setton, R. *Physica B & C* **1980,** *99,* 525-530.

Figueroa, E.; Brill, J. W.; Selegue, J. P. *J. Phys. Chem. Solids* **1996,** *57,* 1123.

Edman, L.; Herold, A.; Jacobsson, P.; Lelaurain, M.; McRae, E.; Sundqvist, B. *J. Phys. Chem. Solids* **1999,** *60*, 475.

Eklund, P. C.; Doll, G. L., Effects of charge transfer on the optical properties of graphite intercalation compounds. In *Graphite Intercalation Compounds II. Transport and Electronic Properties*, Zabel, H.; Solin, S. A., Eds. Springer-Verlag: UA, 1992; Vol. 18, pp 105-162.

Elmakrini, M.; Guerard, D.; Lagrange, P.; Herold, A. *Physica B & C* **1980,** *99*, 481.

Enoki, T.; Suzuki, M.; Endo, M. *Graphite Intercalation Compounds and Applications*; 1st ed.; Oxford University Press: New York, 2003.

García-Ponce, L.; Moreno-Real, L.; Jiménez-López, A. *Can. J. Chem.* **1990,** *68*, 592.

Geng, Y.; Li, J.; Wang, S. J.; Kim, J. K. *J. Nanosci. Nanotech.* **2008,** *8*, 6238.

Gengler, R. Y. N.; Spyrou, K.; Rudolf, P. *J. Appl. Phys. D* **2010,** *43,* 374015.

Goldmann, M.; Beguin, F. *Phase Transitions* **1991,** *30*, 91.

Goldmann, M.; Pilliere, H.; Beguin, F. *Syn. Met.* **1990,** *34*, 59.

Gopalakrishnan, J.; Uma, S.; Bhat, V. *Chem. Mater.* **1993,** *5*, 132.

Ginderow, D., *Ann. Chim.* **1971,** *6*, 5.

Ginderow, D.; Setton, R. *Carbon* **1968,** *6*, 81.

Hamwi, A.; Touzain, P.; Bonnetain, L., *Comptes Rendus De L Academie Des Sciences Serie Ii* **1984,** *299*, 1385.

Han, S. S.; Jang, S. S. *Chem. Commun.* **2009,** 5427.

Haynes, W. M., ed., *CRC Handbook of Chemistry and Physics;* 91st Edition (Internet Version 2011), CRC Press/Taylor and Francis: Boca Raton, FL, 2011.

Herold, A.; Mareche, J. F.; Lelaurain, M. *Carbon* **2000,** *38*, 1955.

Herold, C.; Herold, A.; Lagrange, P. *Solid St. Sci.* **2004,** *6*, 125.

Herold, C.; Pruvost, S.; Herold, A.; Lagrange, P. *Carbon* **2004,** *42*, 2122.

Herrera-Alonso, M.; Abdala, A. A.; McAllister, M. J.; Aksay, I. A.; Prud'homme, R. K. *Langmuir* **2007,** *23*, 10644.

Hick, S. M.; Griebel, C.; Blair, R. G. *Inorg. Chem.* **2009,** *48*, 2333.

Ikuta, S. *Chem. Phys.* **1986,** *108*, 441.

Inagaki, M. *J. Mater. Res.* **1989,** *4*, 1560.

Inagaki, M.; Kang, F.; Toyoda, M. *Chem. Phys. Carbon* **2004,** *29*, 1.

Isaev, Y. V.; Guerard, D.; Blumenfeld, A. L.; Lenenko, N. D.; Novikov, Y. N. *Carbon* **1996,** *34*, 97.

Isaev, Y. V.; Lenenko, N. D.; Gumileva, L. V.; Buyanovskaya, A. G.; Novikov, Y. N.; Stumpp, E. *Carbon* **1997,** *35*, 563.

Isaev, Y. V.; Novikov, Y. N.; Volpin, M. E. *Syn. Met.* **1982,** *5*, 23.

Isaev, Y. V.; Novikov, Y. N.; Volpin, M. E.; Rashkov, I.; Panayotov, I. *Syn. Met* **1983,** *6*, 9.

Jang, B. Z.; Zhamu, A. *J. Mater. Sci.* **2008,** *43*, 5092.

Janiak, C. *Chemische Berichte-Recueil* **1993,** *126*, 1603.

Jegoudez, J.; Mazieres, C.; Setton, R. *Syn. Met.* **1983,** *7*, 85.

Jegoudez, J.; Mazieres, C.; Setton, R. *Carbon* **1986,** *24*, 747.

Jimenez, P. V.; Martinez, M. I. A.; Rodriguez, A. M. *Carbon* **1985,** *23*, 473.

Jones, J. E.; Cheshire, M. C.; Casadonte, D. J.; Phifer, C. C. *Org. Lett.* **2004,** *6*, 1915.

Jordan, V.; Behrens, U.; Olbrich, F.; Weiss, E. *J. Organomet. Chem.* **1996,** *517*, 81.

Joy, P. A.; Vasudevan, S. *Chem. Mater.* **1993,** *5*, 1182.

Kargina, I.; Richeson, D. *Chem. Mater.* **1996,** *8*, 480.

Katayama, Y.; Yukumoto, M.; Miura, T. *Electrochem. Solid St. Lett.* **2003,** *6*, A96.

Kijima, T.; Ohe, K.; Sasaki, F.; Yada, M.; Machida, M. *Bull. Chem. Soc. Jpn.* **1998,** *71*, 141.

Kimmel, T.; Becker, D. *J. Org. Chem.* **1984,** *49*, 2494.

Kirczenow, G., Staging and Kinetics. In *Graphite Intercalation Compounds I. Structure and Dynamics*, 1st ed.; Zabel, H.; Solin, S. A., Eds. Springer-Verlag: Germany, 1990; Vol. 14, pp 59-100.

Klein, H. F.; Gross, J.; Besenhard, J. O. *Angew. Chem. Int. Ed. Engl.* **1980,** 19, 491-492.

Komori, Y.; Sugahara, Y.; Kuroda, K. *Appl. Clay Sci.* **1999,** *15*, 241.

Kumar, M. K.; Rao, J. S.; Prabhakar, S.; Vairamani, M.; Sastry, G. N. *Chem. Commun.* **2005,** 1420.

Lazarin, A. M.; Morales, G. C.; Sernaglia, R. L.; Andreotti, E. I. S.; Airoldi, C. *J. Phys. Chem. Solids* **2011,** *72*, 637.

Lee, J. H.; Shin, D. W.; Makotchenko, V. G.; Nazarov, A. S.; Fedorov, V. E.; Kim, Y. H.; Choi, J. Y.; Kim, J. M.; Yoo, J. B. *Adv. Mater.* **2009,** *21*, 4383.

Leung, S. Y.; Underhill, C.; Dresselhaus, G.; Krapchev, T.; Ogilvie, R.; Dresselhaus, M. S. *Solid St. Commun.* **1979,** *32*, 635.

Li, Y. Q.; Ishida, H. *Chem. Mater.* **2002,** *14*, 1398.

Li, Y. Q.; Ishida, H. *Langmuir* **2003,** *19*, 2479.

Liang, M. H.; Zhi, L. J. *J. Mater.Chem.* **2009,** *19*, 5871.

Liau, Y. H.; Su, T. M. *J. Am. Chem. Soc.* **1992,** *114*, 9169.

Liu, D. R.; Yang, Z. H.; Li, W. X.; Qiu, S. L.; Luo, Y. T. *Electrochim. Acta* **2010,** *55*, 1013.

Mackenzie, F. M.; Mulvey, R. E.; Clegg, W.; Horsburgh, L. *Polyhedron* **1998,** *17*, 993.

Maluangnont, T.; Bui, G. T.; Huntington, B. A.; Lerner, M. M. *Chem. Mater.* **2011,** *23*, 1091.

Maluangnont, T.; Gotoh, K.; Fujiwara, K.; Lerner, M. M. *Carbon* **2011,** *49*, 1040.

Maluangnont, M.; Lerner, M. M. *submitted to Inorg. Chem.*

Maluangnont, T.; Sirisaksoontorn, W.; Lerner, M. M. *Carbon* doi: 10.1016/j.carbon.2011.09.018

Manthiram, A.; Kim, J. *Chem. Mater.* **1998,** *10*, 2895.

Marcus, B.; Touzain, P. *J. Solid St. Chem.* **1988,** *77*, 223.

Markevich, E.; Baranchugov, V.; Salitra, G.; Aurbach, D.; Schmidt, M. A. *J. Electrochem. Soc.* **2008,** *155*, A132.

Martin, D. S.; Weightman, P. *Surf. Sci.* **2000,** *450*, 171.

Matsumoto, R.; Arii, T.; Oishi, Y.; Takahashi, Y. *Thermochim. Acta* **2005,** *431*, 53.

Matsumoto, R.; Takahashi, Y.; Akuzawa, N. *Mol. Cryst. Liq. Cryst.* **2000,** *340*, 43.

Matsuo, Y.; Miyabe, T.; Fukutsuka, T.; Sugie, Y. *Carbon* **2007,** *45*, 1005.

Medjahed, D.; Merlin, R.; Clarke, R. *Phys. Rev. B* **1987,** *36*, 9345.

Melero, C.; Guijarro, A.; Yus, M. *Dalton Trans.* **2009**, 1286.

Merle, G.; Beguin, F. *Carbon* **1980,** *18*, 371.

Merle, G.; Letoffe, J. M.; Rashkov, I. B.; Claudy, P. *J. Therm. Anal.* **1978,** *13*, 293.

Merle, G.; Mai, C.; Gole, J.; Rashkov, I. *Carbon* **1977,** *15*, 243.

Merle, G.; Rashkov, I.; Mai, C.; Gole, J. *Mater. Sci. Eng.* **1977,** *31*, 39.

Metrot, A.; Guerard, D.; Billaud, D.; Herold, A. *Syn. Met.* **1980,** *1*, 363.

Mizutani, Y.; Abe, T.; Ikeda, K.; Ihara, E.; Asano, M.; Harada, T.; Inaba, M.; Ogumi, Z. *Carbon* **1997,** *35*, 61.

Mizutani, Y.; Abe, T.; Inaba, M.; Ogumi, Z. , *Syn. Met.* **2002,** *125*, 153.

Mizutani, Y.; Ihara, E.; Abe, T.; Asano, M.; Harada, T.; Ogumi, Z.; Inaba, M. *J. Phys. Chem. Solids* **1996**, *57*, 799.

Morales, J.; Santos, J.; Barrado, J. R. R.; Espinos, J. P.; Gonzalez-Elipe, A. R. *J. Solid St. Chem.* **2000,** *150*, 391.

Moreh, R.; Pinto, H.; Finkelstein, Y.; Beguin, F. *J. Phys. Chem. Solids* **1996,** *57*, 909.

Morlat-Therias, S.; Mousty, C.; Palvadeau, P.; Molinie, P.; Leone, P.; Rouxel, J.; Taviot-Gueho, C.; Ennaqui, A.; de Roy, A.; Besse, J. P. *J. Solid St. Chem.***1999,** *144*, 143.

Müller-Warmuth, W.; Schollhorn, R. *Progress in Intercalation Research;* Kluwer Academic Publishers: The Netherlands, 1994.

Nakayama, H.; Hayashi, A.; Eguchi, T.; Nakamura, N.; Tsuhako, M. *J. Mater. Chem.* **2002,** *12*, 3093.

Noel, M.; Santhanam, R. *J. Power Sources* **1998,** *72*, 53.

Novoselov, K. S.; Geim, A. K.; Morozov, S. V.; Jiang, D.; Zhang, Y.; Dubonos, S. V.; Grigorieva, I. V.; Firsov, A. A. *Science* **2004,** *306*, 666.

Ogawa, M.; Kuroda, K. *Bull. Chem. Soc. Jpn.* **1997,** *70*, 2593.

Ogumi, Z.; Inaba, M. *Bull. Chem. Soc. Jpn.* **1998,** *71*, 521.

Ohzuku, T.; Iwakoshi, Y.; Sawai, K. *J. Electrochem. Soc.* **1993,** *140*, 2490.

Okuyama, N.; Takahashi, T.; Kanayama, S.; Yasunaga, H. *Physica B & C* **1981,** *105*, 298.

Osada, M.; Sasaki, T. *J. Mater. Chem.* **2009,** *19*, 2503.

Ottmers, D. M.; Rase, H. F. *Carbon* **1966,** *4*, 125.

Ottolenghi, M.; Bar-Eli, K.; Linschitz, H.; Tuttle, T. R. *J. Chem. Phys.* **1964,** *40,* 729.

Papp, S.; Dekany, I. *Colloid Polym. Sci.* **2005,** *283,* 1116.

Pilliere, H.; Beguin, F. *Carbon* **1993,** *31,* 654.

Pilliere, H.; Goldmann, M.; Beguin, F. *J. Mater. Res.* **1993,** *8,* 2288.

Pilliere, H.; Soubeyroux, J. L.; Beguin, F. *Phase Transitions* **1993,** *46,* 27.

Pittman, C. U.; He, G. R.; Wu, B.; Gardner, S. D. *Carbon* **1997,** *35,* 317.

Prasad, B. L. V.; Radhakrishnan, T. P. *Syn. Met.* **1996,** *81,* 9.

Pruvost, S.; Herold, C.; Herold, A.; Lagrange, P. *Eur. J. Inorg. Chem.* **2004,** 1661.

Rhine, W. E.; Stucky, G. D. *J. Am. Chem. Soc.* **1975,** *97,* 737.

Rida, H.; Cahen, S.; Herold, C.; Lagrange, P. *Carbon* **2010,** *48,* 3190.

Rocher, N. M.; Frech, R.; Powell, D. R. *J. Phys. Chem. B* **2006,** *110,* 15117.

Rüdorff, W. *Adv. Inorg. Chem. Radiochem.* **1959,** *1,* 223.

Rüdorff, W. *Chimia* **1965,** *19,* 489.

Rüdorff, W.; Schulze, E. *Angew. Chem.* **1954,** *66,* 30

Rüdorff, W.; Schulze, E.; Rubisch, O. *Z. Anorg. Allg. Chem.* **1955,** *282,* 232.

Safran, S. A. *Solid St. Phys.* **1987,** *40,* 183.

Sanders, R. A.; Frech, R.; Khan, M. A. *J. Phys. Chem. B* **2003,** *107,* 8310.

Scharff, P.; Alheid, H. *Phys. Status Solidi A* **2000,** *177,* 93.

Schlögl, R.; Boehm, H. P. *Carbon* **1984,** *22,* 341.

Schlögl, R.; Boehm, H. P. *Carbon* **1984,** *22,* 351.

Schmidt, C.; Rosen, M. E.; Caplan, D. F.; Pines, A.; Quinton, M. F. *J. Phys. Chem.* **1995,** *99,* 10565.

Setton, R. *Syn. Met.* **1988,** *23,* 467

Setton, R. *Syn. Met.* **1989,** *34,* 279.

Setton, R., Ternary Systems. In *Graphite intercalation compounds I. Structure and Dynamics,* Zabel, H.; Solin, S. A., Eds. Springer-Verlag: Germany, 1990.

Setton, R.; Beguin, F.; Facchini, L.; Quinton, M. F.; Legrand, A. P.; Ruisinger, B.; Boehm, H. P. *J. Chem. Soc. Chem. Commun.***1983,** 36.

Shioyama, H. *Carbon* **1997,** *35,* 1664.

Shioyama, H. *Syn. Met.* **2000,** *114,* 1.

Shioyama, H.; Tatsumi, K.; Iwashita, N.; Fujita, K.; Sawada, Y. *Syn. Met.* **1998,** *96,* 229.

Shu, Z. X.; McMillan, R. S.; Murray, J. J. *J. Electrochem. Soc.* **1993,** *140,* 922.

Sirisaksoontorn, W.; Adenuga, A. A.; Remcho, V. T.; Lerner, M. M. *J. Am. Chem. Soc.* **2011,** *133,* 12436.

Skipper, N. T.; Walters, J. K.; Lobban, C.; McKewn, J.; Mukerji, R.; Martin, G. J.; de Podesta, M.; Hannon, A. C. *J. Phys. Chem. B* **2000,** *104,* 10969.

Solache-Rios, M.; Garcia-Sosa, I.; Sosa-Reyes, S. *J. Radioanal. Nucl. Chem.* **1998,** *237,* 151.

Solin, S. A. *Ann. Rev. Mater. Sci.* **1997,** *27,* 89.

Solin, S. A.; Chow, P.; Zabel, H. *Phys. Rev. Lett.* **1984,** *53,* 1927.

Solin, S. A.; Zabel, H. *Adv. Phys.* **1988,** *37,* 87.

Strohmann, C.; Gessner, V. H. *Angew. Chem. Int. Ed. Engl.* **2007,** *46,* 4566.

Stumpp, E.; Alheid, H.; Schwarz, M.; Janssen, J. J.; Müller-Warmuth, W. *J. Phys. Chem. Solids* **1996,** *57,* 925.

Sugimoto, W.; Ohuchi, K.; Murakami, Y.; Takasu, Y. *Bull. Chem. Soc. Jpn.* **2005,** *78,* 633.

Sutto, T. E.; Duncan, T. T.; Wong, T. C. *Electrochim. Acta* **2009,** *54,* 5648.

Sutto, T. E.; Trulove, P. C.; De Long, H. C. *Electrochem. Solid St. Lett.* **2003,** *6,* A50.

Takahashi, Y.; Akuzawa, N.; Beguin, F. *Syn. Met.* **1995,** *73,* 45.

Tanaike, O.; Inagaki, M. *Syn. Met* **1998,** *96,* 109.

Tatsumi, K.; Zaghib, K.; Sawada, Y.; Abe, H.; Osaki, T. In *Rechargeable lithium and lithium-ion batteries,* Megahed, S.; Barnett, B. M.; Xie, L., Eds. The Electrochemical Society: 1994; pp 97-109.

Thomas, J. M.; Millward, G. R.; Schlogl, R. F.; Boehm, H. P. *Mater. Res. Bull.* **1980,** *15,* 671.

Toyoda, M.; Inagaki, M. *Carbon* **2000,** *38,* 199.

Viculis, L. M.; Mack, J. J.; Kaner, R. B. *Science* **2003,** *299,* 1361.

Walters, J. K.; Skipper, N. T.; Soper, A. K. *Chem. Phys. Lett.* **1999,** *300,* 444.

Wang, B. S.; Dong, X. W.; Pan, Q. Y.; Cheng, Z. X.; Yang, Y. Z. *J. Solid St. Chem.* **2007,** *180,* 1125.

Wasse, J. C.; Hayama, S.; Skipper, N. T.; Benmore, C. J.; Soper, A. K. *J. Chem. Phys.* **2000,** *112,* 7147.

Weller, T. E.; Ellerby, M.; Saxena, S. S.; Smith, R. P.; Skipper, N. T. *Nature Physics* **2005,** *1,* 39.

Whittingham, M. S.; Jacobson, A. J. *Intercalation Chemistry;* Academic Press: New York, 1982.

Widenkvist, E.; Boukhvalov, D. W.; Rubino, S.; Akhtar, S.; Lu, J.; Quinlan, R. A.; Katsnelson, M. I.; Leifer, K.; Grennberg, H.; Jansson, U. *J. Phys. D Appl. Phys.* **2009,** *42,* 112003.

Wortham, E.; Bonnet, B.; Jones, D. J.; Roziere, J.; Burns, G. R. *J. Mater. Chem.* **2004,** *14,* 121.

Wotiz, J. H.; Barelski, P. M.; Hinckley, C. C.; Koster, D. F.; Kleopfer, R. D. *J. Org. Chem.* **1972,** *37,* 1758.

Yan, W.; Lerner, M. M. *Carbon* **2004,** *42,* 2981.

Yazami, R.; Guerard, D. *J. Power Sources* **1993,** *43,* 39.

Yin, S. Y.; Zhang, Y. Y.; Kong, J. H.; Zou, C. J.; Li, C. M.; Lu, X. H.; Ma, J.; Boey, F. Y. C.; Chen, X. D. *ACS Nano* **2011,** *5,* 3831.

Zabel, H.; Solin, S. A. *Graphite Intercalation Compounds I. Structure and Dynamics.* 1st ed.; Springer-Verlag: Germany, 1990; Vol. 14.

Zabel, H.; Solin, S. A. *Graphite intercalation compounds II. Transport and electronic properties.* 1st ed.; Springer-Verlag: US, 1992; Vol. 18.

Zhang, Y. P.; Scott, K. J.; Clearfield, A. *Chem. Mater.* **1993,** *5,* 495.

Zhang, Y. P.; Scott, K. J.; Clearfield, A. *J. Mater. Chem.* **1995,** *5,* 315.

Zhao, Y. F.; Kim, Y. H.; Simpson, L. J.; Dillon, A. C.; Wei, S. H.; Heben, M. J. *Phys. Rev. B* **2008,** *78,* 144102.

Zhao, Y. H.; Abraham, M. H.; Zissimos, A. M. *J. Org. Chem.* **2003,** *68,* 7368.

Zheng, H. H.; Jiang, K.; Abe, T.; Ogumi, Z. *Carbon* **2006,** *44,* 203.

Zhou, J. S.; Cai, J. W.; Wang, L.; Ng, S. W. *Dalton Trans.* **2004,** 1493.